Field reconnaissance geologic mapping of the Columbia Hills, Mars, based on Mars Exploration Rover Spirit and MRO HiRISE observations

L. S. Crumpler,[1] R. E. Arvidson,[2] S. W. Squyres,[3] T. McCoy,[4] A. Yingst,[5] S. Ruff,[6] W. Farrand,[7] Y. McSween,[8] M. Powell,[9] D. W. Ming,[10] R. V. Morris,[10] J. F. Bell III,[3] J. Grant,[4] R. Greeley,[6] D. DesMarais,[11] M. Schmidt,[12] N. A. Cabrol,[11] A. Haldemann,[13] Kevin W. Lewis,[14] A. E. Wang,[2] C. Schröder,[15,16] D. Blaney,[9] B. Cohen,[17] A. Yen,[9] J. Farmer,[6] R. Gellert,[18] E. A. Guinness,[2] K. E. Herkenhoff,[19] J. R. Johnson,[20] G. Klingelhöfer,[20] A. McEwen,[21] J. W. Rice Jr.,[22] M. Rice,[3] P. deSouza,[23] and J. Hurowitz[9]

[1] Chemical, mineralogic, and lithologic ground truth was acquired for the first time on Mars in terrain units mapped using orbital Mars Reconnaissance Orbiter's High Resolution Imaging Science Experiment (MRO HiRISE) image data. Examination of several dozen outcrops shows that Mars is geologically complex at meter length scales, the record of its geologic history is well exposed, stratigraphic units may be identified and correlated across significant areas on the ground, and outcrops and geologic relationships between materials may be analyzed with techniques commonly employed in terrestrial field geology. Despite their burial during the course of Martian geologic time by widespread epiclastic materials, mobile fines, and fall deposits, the selective exhumation of deep and well-preserved geologic units has exposed undisturbed outcrops, stratigraphic sections, and structural information much as they are preserved and exposed on Earth. A rich geologic record awaits skilled future field investigators on Mars. The correlation of ground observations and orbital images enables construction of a corresponding geologic reconnaissance map. Most of the outcrops visited are interpreted to be pyroclastic, impactite, and epiclastic deposits overlying an unexposed substrate, probably related to a modified Gusev crater central peak. Fluids have altered chemistry and mineralogy of these protoliths in degrees that vary substantially within the same map unit. Examination of the rocks exposed above and below the major unconformity between the plains lavas and the Columbia Hills directly confirms the general conclusion from remote sensing in previous studies over past years that the early history of Mars was a time of more intense deposition and modification of the surface. Although the availability of fluids and the chemical and mineral activity declined from this early period, significant later volcanism and fluid convection enabled additional, if localized, chemical activity.

Citation: Crumpler, L. S., et al. (2011), Field reconnaissance geologic mapping of the Columbia Hills, Mars, based on Mars Exploration Rover Spirit and MRO HiRISE observations, *J. Geophys. Res.*, *116*, E00F24, doi:10.1029/2010JE003749.

[1]New Mexico Museum of Natural History and Science, Albuquerque, New Mexico, USA.

[2]Department of Earth and Planetary Sciences, Washington University, St. Louis, Missouri, USA.

[3]Department of Astronomy, Cornell University, Ithaca, New York, USA.

[4]National Museum of Natural History, Smithsonian, Washington, D. C., USA.

[5]Planetary Science Institute, Tucson, Arizona, USA.

[6]School of Earth and Space Exploration, Arizona State University, Tempe, Arizona, USA.

[7]Space Science Institute, Boulder, Colorado, USA.

[8]Department of Earth and Planetary Sciences, University of Tennessee, Knoxville, Tennessee, USA.

[9]Jet Propulsion Laboratory, Pasadena, California, USA.

[10]Johnson Space Center, Houston, Texas, USA.

[11]NASA Ames Research Center, Moffett Field, California, USA.

[12]Department of Earth Sciences, Brock University, St. Catharines, Ontario, Canada.

[13]ESA/ESTEC, Noordwijk, Netherlands.

[14]Division of Geological and Planetary Sciences, California Institute of Technology, Pasadena, California, USA.

[15]Center for Applied Geoscience, Universität of Bayreuth and Eberhard Karls Universität, Tübingen, Germany.

[16]Now at Johnson Space Center, Houston, Texas, USA.

[17]NASA Marshall Spaceflight Center, Huntsville, Alabama, USA.

[18]Department of Physics, University of Guelph, Guelph, Ontario, Canada.

[19]U.S. Geological Survey, Flagstaff, Arizona, USA.

[20]Institut für Anorganische und Analytische Chemie, Johannes Gutenberg-Universität, Mainz, Germany.

[21]Lunar and Planetary Lab, University of Arizona, Tucson, Arizona, USA.

[22]NASA Goddard Space Flight Center, Greenbelt, Maryland, USA.

[23]Tasmanian ICT Centre, CSIRO, Hobart, Tasmania, Australia.

1. Introduction

[2] The traverse through the Columbia Hills by the Mars Exploration Rover (MER) Spirit began on the 156th sol after landing [*Arvidson et al.*, 2006, 2008; *Squyres et al.*, 2006] (Figure 1a). The crossing of the contact between the lava plains and the older Columbia Hills represents an historic first crossing and documentation of a major stratigraphic unconformity on Mars. This unconformity records conditions extant at two significantly different points in Martian geologic time. Using the Athena Instruments [*Arvidson et al.*, 2003; *Bell et al.*, 2003; *Christensen et al.*, 2003; *Gorevan et al.*, 2003; *Herkenhoff et al.*, 2003; *Klingelhöfer et al.*, 2003; *Rieder et al.*, 2003; *Squyres et al.*, 2003] to replicate the basic capabilities of a field geologist, a field assessment of the mineralogy, chemistry, and microscopic character of outcrops and samples was made at representative sites throughout the traverse, and the locations of these observations were mapped onto Mars Reconnaissance Orbiter's High Resolution Imaging Science Experiment (MRO HiRISE) [*McEwen et al.*, 2007, 2010] orbital image data. Using the HiRISE data as a base along with concurrent photogeologic mapping of units and their contacts, the resulting summary of the geology provides geologic context for some of the more important in situ results of the MER mission. This simple coordination between orbital and surface data also enables some inferences about the distribution of differing lithologies in the Columbia Hills beyond the immediate areas actually sampled by the traverse. The traverse by Spirit through a photogeologic map also represents the first time that photogeologic units have been examined in the field on Mars.

[3] The mineralogy and chemistry of outcrops in the Columbia Hills are moderately complex, geologically challenging to interpret, and certainly not easily interpreted using a simple, monotonic geologic setting. Several perspectives on the categorization of the disparate outcrops and samples analyzed during the mission have been discussed based on collective properties as determined with the Athena instrument suite [*Squyres et al.*, 2006], the elemental chemistry and iron mineralogy [*Ming et al.*, 2008; *Morris et al.*, 2008], and the visible and near-infrared [*Farrand et al.*, 2008] and thermal infrared [*Ruff et al.*, 2006] spectral character of the rocks and outcrops. The limited information on the geologic context and correlation of outcrops from one site to another within the Columbia Hills has restricted initial efforts to interpret the significance of some of these categorizations. The chemistry of any protoliths is not known, and neither the degree of alteration, nor the timing of alteration events can be easily related to the observed lithologies and mineralogies. The field geologic map provides a context for the lateral correlation of outcrops. And by providing a narrative of the basic field geologic observations, some of the complex relations and many of the otherwise unconnected observations of local setting, morphology, and structure at individual sites are also presented in a broader geologic context from which they may be better appreciated, if not entirely understood.

2. Background: Geologic Setting, Spirit's Traverse, and Rover Location

[4] Details of the geologic setting are succinctly reviewed by *McCoy et al.* [2008]. The following abbreviated outline is provided for context. Gusev crater is a 160 km diameter impact crater of likely Noachian age located near the boundary between the southern highlands and the northern lowlands and is distinguished principally by its location at the terminus of an important large valley, Ma'adim Vallis [*Cabrol et al.*, 2003; *Golombek et al.*, 2003]. The Columbia Hills lie near the center of Gusev crater and consist of a roughly north-south oriented series of rounded peaks forming a continuous range approximately 6.6 km in north-south extent and range in width from 0.4 km on the north to 3.6 km on the south. The range relief gradually diminishes, and the east-west extent narrows to the north where it appears to merge visually with the plains. On the south end, steep range fronts form a clear contact with the surrounding plains lavas. Maximum relief of the Columbia Hills relative to the landing site is 110 m and 90 m above the local plains [*Squyres et al.*, 2006; *Li et al.*, 2008], and slopes range up to approximately 25° [*Li et al.*, 2005, 2006, 2008]. Steeper flanks generally occur midway up the hills, summits have rounded characters, and the basal slopes are low ramps of debris.

[5] Overlapping relations from regional photogeologic mapping [*Milam et al.*, 2003; *Kuzmin et al.*, 2000] showed that the Columbia Hills are older than the plains surrounding them. Estimates of the age of the lava flows that cover the Gusev crater floor vary substantially, from Early Hesperian age (3.7 to 3.0 Ga) [*Greeley et al.*, 2005] to Late Noachian–Early Amazonian (3.7 to 3.0 Ga) [*Martínez-Alonso et al.*, 2005; *Milam et al.*, 2003], placing a lower limit on the age on the Columbia Hills as no older than Late Noachian (3.7 Ga), and an upper limit on the age of the Columbia Hills at around 3.0 Ga. This is more than 2 Ga in the chronology of *Hartmann* [2005].

[6] The pathway of Spirit through the Columbia Hills was dictated mostly by the mission goals, focusing on outcrops with potential for preserving textures, mineral, and chemical records of (sedimentary) environments. Outcrops with sedimentary textures or outcrops that might represent the deep substrate tended to be objects of interest. In practice a balance was sought between competing science and operational needs. The pathway was typically dictated by mobility limits, and the need to be at certain locations by set times of the Martian year, notably winter locations where power-maximizing northward tilts were possible, set a pace that limited the time available at any location of interest. Traverse schedule constraints were compounded by the time necessary for simple in situ observations. Many additional compromises in observations occurred, such as drives across significant contacts without documentation, or the need to divert a traverse route from a stratigraphic sequence for mobility purposes. In other situations, successive drives crossed large areas with few observations, or in some cases postdrive remote sensing was restricted due to small downlink data volume on that particular sol. For these and many additional operational reasons, the geologic observations in some areas were incomplete or imperfect. Nonetheless they represent the first detailed observations on the surface of Mars along a transect over an area of varied geologic materials.

[7] Determination of the position from which Spirit made field observations is an important part of the work reported here. Considerable effort went into development of the required methodology for determining Spirit's position with respect to mapped landscape features (Figure 1a). At least
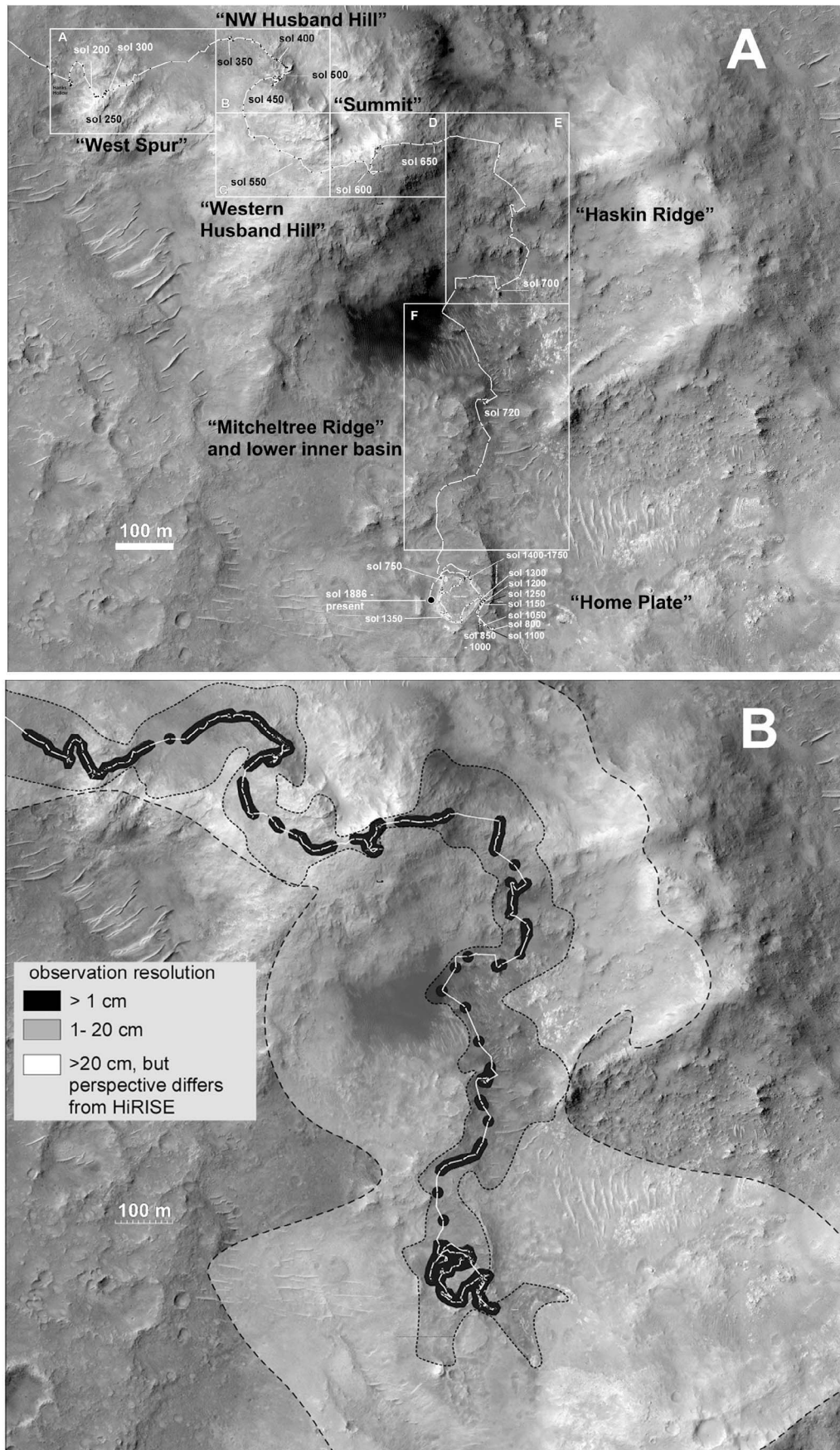
Figure 1

three methods have been used to locate Spirit with respect to the Mars surface coordinate system and with respect to the orbital image data products including position estimates determined by dead reckoning with respect to a starting point [*Arvidson et al.*, 2004]; estimates from two-way Doppler radio positioning, cartographic triangulations, visual odometry, and bundle-adjustment technologies [*Li et al.*, 2005]; and (used in this study) azimuthal centering of the rover position with respect to characteristics identified in a single orbital image and corresponding local panoramas.

[8] In this study we are interested in relating geological observations from the rover perspective to regional geologic characteristics in HiRISE images rather than rover position with respect to a particular map datum or coordinate system. Triangulation in rover perspective with respect to HiRISE image features was facilitated by development of a process [*Powell et al.*, 2010] (Maestro Map View) that merged overhead projections of Navigation Camera (Navcam) panoramas [*Powell et al.*, 2010] with the HiRISE image base using standard data products and flight operations software. Navcam mosaics were acquired in stereo and digital terrain model routinely generated for surroundings out to the limit of useful stereopsis (about 20 m on average) and provided detailed information about ranges to surrounding triangulation targets. Maestro Map View facilitated the process of aligning image mosaics draped onto the local terrain model. When combined with HiRISE image data and the ability to move the Navcam plan view mosaics around with respect to a HiRISE image base and match features, the rover position was accurately established with respect to geologic characteristics mapped previously. The flight operations software Science Activity Planner (SAP) integrated this information for use in daily science activities on both rovers [*Norris et al.*, 2005].

3. Observation Naming Conventions and Geologic Mapping Methods

[9] Names of features and naming conventions throughout the mission are informal, but followed a well-defined system that identified larger geographic features, outcrops, and in situ observations according to predefined themes (for example, sailing ships, sailing ship parts). The themes were often restricted to individual outcrops or series of outcrops in a larger geographical division such as "the west side," "the summit," or "the south flank." The observations made by each of the Athena Instruments, Pancam, Min-iTES, APXS, Mossbauer, Rock Abrasion Tool (RAT), and Microscopic Imager (MI), were each identified with an informal target name keyed to a location, or sample, on a larger feature, usually the outcrop (feature name). For example, the target Plano was on the outcrop feature Clovis in the geographic

area West Spur. In most cases, observations on a given target have similar names for each instrument, although the in situ instruments (APXS, Mossbauer, MI, and RAT) and the remote sensing instruments (Pancam and Min-iTES) frequently examined different features and targets. Even with this rigorous naming convention for each observation, the variety and abundance of names and locations can be confusing. To clarify the usage of names, some of the larger location names are shown in Figure 1, the important outcrops and sample name localities are labeled in Figure 3, and finally, Table 1 compiles the target, feature, and outcrop names and their respective locations (Table 2 of *Arvidson et al.* [2008] is also an important resource in this regard).

[10] Geologic mapping followed terrestrial field geologic mapping methods [e.g., *Evans*, 2007; *Compton*, 1985; *Barnes*, 1981] and made use of both orbital and surface observations. Fieldwork (Spirit's traverse and in situ observations) was preceded by examination of high-resolution orbital image data, and a preliminary photogeologic map of the area was prepared from the preview. The mapping initially used Mars Global Surveyor (MGS)–Mars Orbiter Camera (MOC) images and was subsequently updated and refined with MRO-HiRISE data. Additional refinements in the map resulted as in situ observations accumulated. The *field reconnaissance geologic map* here combines a photogeological map and the results of in situ examination of outcrops along a limited transect, including the determination of lithology, petrology, and stratigraphic relationships. The Navigation cameras, for which there is the most continuous record, have <1 mrad/pixel resolution [*Maki et al.*, 2003] which enables identification of details smaller than 1 cm within 10 m. Within 100 to 150 m of the rover, Navcam data exceeds the resolution of MRO/HiRISE (Figure 1b). Beyond 150 m, where the surroundings were not obscured by local horizons, to a distance of 1 km the resolution is less than MRO/HiRISE. But the Navcam images, in combination with limited Pancam data, provides additional ground-based perspectives useful for identifying details of the stratigraphy and geologic structure. The final geologic map (Figures 2 and 3) represents the merged results from observations based on orbital data, and proximal remote sensing and in situ observations from the rover.

[11] The photogeological mapping part of the analysis followed methods used to prepare planetary geologic maps from orbital remote sensing data [e.g., *Tanaka et al.*, 2009; *Greeley and Batson*, 1990; *Wilhelms*, 1990]. Units were identified and contacts located using left and right stereoptic pairs examined at full resolution (*not* anaglyphs). The stereo is based on HiRISE images acquired at differing emission angles (PSP_001513_1655, "left" and PSP_001777_1650, "right") [*McEwen et al.*, 2010]. Mapping in the stereo pairs, as in terrestrial field geologic mapping, enables correlation of surface relief characteristics at large scales with surface

Figure 1. (a) Traverse locations on HiRISE image base (PSP_001777_1650) showing the position of Spirit for sols 156 through the present as determined through methods of rover location discussed in the text. Regional names used throughout the text are also shown. Outlined areas A–F are shown in detail in Figure 3. (b) Map showing the approximate area and resolution of field observations assuming 1 mrad resolution and local ridgeline horizons. The most detailed observations at centimeter scale occurred along a corridor within 20 m of the rover at the sites of Navcam panoramas. Observations outside the light shaded area were not made from the rover and are assigned geologic units based on characteristics in HiRISE image data as correlated with known units along the traverse.

Table 1. Summary of Nomenclature (Sample, Class, and Outcrop Names) and Sample Characteristics[a]

Location	Map Unit Label	Sample Type	Outcrop/Field Site	Feature[b]	Unit Strike and Dip[c]	Unit Thickness	Target on Feature/Outcrop[d]	Petrographic Class[e]	Map Unit Name
Summit	(dmf)	Soil	summit ridgeline	Cliffhanger			Lands End, Hang Two	Basaltic sand	drifted mobile fines
Husband Hill northwest slope		Soil	Soil	Pasadena			Paso Robles, Marengo	Sulfate rich fines	
Husband Hill northwest slope		Soil	Soil	Paso Robles 2			Ben's Clod, Big Clod, Bitty Clod, Paso Dark, Paso Light	Sulfate rich fines	
Cumberland Ridge	f	Float rock	Dead Sea	Backstay			Scuppers, Scurvy	Adirondack class	float (basalt)
South (Inner) Basin		Float rock		Arad			Masada	Irvine class	
West flank Husband Hill		Float rock	Independence				Missile		
Valley between West Spur and NW Husband Hill	dmf	Soil	Thanksgiving Flats	Yams			Tofurkey	mobile fines	drifted mobile fines
South (Inner) Basin		Soil	Dead Sea	Arad			Samra, Hula	Sulfate rich fines	drifted mobile fines
West Spur	pl	Float rock		Loofah			Jerry	Adirondack class	Plains lava
Summit Region, Husband Hill	ch	rock	(summit)	Tenzing	18S at N15E(M); SE at N60E (A)	>2 m	Everest, Montagsdem Pangboche, Phortse, Phakding, Naboche Namche Bazaar, Khumjung	Watchtower class	Columbia Hills Summit outcrops
East flank Husband Hill	ch	rock outcrop	Hillary Kansas	Tenzing	18S at N15E(M); SE at N60E (A)	>2 m	Kestrel	Watchtower class	Columbia Hills Summit outcrops
Cumberland Ridge, northwest Husband Hill	lcr	rock outcrop	Alligator		N45E	~23 m	Jambalaya	Peace class	northwest Cumberland Ridge outcrops
		rock outcrop	Jibsheet	Keel			Reef	Watchtower class	
		rock outcrop	Jibsheet	Keel			Davis		
		rock outcrop	Larrys Lookout	Watchtower			Joker, Firetower, Sentinel, Bulwark, Citadel		
		rock outcrop	Larrys Outcrop	Pequod			Ahab, Moby, Moby Dick, Doubloon		
		rock outcrop	Larrys Outcrop	Paros			Paros	Peace class	
		rock outcrop	Methuselah				Keystone		
		rock outcrop	Peace				Justice 2, Equality	Peace class	
South Husband Hill	ed	soil	El Dorado				Gallant Knight Edgar Shadow	Basaltic Sand	El Dorado ripple field
South of summit Husband Hill	f	float rock	summit region	Irvine			Shrewsbury 2	Irvine class	float
Summit	soil	summit	Lambert			Couzy Whymper	mobile fines?		
Crest of Haskin Ridge	h	rock outcrop	Larrys Bench				Thrasher, Bluestem Zizia Muscogee Yeehaw	Wishstone class	Haskin Ridge
Upper slopes of Inner basin	lib	rock outcrop	Comanche Spur		>15 S	>10 m	Horseback	Watchtower class	lower Inner Basin

Table 1. (continued)

Location	Map Unit Label	Sample Type	Outcrop/Field Site	Feature[b]	Unit Strike and Dip[c]	Unit Thickness	Target on Feature/Outcrop[d]	Petrographic Class[e]	Map Unit Name
South flank Haskin Ridge	uib	rock outcrop rock outcrop rock outcrop	Comanche Spur Algonquin Seminole		15 S at N53E(M)	20 m	Palomino Iroquois Osceolan Abiaka	Algonquin class	upper Inner Basin
Husband Hill northwest slope	dcr	Float rock	northwest Husband Hill slope	Wishstone			La Brea, Chisel	Wishstone class	bright unconformable deposits of Cumberland Ridge
				Wishing Well			La Brea Chisel Champagne Dreaming Piper Piping		
West flank of Husband Hill	wh	rock outcrop	Independence	Independence			Jefferson, Livingston, Penn2, Franklin, Liberty Bell 2	Independence class	western Husband Hill
		rock	Voltaire	Descartes			Discourse, Enlightenment, Paris, Versailles, Napolean, Fraternite		
		rock		Haussmann			Rue Legendre, Rue Laplace, Sophie Germain		
		rock		Assemblee			Gruyere		
		rock		Bourgeoisie			Chic, Gentil Matrice		
West Spur	lws	rock outcrop	Hanks Hollow		~0–15 N at bN85W (M)	~8 m	Pot-of-Gold, Breadbox, Fort Knox, String of Pearls	Peace class?	lower West Spur outcrops
	uws	rock	West Spur Crest and upper slopes	Wooly Patch	~0	≥2 m	Cratchit, Tiny Tim, Scrooge	Clovis class	upper West Spur outcrops
		rock	Tetl				Clump, Squeeze, Edge		
		rock	Palinque				–		
		rock	Uchben				Koolik		
		rock	Lutefisk				FlatFish, Pickled, Twins, Fisheyes, Ratfish		
		rock outcrop	Turkey Leg				Sabre, Mastodon		
		rock	Wooly Patch	Wooly Patch			Plano, Cochiti, Jemez		
		rock	Wooly Patch	Wooly Patch					

[a]Parentheses indicate that the associated mapped lithology is identified but the sample is too small to represent in the regional map.

[b]Some outcrops are large enough that multiple locations or features were investigated, each with multiple targets. The feature is not given for some locations because other outcrops are small and the feature and target are the same in situ analysis location.

[c]Strike and dip from M, McCoy et al. [2008], and A, Arvidson et al. [2008].

[d]Names used for targets planned with Athena instruments.

[e]Petrographic class is defined on hand scale and microscopic imager detected character of the rock texture, grain size, and lamination and is largely independent of chemistry as used in this sense of correlation. Note that the petrographic class is used inclusively based on outcrop lithology. Individual outcrops may be very different in chemical and mineral parameters.
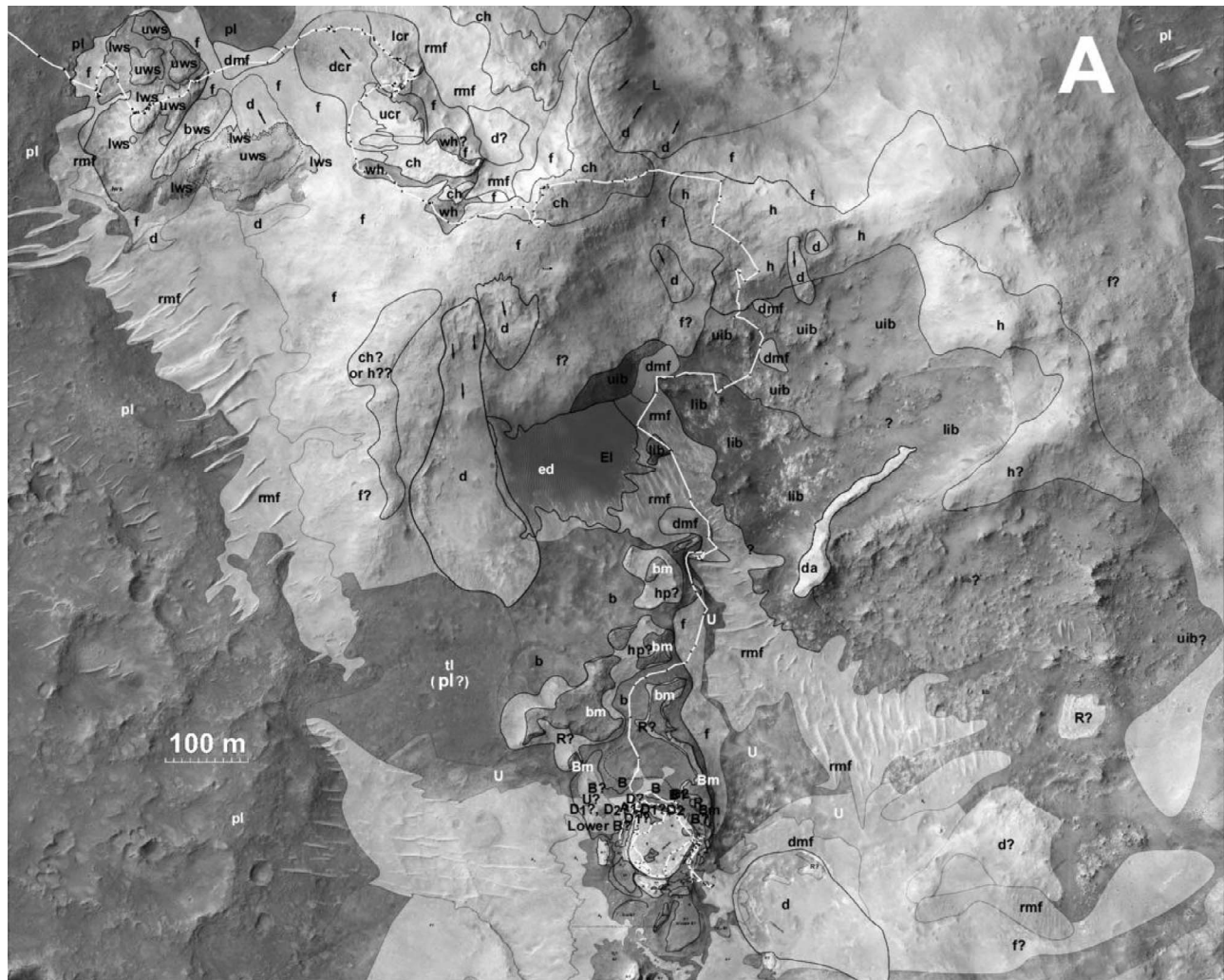
Figure 2. (a) Geologic map of the Columbia Hills prepared from photogeologic mapping on HiRISE image base merged with in situ observations. Contacts in this map were located using stereo image pairs PSP_001513_1655 and PSP_001777_1650. (Note that units Bm, R, and B are not discussed in this work and refer to units exposed near the southern end of the traverse near the feature Home Plate.) (b) Correlation of units as determined from final analysis. This represents a combination of stratigraphy from the photogeologic mapping as well as the in situ inferences regarding stratigraphy from Spirit's traverse.

textural differences, tone, and small-scale physical features many of which are not apparent in monoscopic images or in anaglyph stereo. Mapping in the orbital data also served to identify areas where the detection of differing lithologies and stratigraphy based on photo mapping was ambiguous, and where more focused attention on the ground could assist in resolving questions of stratigraphy, structure, and unit correlation. In practice geologic context was only one of many science objectives of the mission, few such sites were visited due to other scientific and operational requests, and the observations necessary for accurate reconnaissance mapping were done at few of the traverse stops.

4. Descriptions and Comparison of Units in Photogeologic and Field Maps

[12] Here we describe the regional photogeologic map units (Figures 2 and 3), and where possible by identification

of contact relations, overlapping relations, and possible stratigraphic correlations. We start each discussion with a brief synopsis of the combined interpretation, followed by a description of the observations and analysis of HiRISE data, then discuss the relevant Mars Exploration Rover observations (Table 2), proximal remote sensing and in situ investigations of representative outcrops, and conclude with an overall analysis and interpretation of the unit. (Auxiliary material Figure S1 illustrates an example of the HiRISE image from each unit.)[1] Details of observations beyond that included in Table 2, such as observation geometry and sampling characteristics, are available in the online MER Field Analyst's Notebook (http://an.rsl.wustl.edu/mer/).

[13] Using Figure 2b (correlation chart) as a guide, the discussion order proceeds from left to right and top to bottom,

---
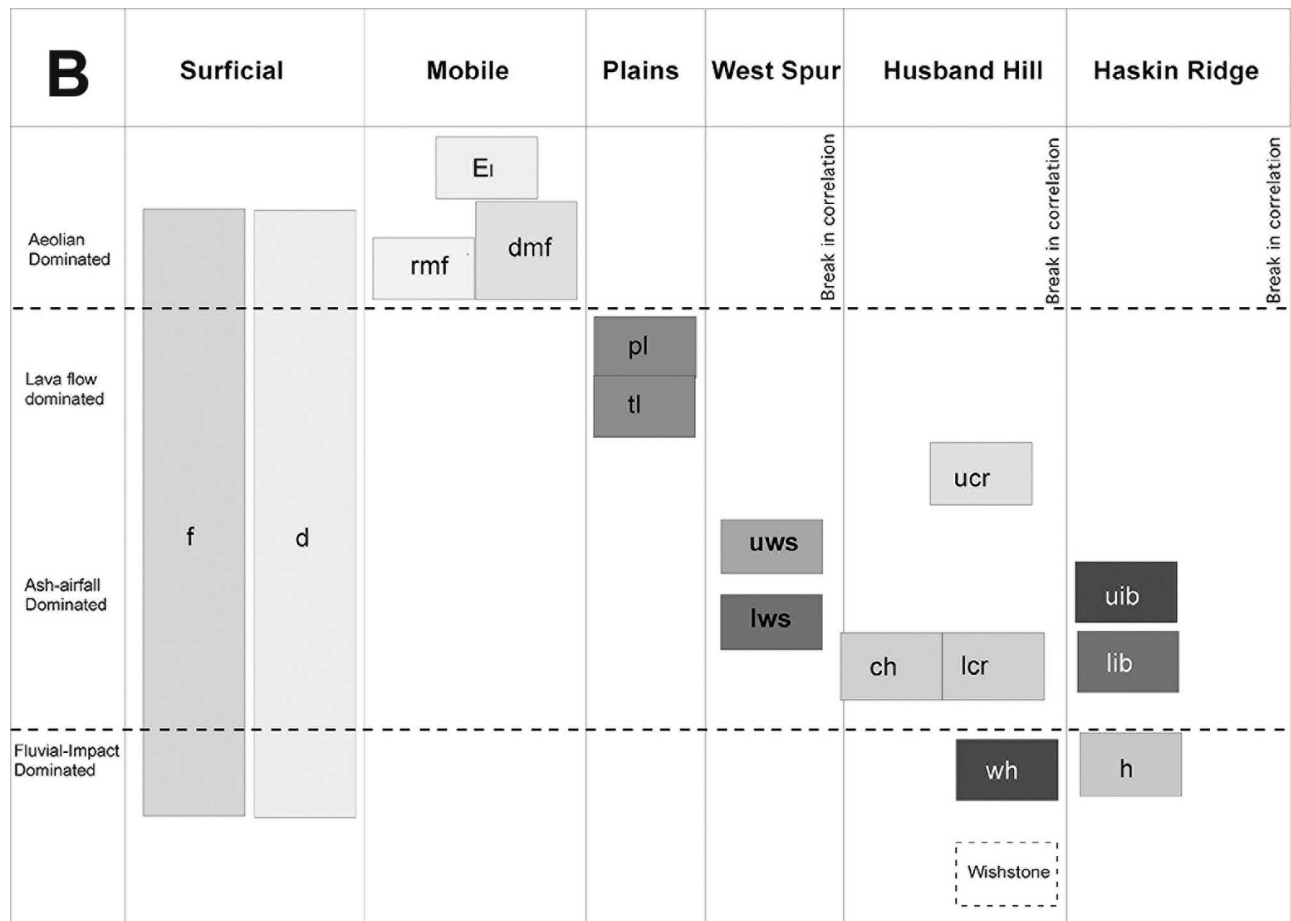
Figure 2. (continued)

with departures in a few places to accommodate the local order in which the units were encountered. This order of discussion differs from the mapping convention of older to younger, but we believe that in this case it follows a mission time-progressive narrative that works better in understanding the analyses, correlations, and conclusions.

[14] Figures 2 and 3 show the traverse and geologic mapping through the last sol near the feature dubbed Home Plate. We discuss the geology of the traverse only though approximately sol 720 because the information accumulated subsequently from detailed studies near the feature Home Plate is much greater than elsewhere and requires a separate discussion.

4.1. El Dorado Drifted Mobile Fines (Unit ed)

[15] Several dark areas around the Columbia Hills appear similar to dark ripple fields on crater floors elsewhere on Mars (Figures 2 and 3f). In situ studies by Spirit show that at least this example consists of sand-sized basaltic grains and the dark character reflects scouring of dust by active turbulence at these locations, but insufficient wind to remove the sands from the local relief trap.

4.1.1. Orbital Observations

[16] El Dorado is the largest (200 m × 150 m) area of dark ripple bed forms and is situated on the southeast facing lower slope of Husband Hill. Individual ripples have wavelengths

on the order of 1 to 3 m. This area is unusually dark and is similar to many much larger areas of dark ripple bed forms elsewhere on Mars [*Sullivan et al.*, 2008] often on large impact crater floors. It appears to onlap adjoining larger, light-toned transverse ridges (unit rmf) and the slope debris from Husband Hill.

4.1.2. Field Observations

[17] The contact with the surrounding landscape is sharply defined such that Spirit was able to examine the material while parked on the adjacent unit. In situ observations of the eastern edge of El Dorado during sols 706–710 show that these consist of ripples similar in morphology and size to those seen within craters on the plains [*Squyres et al.*, 2004]. Individual ripples have wavelengths on the order of 1 to 3 m and relief of about 30 cm [*Sullivan et al.*, 2008]. Remote rover-based observations during the third winter [*Sullivan et al.*, 2008] detected periodic changes in light streaks across the surface in El Dorado implying that the surface tone varies according to transient scouring and dust deposition possibly arising from small-scale turbulence in local winds. Trenching of small ripple bed forms in the plains previously (for example, the ripple Serpent on the rim of Bonneville crater [*Squyres et al.*, 2004]) showed that the interiors of ripples consists of dark sand-sized basaltic grains, the ripple exteriors being coated with bright dust. *Sullivan et al.*'s [2008, paragraph 20] analysis of the MI data on wheel
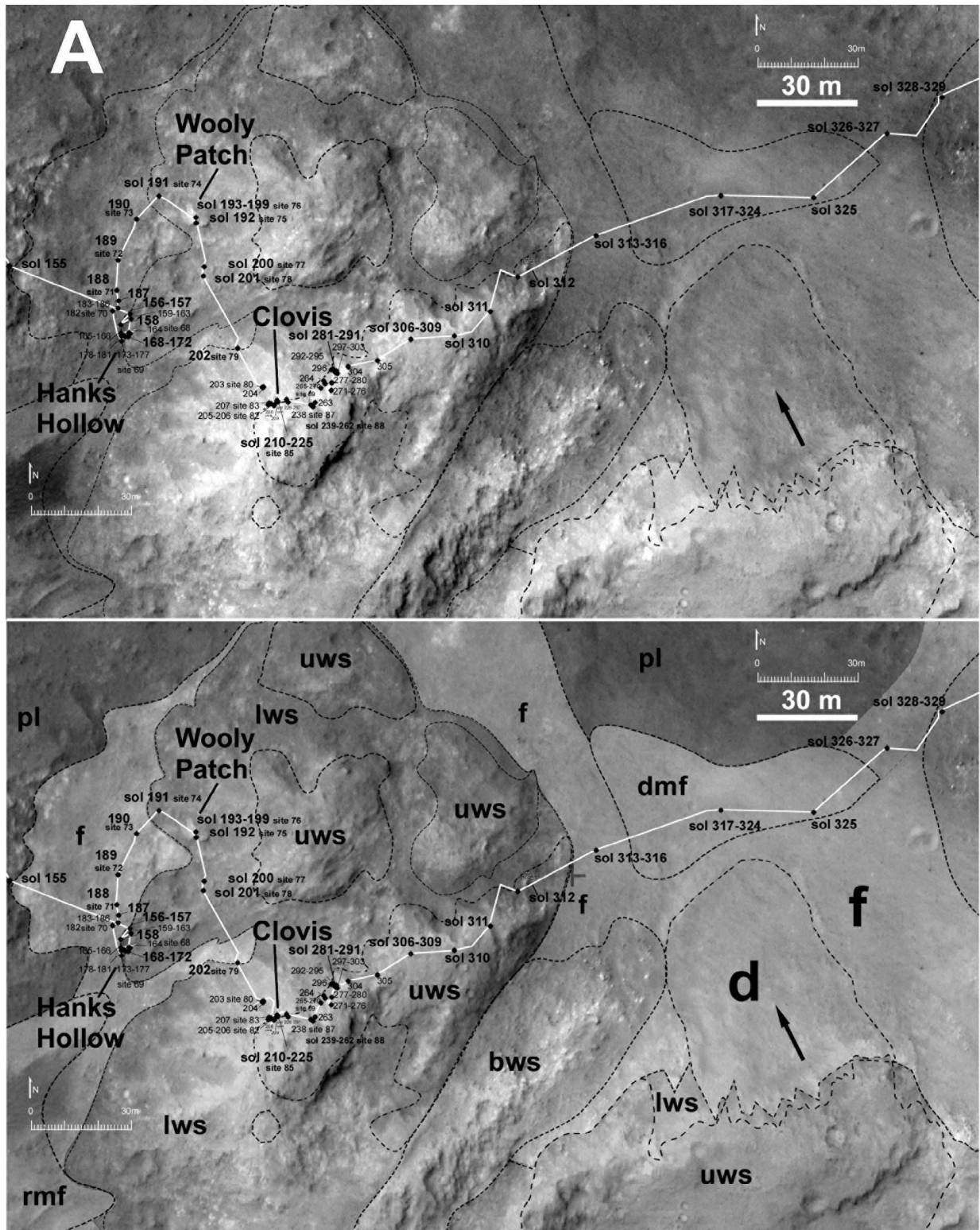
Figure 3. Detailed views of the individual sub areas identified in Figure 1. All rover locations shown here were determined with respect to local HiRISE image base using the MER data tool Maestro. Figures 3a–3d (top) and Figures 3e and 3f (left) show the image base with contacts. Figures 3a–3d (bottom) and Figures 3e and 3f (right) show the geologic units and unit labels on the image base map. (a) West Spur to northwest Husband Hill. (b) Northwest Husband Hill–Larrys Lookout. (c) Western Husband Hill–Voltaire outcrop. (d) Summit Region–Hillary outcrop. (e) Haskin Ridge–Larrys Bench–Seminole–Algonquin–Comanche outcrops. (f) El Dorado to Arad–Mitcheltree Ridge. HiRISE image base (PSP_001777_1650).
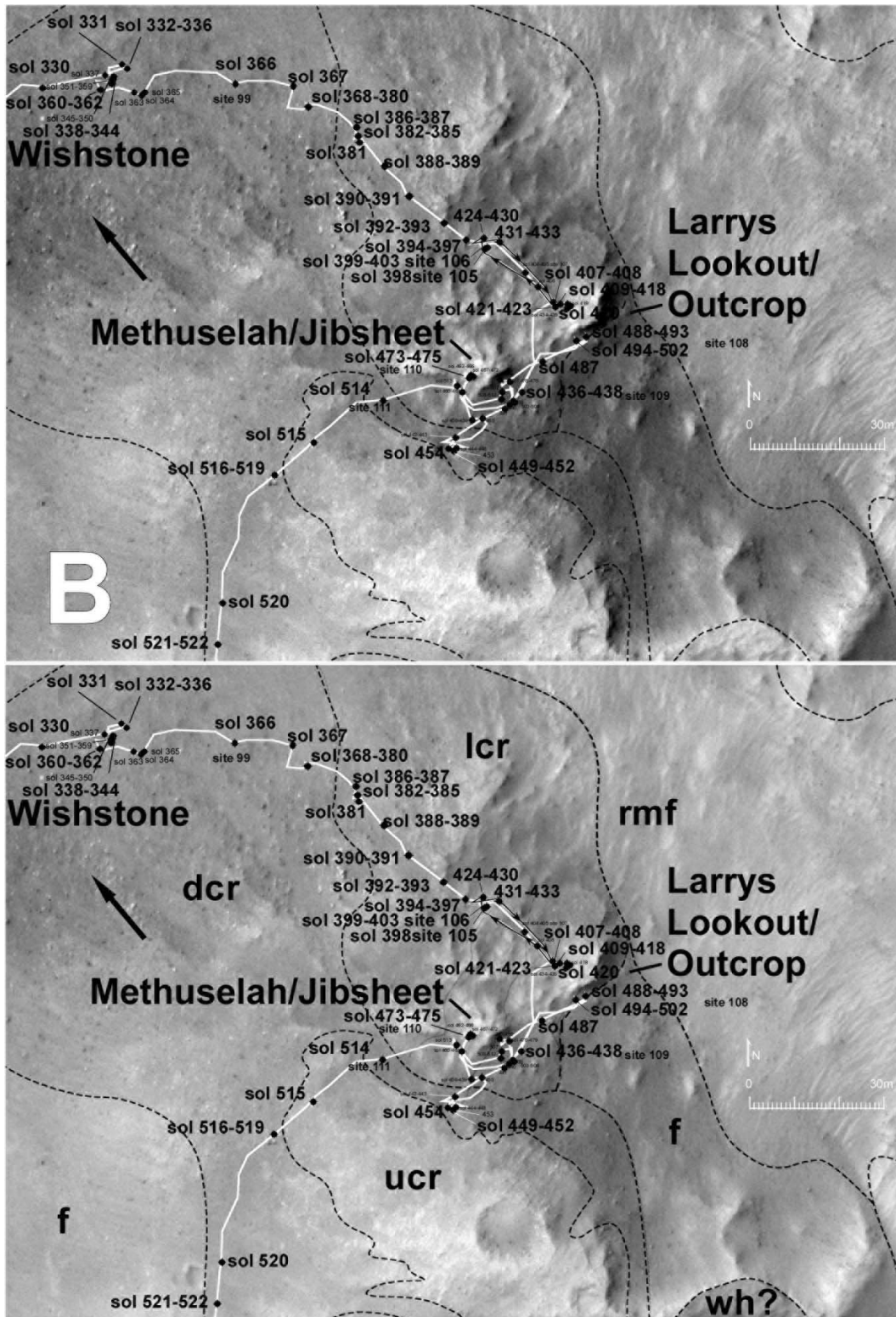
Figure 3. (continued)

scuffs indicates that El Dorado materials are similarly "dominated by poorly sorted sand with maximum grain size of around 300 μm, but with most sand around 100 μm and somewhat smaller…. Materials right at the surface are 200–300 μm sand with minor amounts of air fall dust." Pancam, Mössbauer, APXS, and Min-iTES results at El Dorado [*Sullivan et al.*, 2008; *Morris et al.*, 2008; *Ming et al.*, 2008; *Arvidson et al.*, 2008] are consistent with El Dorado sand
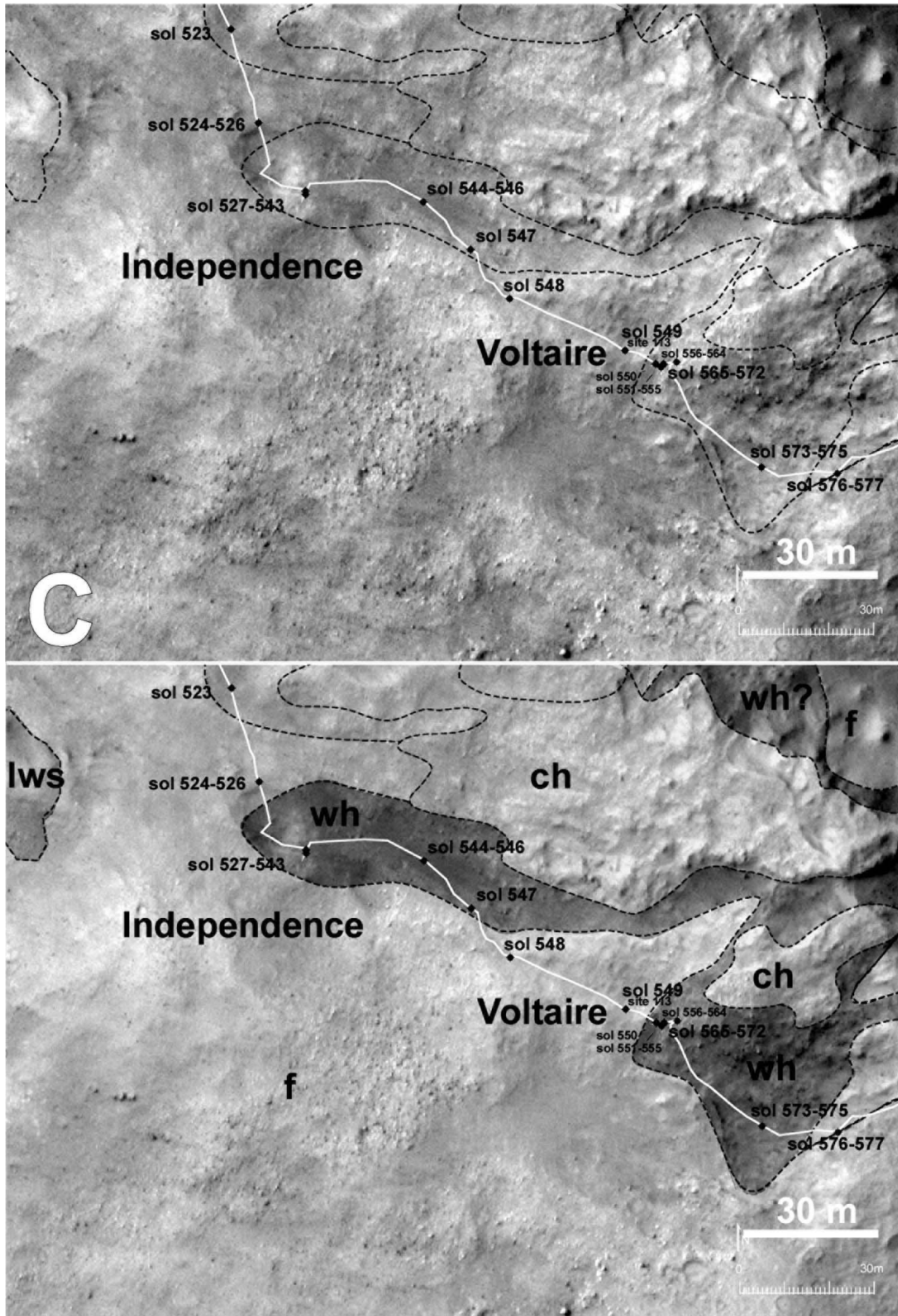
Figure 3. (continued)
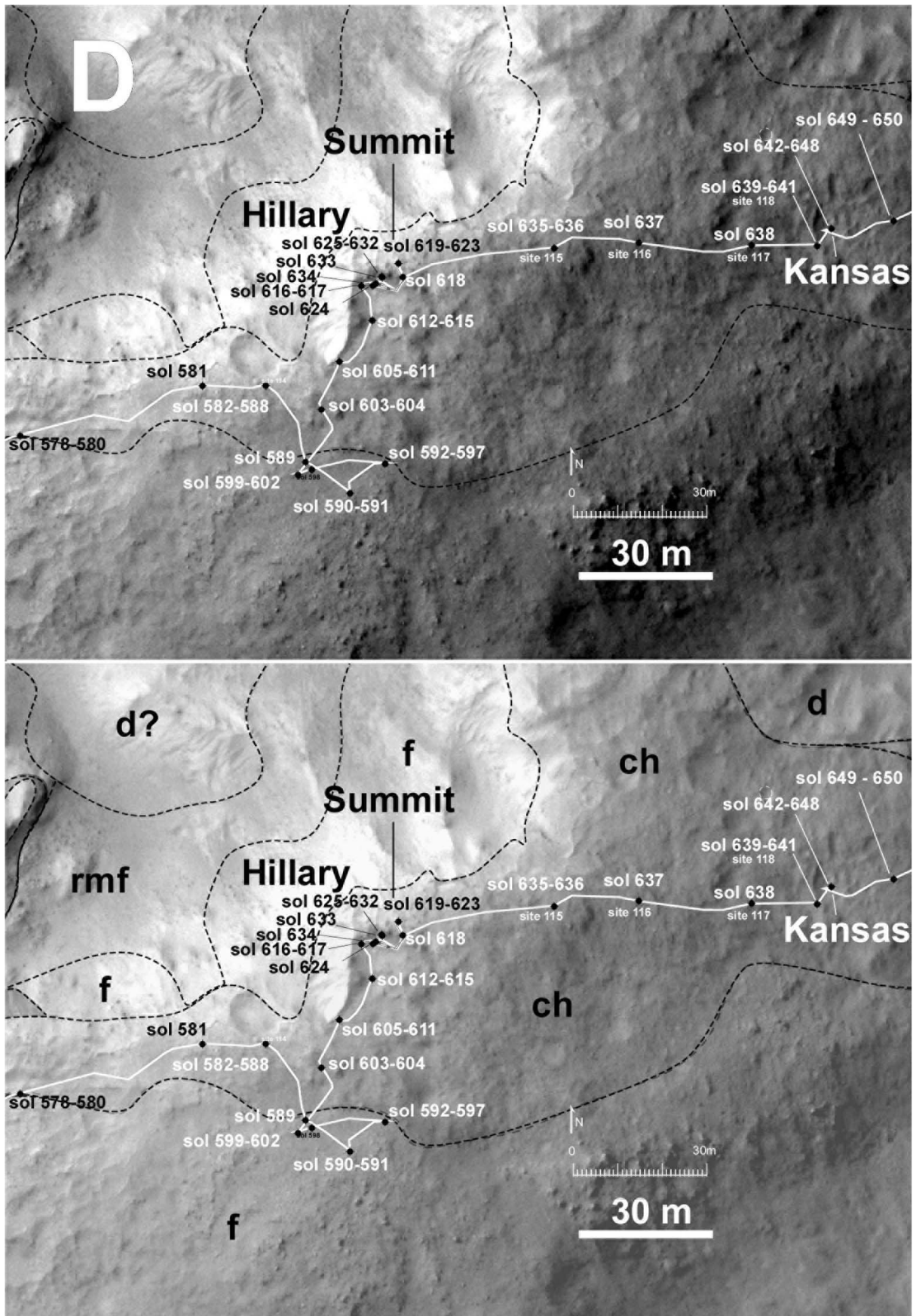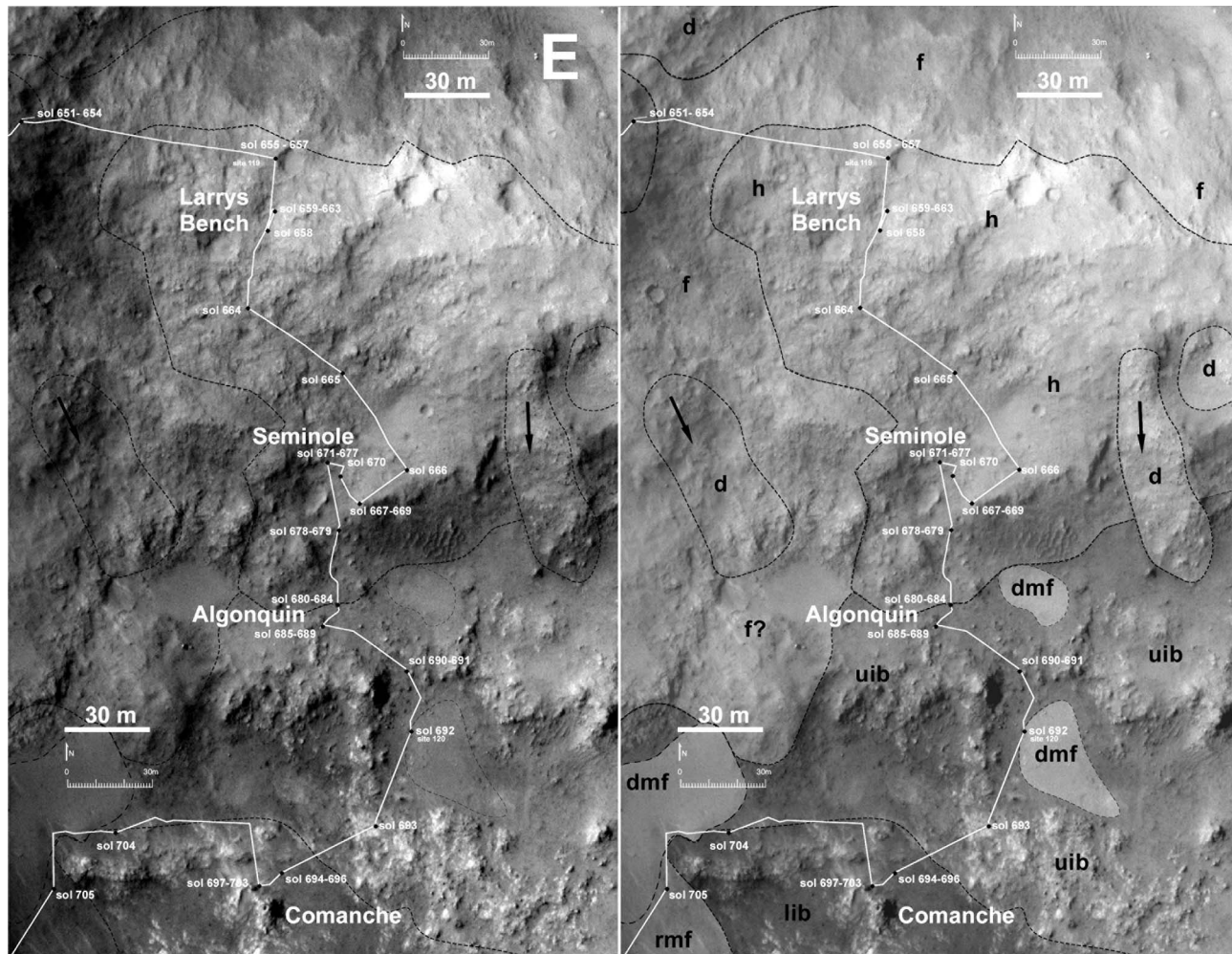
Figure 3. (continued)

Figure 3. (continued)

grains consisting of mostly mafic (olivine and pyroxene rich) materials mixed with small amounts of dust.

4.1.3. Analysis and Interpretation

[18] On the basis of the similarity of El Dorado with the dark ripple patterns within craters on the plains in orbital remote sensing, El Dorado is a collection trap on the lee side of Husband Hill for sand grains sourced in the surrounding plains [*Greeley et al.*, 2006]. The grains arrive through episodic saltation in a dominantly west-northwest-east-southeast orientation across the top of Husband Hill. Sands that are mobile in specific conditions of slope, surface roughness, and wind velocity become trapped in lee basal slopes. Persistent and repeating changes in azimuth of wind associated with the natural turbulence of winds flowing around the Columbia Hills result in distinct cross-ripple orientations as well as scouring of dust that normally settles on the surface and results in most bed forms (such as unit rmf) being lighter in tone. Although the El Dorado bed form field blends with surrounding mobile fines deposits, the active mafic component appears to be responsible for the sharply defined brightness boundary. What is not clear from remote sensing alone is why it is dark as opposed to the lighter tone common to ripples elsewhere around the Columbia Hills. *Sullivan et al.* [2008, paragraph 1] con-cluded that El Dorado represents an unusual setting where "active mafic sand ripples and larger inactive coarse-grained ripples interact."

4.2. Rippled Mobile Fines (Unit rmf)

[19] Elongated or transverse ridges in the vicinity of the Columbia Hills are similar in morphology to the ripples sampled during the traverse, but larger in size such as those common across the surface of Mars (Figures 2 and 3f). They are accordingly interpreted as aeolian bed forms. The details of the constituent grains in these larger bed forms were not examined by Spirit, but they bear some similarity to the El Dorado bed forms.

4.2.1. Orbital Observations

[20] Localized fields of longitudinal ripple bed forms several meters long, and one to two meters wide occur throughout the plains and within the Columbia Hills, par-ticularly on the west side of the Columbia Hills south of West Spur, and within the Inner Basin (between Husband Hill and McCool Hill). These characteristically occur as multiple parallel, straight to slightly sinuous ridges, many with a superimposed second set of smaller ridges that are at approximately right angles to the orientation of the main ridge. Locally, these grade laterally into smooth drifted

Figure 3. (continued)

mobile fines (dmf) but in places appear to rest directly on relatively exposed substrate lithologies.

4.2.2. Field Observations

[21] Only a few proximal observations of ripple bed form fields were done during the traverse simply because large ripples and transverse ridges represented mobility hazards to be avoided. The larger examples were on the order of a meter or slightly more high, and up to 50 m long, often with smaller or secondary set of ripples on their slopes oriented at right angles to the primary ridge form. Drives along the strike of several ridges and down the regional slope occurred after leaving the margins of El Dorado on sol 711. Drives through this transverse ridge field continued until sol 716 where a notably large transverse ridge temporarily obstructed progress near the Dead Sea site and the rock feature Arad and soil feature Samra (sol 716–718).

[22] Transverse ridges within this unit were not examined directly with the Athena instruments, so we cannot say for certain whether significant differences occur in the particles in bed forms of different relief and distribution. MI data show that the sand-sized particles in Cliffhanger, a smaller ripple bed form examined near the summit of Husband Hill (sols 605–611), appear more angular than those out on the plains, supporting a local derivation. The mineralogical and chemical results of analysis at Cliffhanger [*Sullivan et al.*,

2008] were also consistent with local derivation from the flanks of Husband Hill, consisting of Wishstone class materials (see section 4.16) mixed with average Gusev soils of the Laguna (i.e., typical Gusev plains) class [*Ming et al.*, 2008]. And on the basis of the Wishstone class component, the source could be as nearby as Cumberland Ridge to the northwest.

4.2.3. Analysis and Interpretation

[23] Ripple and ridge fields consist of coarse-grained sand-sized materials transported mostly through saltation in generally recurring patterns of winds. We interpret these primarily based on previous studies of similar features. In situ examination of several smaller ripples throughout the traverse show that the locations and orientations tend to be influenced by characteristics of the particles supplied, consistent wind orientations, and local topography [*Greeley et al.*, 2008]. No changes were noted on any of the transverse ridges from rover perspective, so most ripples appear to have relatively stable exteriors and are interpreted to be active only during exceptional conditions.

4.3. Drifted Mobile Fines (Unit dmf)

[24] In orbital images there are many featureless areas in the Columbia Hills, mostly in low areas and along the basal west facing slopes (Figures 2, 3a, and 3e). Many examples of restricted rover mobility, as well as in situ measurements,

Table 2 (Sample). Photogeologic Map Units, Representative Observations With the Athena Instruments on Outcrops and Rocks Within Each Unit, and Summary Interpretations of Lithology, Mineralogy, and Chemistry[a] [The full Table 2 is available in the HTML version of this article]

Photogeologic Map		Location		Traverse-Based Observations		
				Pancam	Remote Sensing	
Map Unit Name	Map Unit Label	MERA Sol Traversed	Representative Rocks/Outcrops	Sample Mosaics/Images	Multispectral	Mini-TES Targets
El Dorado drifted mobile fines	ed	706–710	El Dorado ripple field	El Dorado, Sol708A_P2267; Sol1178A_P2359 L257; Sol699A_P2589; Sol711A_P2536	Sol 711_P2535; Sol711_P2536	Sol 707–708 P3681 ti vscan_el_dorado, Sol 708–709 P3680 ti raster el_dorado, Sol 711 P3353 El Dorado Scuff
Rippled mobile fines	rmf	not traversed (proximal observations, sol 716–718); related obs sol 605–611?	(related observation? = Cliff_Hanger drift)	(see Navcam 2 N190016113 EFFAM CW P0735 L0 M1); Sol1374A_P2421_L257	e.g., Sol 589_P2559	
Drifted mobile fines	dmf	314–316; 705, 716–727; 782–801, 1095–1101	Thanksgiving Flats–sol 313–320 drift deposits; Dead Sea; Tyrone	2 P154430448 EFF 9300 P2559 L2 C1; 779A_P2389 drivedirection_L7; "Tyrone," Sol788A_P2396_L257; "Thanksgiving Pan" (foreground);	Sol324A_P2261; Sol721A_P2538; Sol1098A_P2548	Sol 721 P3357, Arad1; Sol 721 P3358. Arad2; Sol 722 P3359, Arad_tracks1; Sol 722 P3360, Arad_tracks2; Sol 724 P3366, Lot: Sol 724 P3367, LotsWife
Plains lava	pl	(01–155)	Adirondack, Humphrey, Mazatz, (Loofah–sol 191)	2 P 140138483 EFF 67 00 P2371 R1 C1	(Sol 35_P2578; Sol 55_P2583, Sol 60_P2597)	Sol 014 P3109, Adirondack; Sol 041 P3148. Sarah; Sol 047 P3154, Beacon; Sol 060 P3178, Humphrey; Sol 100 P3229, Route66
Trough lava	tl	not traversed		NA		NA
Upper caprock of West Spur	uws	(192–209) 210–262, 305–313	(Wooly Patch); Clovis; Ebenezer; Tetl, Palinque; Uchben; Lutefisk	Cahokia Pan; Sol210A_P2398 L257; Turkey Leg, Sol313A_P2431_L357; Sol278A_P2415; Sol531A_P2443; Sol217A_P2277; Sol226A_P2569; Sol304A_P2553; Sol322A_P2298; Sol526A_P2439;	A227 Frio P2571, P2572 (Wooly Patch, sol 200 P2556)	P3300_sol194_viera_cairns, P3318_sol216_bramsen, P3322_sol219_toltecs, P3324_sol220_plate, P3330_sol225_pico, P3331_sol226_clovis_brushed, P3333_sol227_ebenezer, P3382_sol290_palenque 1630, P3398_sol308 cocomama
Slopes of West Spur	lws	156–181, 192–209, 263–304	Pot-of-Gold/Hanks Hollow; [Hanks Hollow lithologies covered with Clovis-type float]	Archipelago, Sol165A_P2377_L257; Sol158A_P2595; Sol158A_P2594; 2P140936727	Pot of Gold sol159_P2597, sol 176_P2543	Sol 159 P3257 Roger_Dean, Sol 160 P3262 Pancake, Sol 165 P3282 Breadbox, Sol 167 P3288 Pot of Gold, Sol 169 P3291 Pudgie
Upper Cumberland Ridge materials	ucr	515–523	None (Wishstone, Champagne); see unit dcr description	Sol459A_P2412; Sol519A_Sunset_Ridge_L256; Sol519A_P2291	(a332 Wishbone p2563; a337 Wishbone RATed p2569; a343 LaBrea p2574; a362 Champagne RATed p2530)	Sol 335_P3811_Wishbone, Sol 341_P3820_La Brea, Sol 341_P3819_Golden_rings, Sol 344_P3830_Pipers_piping

[a]Dash indicates that the unit may also be present within the sample field during these sols although another unit is mapped as occurring in these locations.
[b]References are F, Farrand et al. [2008]; M, McSween et al. [2006a, 2006b]; Mi, Ming et al. [2008]; Mo, Morris et al. [2008]; R, Ruff et al. [2006]; S, Squyres et al. [2006]; Y, Yen et al. [2008]; W, Wang et al. [2008].
[c]Results from Pancam, Navcam, and MI.
[d]Results from Min-iTES, APXS, Mossbauer.

show that there are very fine materials. Proximity to ripples and other Aeolian characteristics suggests that these are areas were the fine component becomes trapped during Aeolian transport of mobile fines.

4.3.1. Orbital Observations

[25] These are bland-appearing surfaces that occur in topographic lows (based on stereoscopic images), and unlike dark ripple fields that occur on southeast facing slopes, this unit commonly occurs at the west facing base of hills throughout the Columbia Hills. It may also be present adjacent to areas of prominent ripple bed forms (unit rmf). The contact with surroundings ranges from an abrupt to gradational in an area of otherwise distinguishable surface textures and small roughness to adjacent areas where relief characteristics may be visible, but tonal variations and high-frequency surface irregularities appear subdued. In some locations a pattern of parallel streaks may also be present.

4.3.2. Field Observations

[26] These deposits correspond with sites of sulfate-rich soils commonly traversed in local topographic lows [*Wang et al.*, 2008; *Yen et al.*, 2008] including iron sulfates of Paso Robles (sol 398–403, 424–430) and Dead Sea (soil target Samra) (sols 716–725) where large variations in chemistry of the soils occurs over centimeter scales. Other examples are silica-enriched [*Squyres et al.*, 2008; *Wang et al.*, 2008] particularly around the margins of Home Plate. These areas are mostly detectable in HiRISE images, but are too small to be mapped consistently in the regional mapping. Some of the larger mapped deposits are located on the basal northwest slopes of hills.

[27] Some of these deposits have a one to two centimeter thick uppermost layer of somewhat more cohesive fines [*Arvidson et al.*, 2010b] with distinct vertical chemical stratification profiles interpreted to result from downward percolation of fluids through minerals of varying solubilities and corresponding variability in downward transport. The cohesive character of these constitutes a significant mobility hazard. In some cases, such as at *Troy* [*Arvidson et al.*, 2010a], small clasts have been deposited on the surface of these cohesive soils resulting in a surface that appears like a thinly mantle rocky surface but is actually a crusted, cohesionless sand, and a mobility hazard.

4.3.3. Analysis and Interpretation

[28] We identify these as mobile fines because they occur frequently in association with (1) more obvious ripple bed forms and (2) areas where local relief lows are likely to provide a trap for fines. Assuming they are mobile materials, it is likely that they have been trapped in topographic lows and banked against the windward side of steeper slopes where they commonly occur. In this respect the drifted mobile fines deposits (unit dmf) are the results of sorting processes that are different from dark ripples (unit ed), and occur mostly on the windward rather than lee sides of large-scale relief features. Part of the reason for the location on the windward lower slopes of relief feature may relate to the particle sizes. Whereas dark lee slope ripples are sand size materials that are likely to have been transported by saltation, windward mobile fines could consist of a size fraction that is below the threshold necessary for upslope transport through saltation. The transitional contact with surrounding material units is consistent with the obscuring effects of a relatively thin mantle smoothing rougher elements and washing out tonal variations of the surface, and thickly mantling local topographic lows, but accumulating insufficiently to bury typical surface relief.

[29] Sufficient in situ and remote sensing observations have been made on a number of these deposits [*Wang et al.*, 2008; *Squyres et al.*, 2008; *Arvidson et al.*, 2010b] to show that many of the deposits have hydration characteristics. Furthermore the small-scale variations in chemistry appear consistent with volumetrically limited, but locally concentrated, availability of altering fluids. This might include gas-solid interactions or liquid-solid interactions associated with fumaroles or low water to rock ratios [*Wang et al.*, 2006]. A viable hypothesis for the later is an episodic climatic change in the presence of water (ice?) resulting in soil-stratified alteration character that is time-intensive [*Arvidson et al.*, 2010a]. This hypothesis implies that these soils are chemically metastable in the current environment, and may have had considerable residence time in their current form.

4.4. Plains Lava (Unit pl)

[30] The contact between the plains and the Columbia Hills is of interest because it represents a major unconformity, a significant gap in recorded geologic time, and significant differences in the environments of emplacement for rocks above and below the unconformity (Figures 2 and 3a). Also, there has been no previous experience with how such contacts between lava flows and preexisting terrains are preserved. Unlike terrestrial contacts, these contacts have been exposed at the surface for potentially several billion years. Before Spirit's traverse across this contact it was unknown whether major contacts were detectable at meter scales due to the potential diffusion of otherwise distinctive lithologies across contacts through the effects of long-term weathering. Spirit's observations show that such contacts are actually well preserved and are sharp boundary contacts much like many terrestrial contacts between lava flows and preexisting terrains.

4.4.1. Orbital Observations

[31] The rolling plains surface in central Gusev crater is Late Hesperian in age [*Cabrol et al.*, 1998; *Kuzmin et al.*, 2000; *Greeley et al.*, 2005], and is a known basaltic lava unit [e.g., *Golombek et al.*, 2006]. Embayment relations along the contact indicate that the plains unit postdates the Columbia Hills. The contact with the Columbia Hills consists of alternating faint light and dark bands or discontinuous ridges a few meters wide parallel to the contact with the hills resulting in a light and dark aureole in plan view. Despite the young relative age from overlapping relations, the plains record more impact craters.

4.4.2. Field Observations

[32] Characteristics of the plains lava surface [*Golombek et al.*, 2006], mineralogy, and chemistry [*Gellert et al.*, 2004; *McSween et al.*, 2006a, 2008; *Morris et al.*, 2004] have been discussed previously. On sol 154 Spirit entered the light and dark aureole along the contact, but few observations were made while crossing it. On sol 155 Spirit was located at the contact with the Columbia Hills (Figure 4a) where the contact between the basaltic lava plains and the Columbia Hills was surprisingly abrupt and easily identifiable in which surface clasts adjacent to the rover to the east were more fragmental and lighter in tone, whereas the rubble to the west was blocky and dark. On the basis of this single observation,
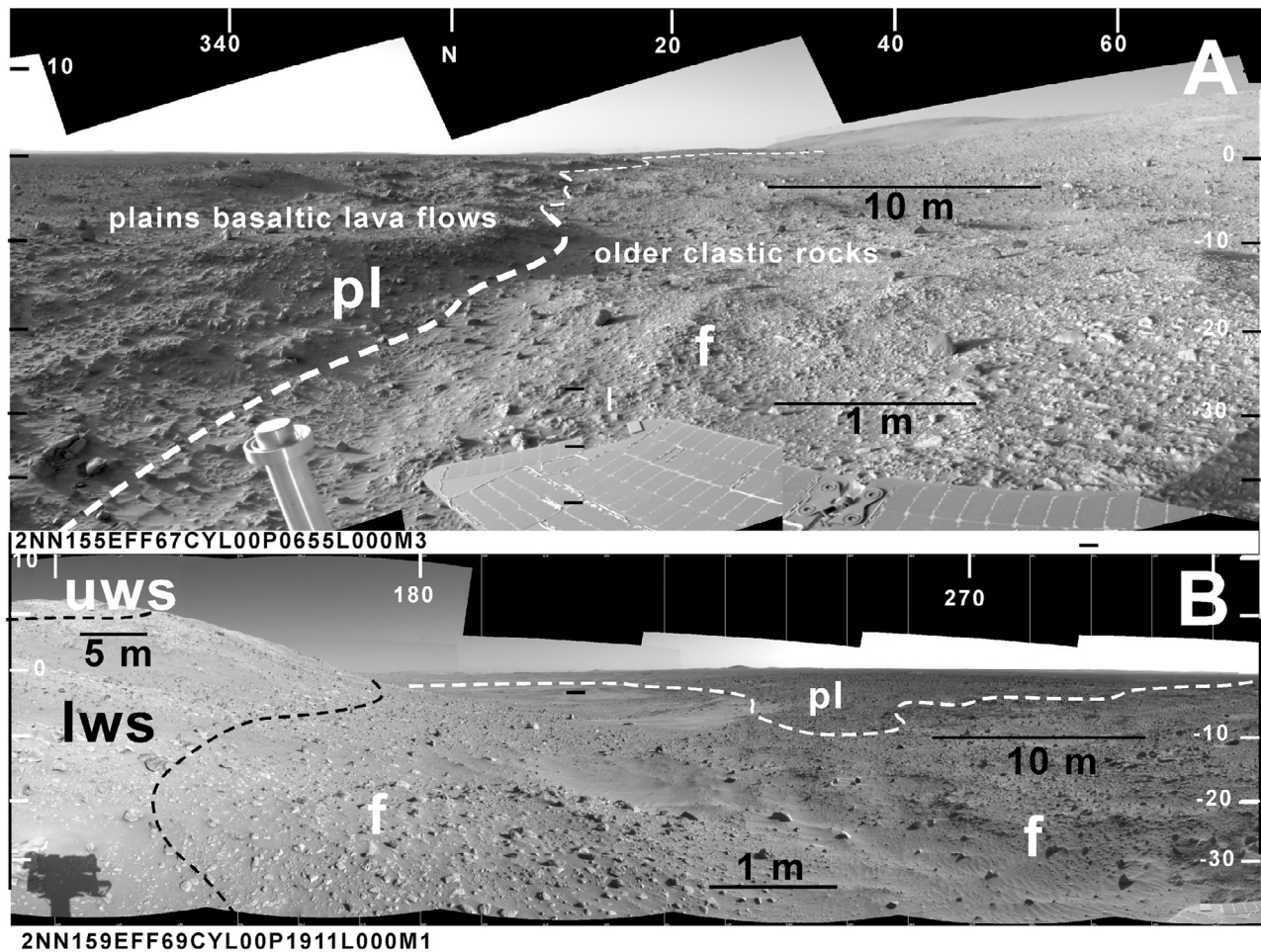
Figure 4. Contact crossed on sol 156 between the lower slopes of West Spur (units lws and f) and the surrounding plains basalt flows (unit pl). (a) View north from a position occupied on sol 155. (b) View south from position occupied on sol 156. The traverse across these two surfaces represents the first crossing of a major geologic unconformity on Mars. The rocks on either side of the contact are of significantly different Martian geologic ages and record the effects of weathering in two entirely different environments. By the time that lava flows were emplaced, the Columbia Hills had already eroded substantially and shed considerable float onto the lower slopes. Observations made on the two sides of this contact physically validate the fundamental geologic interpretation from previous photogeologic studies that earlier Mars was wetter than later Mars. Rover solar panels (0.47 m wide) and shadow of the Pancam assembly (0.40 m wide) provide local scale. Navcam mosaics 2NN155EFF67CYL00P0655L000M3 and 2NN156EFF69CYL00P0665L000M1.

we can estimate that the contact spanned much less than a meter in width. The contact after the sol 156 drive onto the Columbia Hills material is easily traceable remotely in Navcam and Pancam panoramas (Figure 4b), and is locally only slightly obscured by mobile fines and irregularities. Otherwise the contact appears much as any contact between basaltic flows and substrate rocks does on Earth despite the great age of the surface and the obvious gardening of the upper few tens of centimeters by small impact craters.

[33] The plains basalt lavas have Rock Abrasion Tool (RAT) specific grind energies (SGE) [*Bartlett et al.*, 2005] of 50–94 J mm^{-3} [*Arvidson et al.*, 2004; *Squyres et al.*, 2006; *McSween et al.*, 2006a], which is several times harder than any of the measured rocks of the Columbia Hills, but still less than that of typical terrestrial basalts. Since these results are for the outer few millimeters, it is

possible that these values relate to weathered surfaces only and are not representative of the bulk rock. Even the plains basalt measurements are soft by terrestrial standards. For example, the SGE results for Gusev plains lavas appear analogous to the results for well-indurated terrestrial sedimentary rocks [*Arvidson et al.*, 2004].

[34] The Plains lavas (pl), are picritic basalts [*McSween et al.*, 2006b] consisting of abundant olivine megacrysts in a dark sparsely to densely vesicular aphanitic matrix. A variety of observations made on these rocks suggest that sufficient weathering of blocks has occurred to destroy olivine and deposit light-toned veins in cracks since being dislodged and exposed at the surface. These results and the low measured strengths relative to typical terrestrial basalts may mean that the basalts of the Gusev plains have been isochemically altered by reactive fluids more than is otherwise apparent.

[35] Examples of Adirondack class rocks were detected as small isolated clasts on Husband Hill in a few localities where they were likely ballistically emplaced as ejecta from small impacts in the surrounding plains [*Ruff et al.*, 2006; *Grant et al.*, 2006]. One miscellaneous clast, Loofah, was encountered in the float at the base of West Spur a few meters from the plains-hills contact on sol 191 [*Herkenhoff et al.*, 2006]. This sample proved distinctive, as it is one of the few samples of vesicular basalt observed with the Microscopic Imager. The mean vesicle size [*Crumpler and the Athena Science Team*, 2005] of Loofah is approximately 1 mm with a linear semilog size distribution that is, if interpreted as a proxy for volume distribution, indicative of a population inherited from nucleation distributions and initial bubble growth [*Shea et al.*, 2010]. With the exception of a few joined vesicle walls, there is minimal evidence for coalescence. Irregular vesicles are evidence that the lava enclosing them had attained a strength of a few tens of N m^{-2} in order for the irregular shapes to be maintained before solidification [e.g., *Rust et al.*, 2003]. This suggests that the observed vesicles represent the vesicularity at the solidification interface of the lava with slight growth, possibly from exsolution during crystallization at the time the basalt was emplaced. The pervasive sulfate coatings on many of the plains rocks are what we would characterize as sulfate varnishes [*Haskin et al.*, 2005; *McSween et al.*, 2006a] because they are layers on the order of tens to 100 microns thick unconformably coating rock surfaces.

4.4.3. Analysis and Interpretation

[36] The halo visible in orbital images plainsward of the contact with the Columbia Hills is not identifiable from the rover perspective, so its origin remains unclear. Possible origins include: (1) successive onlap of lava sheet flows as on Earth where successive lava sheets encroach and then deflate along a contact with adjoining relief or valley walls; (2) the margins of lava flows may also be areas where the flows thin against topographic relief, solidification was relatively rapid, and distinctive surface textures were developed; (3) interaction of the lavas with a volatile-rich substrate could cause some disruption of lava flows along margins where the hydrostatic balance favors release of gases; and (4) the bands could reflect back wasting of a former steeper buttress formed by the hills and collapse of the lavas during ablation of the underlying Columbia Hills materials.

[37] The surfaces of basalt blocks record other evidence for long-term climatic effects. Several observations imply that fluids have altered the surfaces of basalt and in sufficient amounts since the early disruption of the surface by small impact craters to weather the surface of loose basalt blocks. Varnish-like coatings are common and may be allied in origin with the same intermittent fluid events that altered many loose soils such as the sulfate-rich and crusty soils associated with drifted mobile fines unit (dmf). Because sulfate coatings were measured on ventifact surfaces such as *Mazatzal*, a plains lava block on the rim of Bonneville crater [*Haskin et al.*, 2005], the coatings must have accumulated since the wind abrasion of the block. Similar surface coatings consisting dominantly of sulfates [*Ming et al.*, 2008] are common among the undisturbed surfaces of rocks within the Columbia Hills as well. Several possible mechanism for these coatings were discussed by *Haskin et al.* [2005], including alteration of the surface of the basalt and possible

mechanism analogous to desert vanish on Earth in which rocks exposed to dust and moisture are effectively painted with alteration products from the surrounding environment [*Perry and Adams*, 1978] at scales of a few thousand years. Given the evidence for the intermittent availability of fluids seen elsewhere during Spirit's traverse, the desert varnish model is an important alternative to consider. In the case of Martian sulfate varnishes, only thin films of moisture or melting ice acting on several microns of dust and separated by thousands to millions of years need occur to fix sulfates on the surfaces of rocks. Since Hesperian time (~2 Ga) wetting events need only occur every 100,000 years *or less* to replicate the rates estimated for some terrestrial varnish accumulations during the Quaternary [*Fleisher et al.*, 1999; *Liu and Broecker*, 2000]. This number of wetting cycles (~10^4) is similar to the number of climatic cycles associated with Martian changes in obliquity [*Arvidson et al.*, 2004] assuming cycles of a few tens of thousands of years and an Hesperian age of the surface or slightly younger for the currently exposed surfaces of individual rocks.

[38] Despite the Hesperian age and disturbance of the surface by small impact craters, the lavas forming the plains around the Columbia Hills are still one of the youngest large-scale geologic events in the region. The greater apparent alteration of older rocks in the older hills is primary evidence for significantly more fluids during their formation. Documentation of the different character of rocks on either side of this stratigraphic unconformity validates with in situ studies the general interpretation from several decades of research [e.g., *Carr*, 1996] that substantial changes in the Martian climate have occurred over geologic time.

4.5. Trough Lava (Unit tl)

[39] This is a low surface west of Mitcheltree Ridge and Home Plate, somewhat smoother than plains lavas and lying between the plains lavas (pl) and interior of the Columbia Hills (Figure 2a). Both the high retention of impact craters and a local lobate shaped margin appear more similar to the plains than the rounded shapes of relief within the Columbia Hills. Because it lies in a relatively low-lying area, it appears heavily mantled, most likely by mobile fines, and there are few blocks or small-scale relief characteristics in comparison with the plains lavas (unit pl). The topographic trace of the contact between the plains lava and the Columbia Hills crosses this material, so it appears to be an underlying surface that predates the latest plains lavas sheets. This material was not traversed and there are no relevant observations from the ground. Observations from the summit of Husband Hill and while traversing the west side of Home Plate reveal only extensive mobile fines and ripple bed forms in the low area between the plains basalts (pl) and the Inner Basin.

4.6. Upper Caprock of West Spur (Unit uws)

[40] The upper surface of the West Spur is relatively flat in appearance, yet the flanks are mostly straight slopes (Figures 2 and 3a). This differs from the margins of the Columbia Hills elsewhere where the flanks uniformly slope down into contact with the surrounding plains. So from orbital observations it was unclear whether the West Spur was representative of the Columbia Hills, or something overprinted on the main massif. The abrupt margin of the caprock on West Spur implies that it is now a remnant of a formerly more

widespread surface in which a resistant material had been backwasted on a less resistant substrate long prior to the emplacement of the plains basaltic lavas. The high Cl content is comparable to proposed salient chemical characteristics of a large-scale geologic unit in the eastern equatorial region of Mars.

4.6.1. Orbital Observations

[41] The upper surface of West Spur consists of light-toned slabs and more indurated materials that are apparent in stereo image data as a nearly level caprock on low ridges and hills on the west flank of the Columbia Hills. The margins are relatively abrupt in relief and the caprock material appears to be fragmented and covers the surrounding lower slopes. Small impact craters and residual depressions appear more common than surrounding slopes implying that it represents a local residual surface surrounded by areas of erosion. From the stereo analysis of the apparent disposition of outcrops on the top of the saddle where the eastern end of West Spur abuts Husband Hill, this material appears to overlie the flanks of Husband Hill.

4.6.2. Field Observations

[42] Representative observations on outcrops and rocks of the upper unit of West Spur were made between sol ~210 and sol 312, notably at the outcrop Clovis, but also at the rocks Frio, Ebenezer, Palenque, Uchben, Tetl, and Lutefisk, all along the north upper slope of West Spur. These outcrops and rocks are laminated at scales from a few millimeters to centimeters. On the basis of Navcam ranging data the caprock is estimated to be in excess of 2 m thick. In Microscopic Images and in situ chemical and mineralogical analyses, Clovis and Uchben are poorly sorted fine-grained clastic rocks of basaltic composition [Squyres et al., 2006; Herkenhoff et al., 2008; Wang et al., 2006]. Some isolated larger grains appear matrix supported implying explosively energetic deposition with little sorting. Although this unit occurs as a caprock, clasts and large blocks (Wooly Patch) are pervasive on the slopes of West Spur. Individual rocks (for example, Tetl) have subplanar fabrics or partings but otherwise appear to be part of the same unit. During RAT grinding the tailings from the grinds were voluminous, often settling into the grind cavity indicative of the poor cohesion of the rock mass. Together with the reported RAT grind energy of 4 to 9 J mm^{-3} [Squyres et al., 2006], the overall impression is that this is a poorly consolidated rock of little equivalent compressive strength.

[43] An outcrop imaged but not sampled while departing from West Spur on its east end (Pancam sequence P2431_L357, Turkey Leg, sol 312) (Figure S2) consolidates some stratigraphic inferences made elsewhere along West Spur. The sequence of laminations repeats on one outcrop the fine lamination sequence of the stratigraphic group Tetl, Palenque, and a finely laminated remote sensing target Anasazi. The outcrop also appears to dip conformably with local slope toward the east. The overall impression is that the caprock of West Spur and Clovis class material are the same, constitute a dip slope at this site, and form a conformable drape on an existing relief or have become rotated to follow the relief of an underlying more easily eroded substrate.

[44] Pancam multispectral data for the Clovis-type caprock of West Spur (uws) [Farrand et al., 2008] showed that these rocks had the highest 535 nm band depth of any of the rocks observed by Spirit, an indicator typical of substantial oxidation. That these are altered rocks is consistent with other results. In Miniature Thermal Emission Spectrometer (Min-iTES) deconvolutions [Ruff et al., 2006] of multiple Clovis class rocks on West Spur (unit uws), a substantial component of the rock is an amorphous phase akin to glass (noncrystalline) in addition to a fraction consisting of likely plagioclase and pyroxene. Mössbauer results indicate abundant nanophase iron oxides, goethite, and hematite, and high (0.72) Fe^{3+}/Fe_T [Morris et al., 2008]. The rocks Clovis, Ebenezer, Palenque, Uchben, Tetl, and Lutefisk are fundamentally basaltic in chemistry, bearing abundant normative pyroxene, but are enriched in Cl (1.4 wt %) and Br [Gellert et al., 2006; Ming et al., 2006, 2008], a characteristic sometimes seen in volcanic air fall deposits [Delmelle and Stix, 2000]. A fine ash, which may consist of quenched silica melt comminuted to dust size fractions and subsequently altered, would be consistent with the glassy or dusty character of these rocks from Mini-TES results [Ruff et al., 2006] particularly if the particles were also subsequently weathered. If the upper caprock of West Spur (uws) is a volcanic ash, then the nanophase iron oxides may also represent the results of substantial alteration of the glassy component. We cannot rule out one additional hypothesis for this deposit, namely that the alteration predated the deposition, as might occur with fall out from a distal impact in a previously altered terrain.

[45] Another planar slab, Wooly Patch [Wang et al., 2006], is oriented in conformable repose with the slopes immediately adjacent to the crest of West Spur and appears to have been dropped down the northwest side of West Spur through the gradual retreat of the substrate. Chemical and mineralogical results at Wooly Patch were comparable to the results of subsequent analysis at Clovis [Squyres et al., 2006] although it may be distinguished from other Clovis class rocks by phyllosilicates [Wang et al., 2006]. Regardless of minor differences in chemical character, the outcrop habit and hand specimen petrography of Wooly patch and Clovis are similar. They are probably fragments of outcrops of the same caprock lithology. Additional analyses of the rocks Ebenezer, Tetl, Palenque, Uchben, and Lutefisk bear more similarities to this Wooly Patch and Clovis caprock lithology than to the Hanks Hollow rocks, so they too are displaced caprock fragments despite being down the local slope from the crest of West Spur.

4.6.3. Analysis and Interpretation

[46] The scarp-like margins in orbital data combined with the disparity in crater occurrences between the surface and its margins imply that this material was formerly more extensive and has been reduced in area by erosion of its margins. Because it forms a distinct rock layer capping ridges, it probably rests on a more easily eroded substrate the gradual back wasting of which has cantilevered off chunks of the overlying resistant unit leaving sharp outcrop margins.

[47] From rover-based remote observations, throughout most of the West Spur this unit forms a more competent layer at least several tens of centimeters thick and occupying the crests of ridges. There has been substantial back wasting of the underlying less resistant materials that form the lower slopes of West Spur, but the clasts of fragmented caprock material are persistent and now cover the back wasted slopes. Based in physical, petrographic, chemical, and mineralogical assessment of representative examples, this unit appears to be
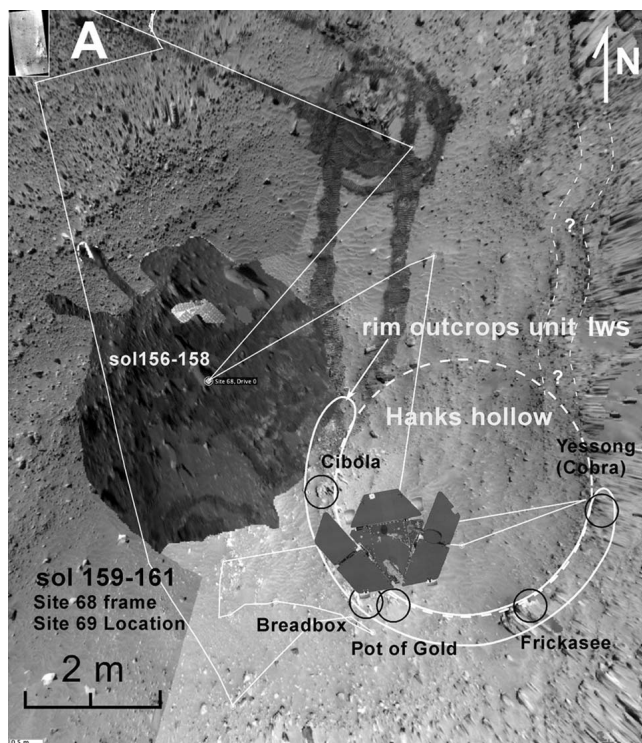
Figure 5. (a) Overhead image composite (in "Maestro Map") of Hanks Hollow positions from Navcam mosaics taken from sols 156 through 161. Exposures here are typical of the outcrop exposures that frequently exist on the floors and rims of small impact craters amid otherwise substantial float. (b) (top) Characteristic textures of rocks exposed in the slopes of West Spur (unit lws). (middle) Pot-of-Gold and Bread Box, and (bottom) Cibola all occur along the exposed rim of a small depression (Hanks Hollow), possibly a small impact crater. Induration along joints followed by ablation results in many examples of fins and angular rocks with casings. All of these rocks appear to be clastic materials that are relatively poorly indurated compared with rocks farther upslope (unit uws) and capping West Spur.

a distal pyroclastic ash or impactite, either altered postdeposition or composed of altered material redistributed as impactite. It appears to be draped on preexisting relief because the apparent dip of bedding surfaces in some of the larger outcrops is roughly conformable to some local slopes.

[48] The chlorine enrichment of Clovis is notable given that *Keller et al.* [2007] found the equatorial area immediately north of Gusev crater to be enriched in chlorine in an area identified [*Newsom et al.*, 2007] as restricted to the Medusae Fossae Formation, a broad equatorial region of thick layered mantling deposits [*Mandt et al.*, 2008; *Kerber and Head*, 2010]. The average value of 1.4 wt% as determined from APXS measurements in Clovis class rocks [*Ming et al.*, 2006] falls within the 1 wt% Cl enrichment contour of *Keller et al.* [2007]. The proximity of Gusev crater to the region over which Medusae Fossae Formation occurs and the chlorine anomaly make the Clovis class materials a viable candidate as a distal outlier of the Medusae Fossae Formation.

4.7. Lower Slopes of West Spur (Unit lws)

[49] The slopes of West Spur were poorly exposed in both orbital and in situ observations, being mostly armored with clasts of the overlying caprock in both data sets (Figures 2 and 3a). The only in situ observations were near the base of the slopes and it is inferred from those observations that the slopes developed in materials that are relatively friable and poorly indurated. Even so, some fracture networks may have carried fluid in volumes great enough to result in some networks of case hardened joint blocks.

4.7.1. Orbital Observations

[50] The slopes around the upper caprock unit of West Spur are distinguished mainly by downslope streaks and chutes, and speckled appearance in orbital images. The latter appears to be rocky debris grading from a meter to dimensions below the resolution of HiRISE image data. It is clear that the caprock unit is resting on an easily eroded substrate, but there are no obvious exposures of that substrate material.

4.7.2. Field Observations

[51] Observations on the lower West Spur unit were made between sol 156 and ~sol 191. Representative rocks include Pot-of-Gold and Breadbox in the outcrop area broadly known as Hanks Hollow, a shallow depression, approximately 4 m across, floored with fines and rimmed with outcrops and float (Figure 5). It is located approximately 10 m from the plains contact at the foot of slopes leading up to a northward projecting thumb of the main east-west oriented mass of West Spur proper. Outcrops positioned in a narrow zone around the rim of the depression appear to be exposures on the former margins of a shallow impact crater now deflated and truncated by wind erosion. The rocks around Hanks Hollow are suborthogonal shaped blocks with smooth, fin-like coatings or with cases enclosing a more granular or cloddy interior. The interiors consist of wind-fluted rounded clasts [*Squyres et al.*, 2006]. Faint subparallel bands visible in overhead views of slopes adjacent to the Hanks Hollow site could be the trace of horizontal layers or lamination in nearby slopes, a characteristic that is repeated in other exposures throughout the Columbia Hills. The known thickness is at least equal to the vertical relief between Hanks Hollow and the base of the West Spur caprock, or about 8 m.

[52] Pot-of-Gold, the first rock investigated within the Columbia Hills [*Squyres et al.*, 2006], is a loosely consolidated clastic rock, bearing uniformly oriented stalk-like textures, probably originating from wind abrasion acting on resistant aggregates, lapilli, or small concretion-like areas set within a more uniform and less cohesive rock mass. The poor consolidation of these outcrops is illustrated by the rock Breadbox (Figure 5b) where a network of vein-like planar structures form open box works consisting of orthogonal networks of vertical fins enclosing poorly consolidated granular materials. Breadbox and Cibola (Figure 5b) are striking examples of case hardening, a characteristic of weathered rock masses in which the more resistant shells on exposed rocks encase more eroded interiors. It is one of the strongest morphological pieces of evidence encountered that fluids were once pervasive in the Columbia Hills [*Farmer*, 2005].

[53] Other rocks nearby with unusual textures are perched on the east rim of Hanks Hollow. Frichasee and Frack on the west rim (Figure 6a) have unusual agglomerated textures, are unlike any other local rocks, and may be exotic. The
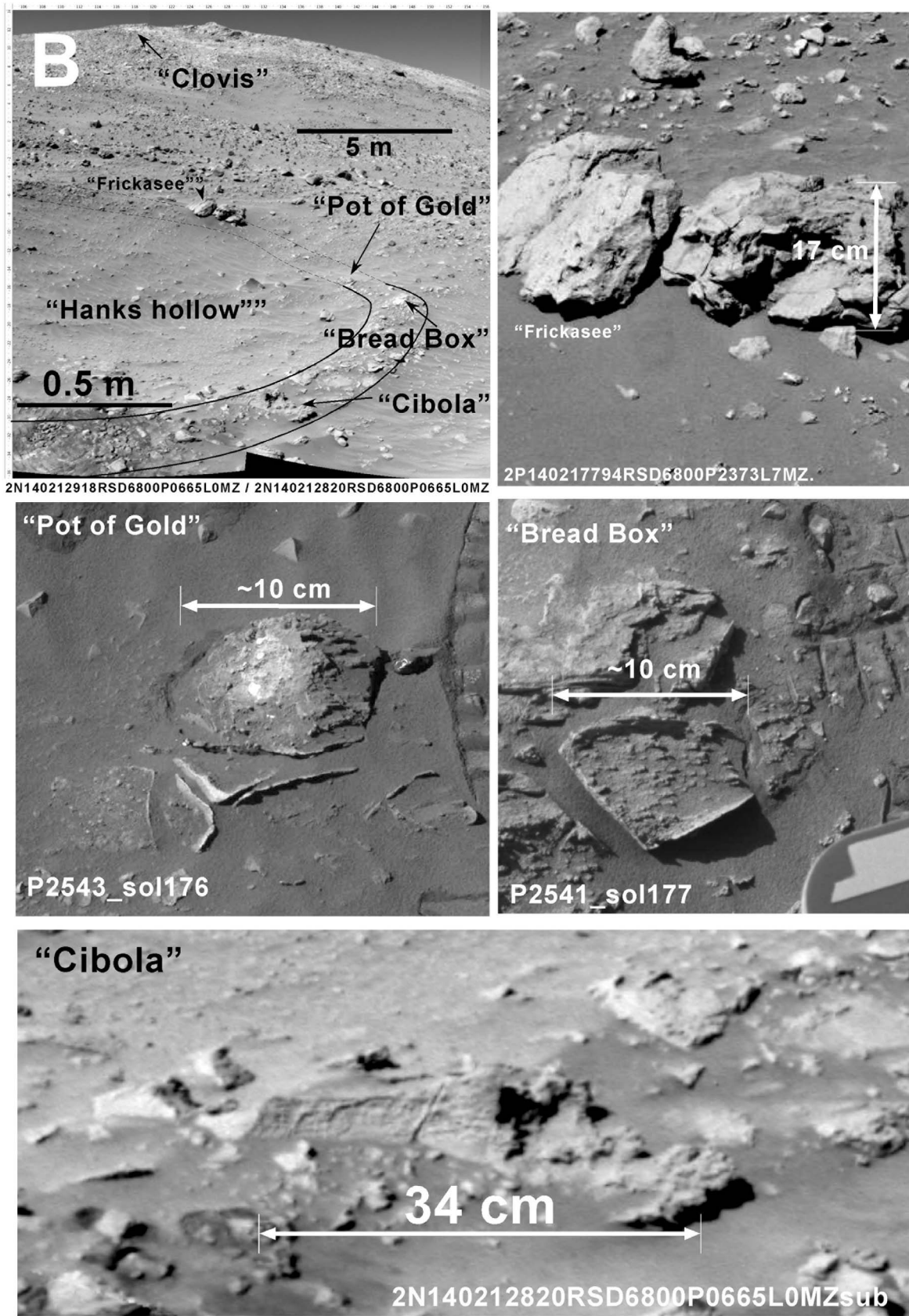
Figure 5. (continued)
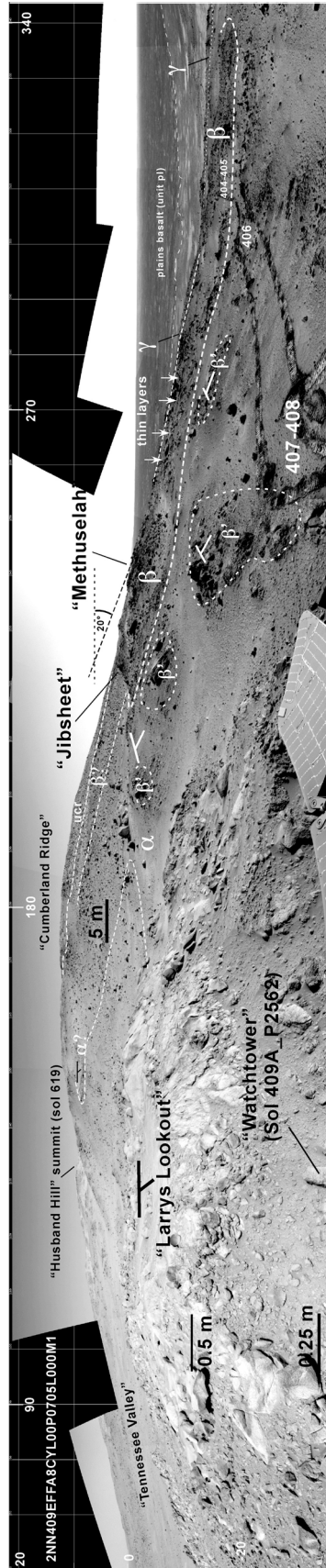
Figure 6. View from Larrys Lookout across the lower Cumberland Ridge unit (lcr). An unusual knob and trough relief throughout this region correlates with dipping layers of a lapilli tuff. The trace shown as a dashed line in the local landscape are the ledge-forming layers α, β, and γ identified in Figure 7c. Individual knobs (β) appear to be residual remnants of layered member β resulting from local ablation and back wasting of member β on α. The ability to identify this level of outcrop detail illustrates the future potential for detailed field stratigraphic studies on Mars. Mapped using Navcam mosaics 2NN409EFFA8CYL00P0705L000M1 and 2NN409EFFA8CYL00P0706R000M1 as stereo pairs.

nearby rock Yessong, also known as the Cobra (NASA image PIA06286), is an example, among many in the Columbia Hills, of the extremely delicate way in which ablation by wind has sculpted unusual shapes, in this case leaving behind a thin delicate stalk supporting a knob of rock.

[54] Chemically, the rocks of Hanks Hollow contained higher Ca, S, and Ni but significantly less Cl and Br than the overlying caprock unit of West Spur [*Ming et al.*, 2006]. The high hematite content of Pot-of-Gold [*Morris et al.*, 2006, 2008] is comparable only to a few other samples in the Columbia Hills, such as the valley floor rocks farther south (lower Home Plate unit (B) near Low Ridge (Halley, Grahamland) and samples at the outcrops Jibsheet and Larrys Outcrop within the lower Cumberland Ridge unit (lcr) on Husband Hill. All of these rocks are notable for their high hematite content, consistent with other evidence for alteration. Due to the limitations of time and the relatively small scale of the rocks around the rim of Hanks Hollow, no comparative analyses of the shells versus interiors of these rocks were possible.

4.7.3. Analysis and Interpretation

[55] Although this unit is not widely exposed in outcrop, the fact that the overlying caprock unit of West Spur appears from HiRISE images to have been back wasted along steep margins implies that the lower slopes of West Spur consist of a less indurated and more easily eroded rock. This interpretation is consistent with rover based observations because few exposures of the slope former were encountered. The lower West Spur materials (lws) appear to disintegrated during erosion and fragmented into material fines rather than rocks. Clasts of the caprock of West Spur (uws) generally a few centimeters in size occurring as slope debris almost completely obscure the underlying slopes, a characteristic of many caprock settings in arid landscapes on Earth where there is a large difference between the competence of the caprock and substrate [e.g., *Easterbrook*, 1999]. Even though the large block Wooly Patch (between sols 192–199) occurs in the middle of this unit, it was found to be Clovis class in both mineralogical and physical characteristics and we suggest that it is instead a block displaced downslope from the overlying caprock unit (uws). Whatever the protolith of this slope forming unit, the few in situ observations imply that it has been substantially altered by fluids and that some of the fluid were transported along a network of joints ultimately responsible for the box-like character of rocks such as Breadbox.

4.8. Upper Cumberland Ridge Materials (Unit ucr)

[56] From orbital images this surface appears to be the relatively bright ejecta surrounding a relatively fresh crater occupying the crest of the Cumberland Ridge, the west rim of a north-south valley on the north flank of Husband Hill (Tennessee Valley) (Figures 2 and 3b). We suspect that this unit is the origin of the blocky materials encountered on the northwest flank of Husband Hill during initial ascent. If so, it appears relatively unaltered compared with most rocks and may be derived from deeper unweathered materials excavated by this small impact along the crest of Cumberland Ridge.

4.8.1. Orbital Observations

[57] This surface consists of light toned streaks and large associated blocks occurring mostly along the crest of Cumberland Ridge, a northwest-southeast oriented rim on northwest Husband Hill. It is largely restricted in area as a mottled surface surrounding a relatively fresh impact crater along the crest of Cumberland Ridge. There is an overall trough and ridge aspect somewhat similar to that seen in the underlying unit (Northwest Cumberland Ridge outcrops, lcr). On the basis of bright streamlines in the lower nearby slopes it appears that some of this light and blocky material has moved directly downslope from the upper Cumberland Ridge unit (ucr), and likely contribute to unit dcr farther downslope.

4.8.2. Field Observations

[58] Where this unit was crossed on the northwest side of Husband Hill between sols 514 and 519 it appears as a field of detached light-toned subangular blocks and small clasts contributing to a rocky general float. In situ analyses of the materials common to this unit were done on the representative float rocks, Wishstone and Champagn*e*, both analyzed farther downslope in the bright unconformable deposits of Cumberland Ridge (unit dcr). On the basis of chemical, spectral, and mineralogical data, Wishstone class [*Squyres et al.*, 2006] rocks are unusual and appear relatively unaltered. Yet some alteration may be present in order to explain unusual elemental abundances, an example being the high phosphorus (see section 4.16). The morphology and spectral character of much of the rocky debris on the northwest flank of Husband Hill shed from the Cumberland Ridge crest are similar to the isolated rocks Wishstone and Champagne. This is supported by Mini-TES spectra of rocks of similar texture that have the plagioclase-rich spectral features comparable to that of Wishstone [*Ruff et al.*, 2006]. Wishstone and Champagne are assumed here to be representative of this unit and are described in more detail in association with the geologic unit where they were encountered (section 4.16, bright unconformable deposits of Cumberland Ridge, unit dcr). Where it occurs on Cumberland Ridge, it appears to be a surficial, thin mantle of rocky material with no substantial thickness.

4.8.3. Analysis and Interpretation

[59] The position of this bright unit downslope from a relatively fresh impact crater was the basis for the hypothesis that this is relatively young, blocky debris from the local ejecta of a ridge crest impact crater. Traverse across this surface did not disprove this hypothesis, and the observation of abundant angular blocks appears consistent with this hypothesis. Unexpected, however, was the fact that the blocks appear to be a rock type not seen elsewhere, and one of the least altered rocks encountered (Wishstone class rocks, see section 4.16). The latter is consistent with these being excavated from deeper than most of the rocks encountered and potentially stratigraphically older as well.

[60] Wishstone class float is common on the west side of Husband Hill, so an excavating impact could be responsible for its widespread distribution and it deep, relatively unaltered origin. The occurrence of this rock class as rind-coated polygonal blocks is suggestive of deep massive rock units bearing abundant joints along which alteration has occurred in restricted volumes adjoining fractures. Projection of outcrop traces of the nearby lower Cumberland Ridge unit (lcr) toward the upper slopes of *Tennessee Valley* shows that the target material is likely to be stratigraphically lower than even the Northwest Cumberland Ridge outcrops (unit lcr, see

below). This finding is further consistent with the presence of clasts of Wishstone class materials in the Voltaire outcrop (unit wh) [*Arvidson et al.*, 2008; *Ming et al.*, 2008] determined to be stratigraphically the lowest demonstrable outcrop in the Columbia Hills. In order for Wishstone class clasts to be present in this unit, the source outcrops for Wishstone class rocks must be considerably lower. Given the source of these rocks is the substrate near the center of the antiformal arrangement of stratigraphy [*McCoy et al.*, 2008] in Husband Hill, it is possible that it has been relatively isolated from any infiltrating fluids over Martian geologic time compared with rocks down gradient.

4.9. Northwest Cumberland Ridge Outcrops (Unit lcr)

[61] Prior to traverse through the area covered by this unit there was little evidence to indicate that the prominent relief features in this area, such as the knob on the west rim of Tennessee Valley, informally named Larrys Lookout, were anything other than large slumps or blocks of material from the main massif of Husband Hill (Figures 2 and 3b). However, these were some of the first clearly layered materials encountered by Spirit. Observations during the traverse of multiple layered outcrops dipping downslope in this area were unanticipated. Dips greater than the hillslope imply that down section is upslope. All of these rocks appear to be altered lapilli tuffs, but might also include air fall impactites.

4.9.1. Orbital Observations

[62] This is one of the few areas within the Columbia Hills that has a surface relief at meter scales consistent with exposed bedrock instead of mantling by fines and loose slope debris. It is limited to a small area on the upper west rim of a broad depression on the north flank of Husband Hill informally named the Tennessee Valley. The relief on this unit consists of a poorly integrated series of troughs, ridges and outcrop knobs. The outcrops are surrounded by mobile fines materials (dmf) and are onlapped on the southwest by unconformable bright slope materials (ucr and dcr).

4.9.2. Field Observations

[63] Several of the important outcrops visited on Husband Hill occur within this photogeologic unit traversed from sols 381 to 513, including Peace, Alligator, Larrys Lookout, Methuselah, Jibsheet, and Larrys Outcrop (Table 1). These outcrops comprise a range of rock classes as identified by *Squyres et al.* [2006] but occur within a distinctive surface textural unit as mapped in HiRISE image data so they are lumped together here. One important rock examined at Larrys Lookout, Watchtower, defines an important class of material seen at other outcrops.

[64] From the rover perspective all of these outcrop exposures lie eastward of a topographic divide between the float-covered outer slopes of Husband Hill and the bedrock-cut surface that forms a general slope leading into the Tennessee Valley where there is an abrupt change in outcrop style from a surface of scattered Wishstone type rocks in a matrix of mobile fines on the west to multiple isolated pedestals of disaggregated rock of darker tone on the east. These form roughly concordant topped ridges of a more indurated material standing as divides between a sinuous pattern of troughs filled with fines (Figure 6).

[65] The outcrop Alligator (Figure S3) examined on sols 381–385 is a light-toned tabular outcrop segmented with suborthogonal fractures or joints. The dip (32°NW) of slabs along the facing edge is greater than other exposures in the Northwest Cumberland Ridge unit (lcr), but occurs in an area where the surface abruptly increases slope, so undermining followed by tilting and detachment of the exposure from the substrate is likely as suggested by *McCoy et al.* [2008]. Petrographically, the MI target Jambalaya is a poorly sorted, fined-grained and cohesive clastic rock bearing subrounded dark lithic fragments.

[66] Downslope from the Alligator outcrop, the outcrop Peace consists of sand-sized grains based on MI mosaics of a RAT abraded surface, a marked contrast to the lapilli-like grains of Jibsheet and Larrys Outcrop. Peace and the nearby outcrop Alligator are fine-grained clastic rocks consisting of sand-sized grains loosely consolidated and have a porous texture in MI data [*Herkenhoff et al.*, 2006]. RAT specific grind energy [*Squyres et al.*, 2006] also indicates that it is a poorly consolidated rock. Peace was found to contain higher Mg and S [*Gellert et al.*, 2006] in accord with Mössbauer results indicating mostly olivine, pyroxene, and magnetite. Fe^{3+}/Fe_T (0.35) [*Morris et al.*, 2008] approaches that of some plains basalt analyses and is comparable to Wishstone class rocks (section 4.16). These results are interpreted to mean that Peace is less altered than most rocks in the Columbia Hills. The higher S in Peace is interpreted as a result of cementation of a relatively unaltered basaltic sand by sulfates [*Squyres et al.*, 2006], and in this respect, Peace bears some similarity to sulfate-rich soils, although not nearly as Fe-enriched. The unusual sulfate-rich soils of Paso Robles [*Yen et al.*, 2008], lies within the area of this unit (sol 399–404, 424–430) although there is nothing in particular to suggest that the two are related since sulfate rich soils occur in a variety of differing terrains and geologic units along the traverse and appear to be mostly associated with local relief characteristics [*Wang et al.*, 2008]. No bedding planes are present in the faces of outcrop exposures, but a subplanar megascopic lamination pervades the outcrops at decimeter (hand specimen) scale yielding strikes and dips of N45°E and 20° (Figure S4).

[67] On the basis of the measure dip and the distance from the bottom of Larrys outcrop to the top of the Alligator outcrop, the estimated thickness is approximately 23 m. Similar subtle lamination occurs in terrestrial lapilli tuffs, and are attributed to rapid deposition of pyroclasts in which vertical (time variable) clast sorting is minor. These are characteristics of violent deposition as might occur from either a volcanic eruption or impact ejecta [*Squyres et al.*, 2006]. Similar MI textures occur in the summit outcrop Hillary and the Comanche Spur outcrop targets Horseback and Palomino.

[68] Clast litter in this unit attained the highest sphericity of any site along the traverse [*Yingst et al.*, 2008]. While transport and emplacement could be a factor, we note simply that the outcrops in this unit tend to consist of more gravel size (>2 mm) particles than other outcrops in the Columbia Hills, and the outcrops tend to disaggregate into more or less equant fragments. The target Davis in the outcrop Jibsheet consists of uniformly packed grains or clasts a few millimeters in size comparable in texture to typical lapilli tuffs. This coarse, subrounded granularity at millimeter scales is also apparent in outcrops from megascopic views (Figure S5).

[69] Mineralogical and chemical analyses include some of the more hematite-rich, highest 535 nm band depth as determined by Pancam, and highest Fe^{3+}/Fe_T ratios as determined by Mössbauer encountered. However, Fe^{3+}/Fe_T ratios vary substantial from outcrop to outcrop implying significant variations in alteration are present. Chemical discriminants used to infer different rock classes [*Squyres et al.*, 2006] separate several of the outcrops into distinct rocks that we have lumped in this unit. Wishstone and Watchtower are similar in elemental details [*Ming et al.*, 2008]. But Watchtower has abundant hematite and nanophase iron oxides, as well as elevated Fe^{3+}/Fe_T (0.74) [*Morris et al.*, 2008] and high 535 nm band depth [*Farrand et al.*, 2008], consistent with Watchtower class rocks being a weathered Wishstone-type protolith. Significantly, low rock-water ratios are applicable to avoid leaching of soluble components, a model supporting slow infiltration of small amounts of sulfate enriched water and downward collection in fractures.

[70] Min-iTES results demonstrate that Watchtower class rocks contain less than half the plagioclase of Wishstone class rocks, but more glass phases and sulfates. Pancam multispectral data [*Farrand et al.*, 2008], shows that Watchtower has one of the most pronounced 904 nm band depth features, a trait shared with the *Seminole* outcrop on the other side of Husband Hill.

4.9.3. Analysis and Interpretation

[71] The trough-and-ridge surface texture of this unit (lcr) may result from trough-like chutes developed in association with debris slides in the adjoining surficial debris unit (dcr) just to the west. Alternatively, the ridges may be exposures of dipping bedding planes. We can construct structural contours [e.g., *Ragan*, 2009] that enable prediction of the trace of clastic ledge-forming outcrops in the surrounding landscape (Figure 7). When compared with the observed trace of ridges, the results support the latter hypothesis. Using a strike (N45°E) and dip (20°) of the outcrops at Larrys Lookout determined by *McCoy et al.* [2008] from analysis of rover acquired stereo image pairs representative of the known outcrop exposures at Jib Sheet, Larrys Outcrop, and the Methuselah outcrop, together with the regional topography from Navcam panorama-based digital elevation models, several of the sinuous ridges and chutes in the local terrain follow the predicted trace of these outcrops (Figure 7). The sinuous ridges and ledges in this part of Husband Hill are predicted to be the trace of these outcrops exposed in the slopes through erosion and ablation of the margins of the Tennessee Valley. The whole area of this unit therefore represents one of the more significant areas of substrate exposure on a hillside that is otherwise buried with thick debris. It offers some insight into the overall structure of the layered units visited along the traverse through the hills in general.

[72] If the Alligator outcrop is in conformable contact with the other layers in this unit, then based on the analysis of structural contours, it is stratigraphically slightly higher than the Methuselah–Larrys Lookout outcrops upslope. If it is in unconformable contact with the layers upslope, then it could be draped on an erosional unconformity cut into the Methuselah–Jib Sheet–Larrys Lookout sequence. From these assessments and the structural analysis (Figure 7) a proposed stratigraphic sequence for the rocks examines

within this unit (bottom to top) would be Wishstone, the target Pequod on the feature Paros (at Larrys Outcrop), Watchtower (Larrys Lookout), the outcrop Jibsheet, the outcrop Methuselah (a few meters west of Jibsheet), Peace, and Alligator.

[73] On the basis of in situ analyses, we would interpret this unit as a layered sequence of clastic materials of basaltic composition, mostly air fall (ash or impactite), draped conformably over slopes of an unknown Columbia Hills precursor hill form and substrate. The poor lamination or bedding form of the outcrops are interpreted to be characteristics derived from rapid and emplacement of voluminous and variably comminuted materials. A strong candidate for the substrate is the Wishstone class source material that is abundant in the float but is otherwise unexposed. The alteration line of descent from Wishstone to Watchtower class rocks would be consistent with a stack of massive air fall pyroclastic or impactite materials altered differently according to the differing exposure to fluids, the variable alteration in turn dependent on differences in rock competence and fracture spacing, compaction, and intergranular porosity with depth.

4.10. Columbia Hills Summit Outcrops (Unit ch)

[74] Aside from scattered blocks the summit region of Husband Hill appears smooth at 10 cm scales and relatively structureless (Figures 2 and 3d). Sufficient rock mass at or near the summit must be present in order to supply the abundance of blocky debris immediately downslope from the summit and in order to support relatively steep scarps along the Tennessee Valley side of the summit. Large blocks of laminated lapilli tuff at the summit bear similarity to the outcrops on the northwest side of Husband Hill (unit lcr). These may be correlated units as they also appear to occupy stratigraphically similar positions besides being mineralogically and chemically similar.

4.10.1. Orbital Observations

[75] Exposures at or near the summit of Husband Hill consist of rolling relief at meter scales, scattered blocks tens of centimeters to one-half meter in size, abundant smooth debris mantles, and numerous circular depressions from likely degraded small impact craters. The rugged and cratered surface bears some resemblance to the surface of West Spur and Haskin Ridge, although there is a greater abundance of loose debris between exposures compared with those two areas. The contact between outcrops and the surrounding float and debris grades downslope into loose debris and float. The principal difference between the two is the abundance of blocks and the change from relief at meter scale to a binary roughness consisting of blocks and smooth-interblock-type surfaces. Although outcrops of the substrate are not apparent, it consists of a lithology that is indurated well enough to support steep scarps like that forming the south boundary of the Tennessee Valley just north of the summit. It also appears competent enough to yield on fragmentation an excess of large blocks that litter the slopes of Husband Hill around the summit region.

4.10.2. Field Observations

[76] This map unit was traversed from sols 581 to 588 and 603 to 654. Only a few large rock exposures are present along the traverse, one of which was the summit outcrop Hillary, examined on sol 625 to 632 and the other the outcrop
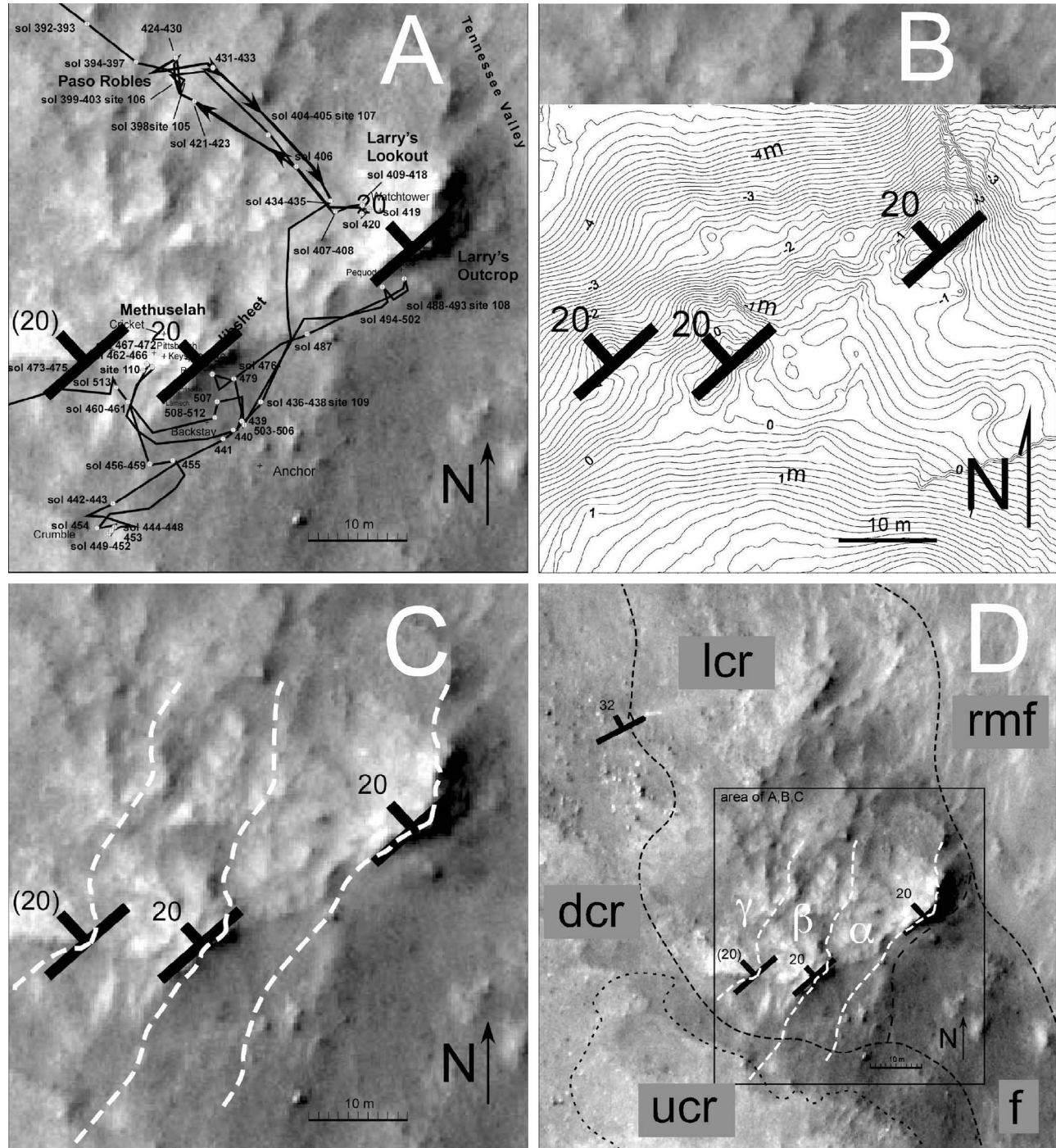
Figure 7. Simple structural analysis of layers dipping northwest at Larrys Lookout. (a) Spirit positions from sol 392 through sol 513 in the vicinity of Larrys Lookout. (b) A ~10 cm contour map of the area shown in Figure 7a derived from Navcam stereo DEM data (S. Thompson, personal communication, 2006). Strike and dip determinations for the local outcrop are from *McCoy et al.* [2008]. (c) Predicted outcrop trace in the local landscape for outcrops exposed at "α, β, γ" as shown in Figure 7b and based on the strike and dip shown. (d) Expanded overhead view of the area showing that the sinuous ridge forms are of the scale and sinuosity predicted for outcrop ledges dipping to the northwest. the interpretation is that the ridges in this slope are outcrop exposures in which the ridges represent slightly more indurated layers now exposed by general erosion of the northwest slope of Husband Hill. This interpretation is consistent with the cross-slope view of outcrops shown in Figure 6.
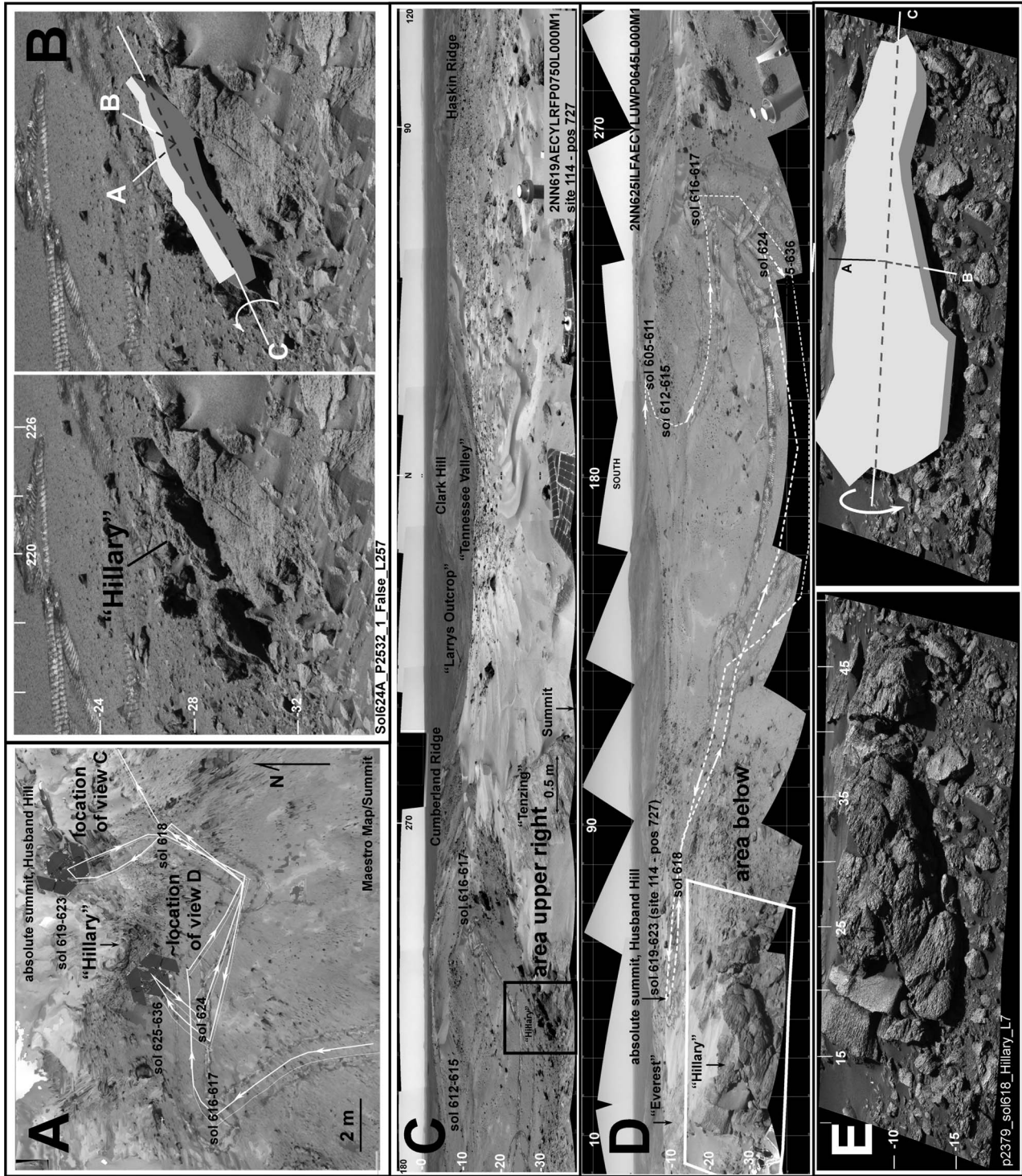
Figure 8

Kansas (sol 642–648). The angular faces of most rocks in the summit area are relatively massive and apparently fine grained as there is little to distinguish them in panoramas. Where apparent planar fabrics occur, they dip southeast [*McCoy et al.*, 2008]. However, many of the summit rocks are also characterized by linear patterns and flutes that are common on ventifacts.

[77] The rock Hillary is a rotated and slumped fragment (Figure 8) forming a west facing ledge a few meters west of the absolute summit. The slab has been undercut, presumably by the prevailing north northwesterly winds that stream across the summit, and has subsequently rotated westward onto the undercut local slope. Hillary illustrates a situation (common in many HiRISE images of resistant laminated outcrops elsewhere on Mars) in which large slabs or blocks become detached from bedrock exposures through initial undercutting, and are then followed by collapse and rotation into slope tiles. In situ observations of the rock between sols 625 and 632 on the accessible, west facing ventifact surface are on a bedding plane, as were most of the rock surfaces examined by Spirit. Tenzing, a rock at the topographic summit, was examined via remote sensing between sols 619 and 623 and appears to be the same rock type. The only additional outcrop successfully examined within the Columbia Hills Summit unit (ch) was the outcrop Kansas located within a shallow depression on the east flank of Husband Hill. Kansas is a flat surface with no megascopic layered structure, so it too is likely a bedding plane if it is layered at all.

[78] In situ observations of the rock Hillary (sols 625–632) included MI data bearing similarity to MI textures in the lower Cumberland Ridge unit (lcr), notably the MI mosaic (Keystone) on the Methuselah outcrop (Figure 9). Since the MI results were acquired on a RAT brushed surface, linear textures could also result from wind abrasion. However, the slab-like character of the outcrop, and its orientation before rotation are consistent with the linear textures arising from etched relief of aligned grains in a layered clastic rock.

[79] In addition to bearing many of the same subtle planar traces and tabular breakage characteristics as seen in the lower Cumberland Ridge unit (lcr), the summit outcrops share mineralogical and chemical similarities with Watchtower class rocks from lower Cumberland Ridge unit (lcr). Both the outcrops Hillary and Kansas are similar to Watchtower class (lower Cumberland Ridge (lcr) in Mössbauer and APXS results [*Morris et al.*, 2008; *Ming et al.*, 2008]. Abundant hematite, elevated Fe^{3+}/Fe_T (~0.6), and substantial nanophase iron oxides are all characteristics of these two outcrops and the outcrops in the Methuselah–Larrys Lookout (Watchtower) area. Likewise Pancam mul-

tispectral observations on the Cumberland Ridge and the Summit (ch) rocks have intermediate 904 nm band depth characteristics, values similar to those in the outcrop Jibsheet (unit lcr). Outcrop and hand specimen scale morphology is largely in agreement with this chemical and spectral similarity between the summit rocks and rocks of Larrys Lookout [*Arvidson et al.*, 2008].

4.10.3. Analysis and Interpretation

[80] Lying along the summit of Husband Hill and unprotected by a thick blanket of float, as are other parts of the hills, the otherwise bland appearance of the summit area could be a result of it being extensively rubblized and ablated as a results of the long-term effects of small impact craters. Some blocks are as large as several tens of centimeters in size suggesting that outcrops are near the surface even if they are not clearly exposed, and that the surface results mostly from rubblized outcrop.

[81] The summit outcrops of Husband Hill and the materials that are exposed in the northwest flank at the outcrops Methuselah and Larrys Lookout are correlatable rock units based on similar stratigraphic position in the overall Columbia Hills stratigraphic stack and similar mineralogical and chemical constituents. The protolith appears to be ash or impactite draped conformally over slopes of a Columbia Hills substrate. The substrate consists in part of the western Husband Hill unit (unit wh) and that in turn overlies the source substrate for Wishstone class materials. We suspect that the Summit unit (ch) together with the alternating large-scale outcrop laminations of the northwest Husband Hill unit (lcr) and other crudely bedded outcrops of approximately similar stratigraphic position on Husband Hill are part of a sequence of explosively emplaced units that were draped over an initial hill relief feature.

4.11. Western Husband Hill (Unit wh)

[82] This exposure on the upper western flanks of Husband Hill is a good example of a material that is not obvious until seen in outcrop and noted for its unusual properties of petrography and stratigraphic position (Figures 2 and 3c). But once identified in outcrop, it can be correlated relatively easily with distinctive orbital image characteristics. This shows the value of both orbital and surface data in defining important geologic units, since neither data set alone assures identification of a material or its lateral extent. The overall conclusion is that the western Husband Hill (wh) unit is a coarse impactite that postdates early Wishstone class materials of the Columbia Hills, but predates the other units examined on the west side of Husband Hill.

4.11.1. Orbital Observations

[83] The upper west slopes of Husband Hill are characterized by a broad depression or shallow valley together

---

Figure 8. (a) The relative positions of Spirit as determined in Maestro Map from convergence of targets in multiple overhead Navcam mosaics. (b) (left) The summit outcrop and rock feature Hillary as viewed from a position on the summit in Pancam mosaic sol 624 sequence 2532 and (right) schematic depiction. (c) Navcam mosaic 2NN619AECYLRFP0750L000M1 from the summit. (d) Navcam mosaic 2NN625ILFAECYLUWP0645L000M1 and (e) Pancam sol 618 predrive mosaic sequence p2379) where in situ observations were made of the rock Hillary between sols 625 and 636. In Figure 8b the view is directed west from on top of the summit outcrop. The rock Hillary has cantilevered eastward and downward from this outcrop. The schematic version of the slab illustrates the slab rotation. (e) (left) The view looking east at the rotated top of the Hillary outcrop slab. (right) The geometry illustrated schematically.
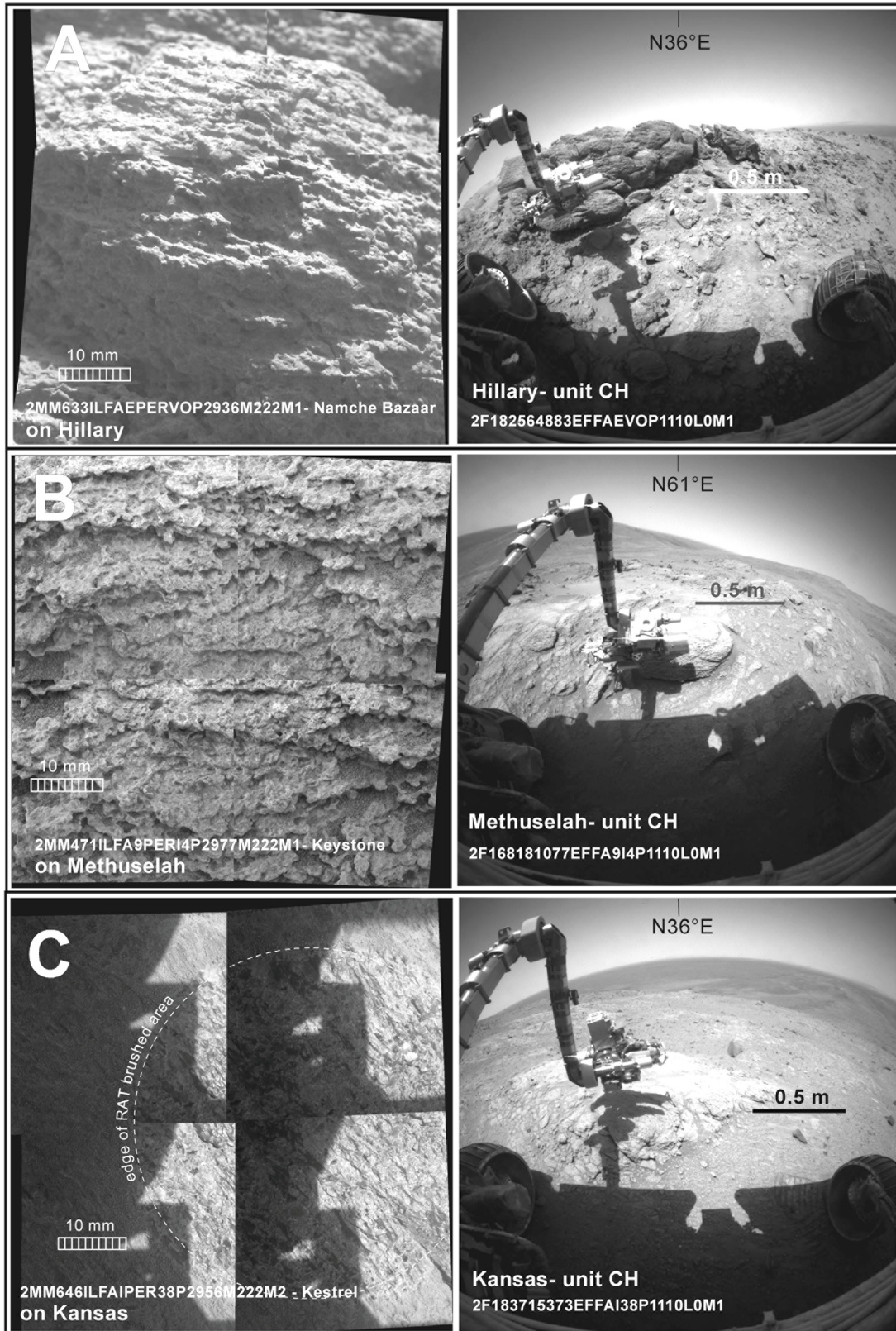
Figure 9. Comparison of Microscopic Imager (MI) mosaics on the Columbia Hills summit outcrop unit (ch) exposed at the outcrops (a) Hillary, (b) Methuselah (β member of lower Cumberland Ridge unit, lcr, see Figures 6 and 7), and (c) *Kansas*. A laminated granularity of 1 to 2 mm particles is common to many of the Columbia Hills ledge-forming outcrops. Paired images show the MI mosaic and position of MI on the outcrop where the mosaic was acquired.

with a varied but generally rougher surface texture than is common elsewhere. There are fewer blocks and mottled textures than the surrounding units, and particularly fewer bright toned blocks. Inspection of stereo pairs shows that there is a prominent step in relief at the contact between this terrain and smoother appearing downslope areas.

[84] The surface texture transitions upslope to a smooth surface bearing blocks and intervening fines common near the summit Columbia Hills summit (unit ch). That unit appears to overlie the western Husband Hill (wh) unit and therefore is a window in an overlying Columbia Hills unit (ch) and a thick float layer. It is consistent with the lower stratigraphic position inferred for the western Husband Hill (wh) unit.

4.11.2. Field Observations

[85] The western Husband Hill unit was traversed between sols 527 to 575 after leaving the Methuselah–Larrys Lookout area and during the climb and approach to the summit. The west side of Husband Hill is covered with large blocks, possibly rubblized outcrop from upslope, and there are few outcrops. Elevated rocky platforms and intervening troughs that continue from midflank to the crest of Cumberland Ridge dominate the terrain. The troughs are relatively free of large blocks and expose relatively homogeneous, nonjointed, and granular-appearing light toned to dark bedrock surfaces, typified by the irregular shaped outcrop Independence. Although not defined in a specific observation, similar granular light toned surfaces are noted in L2-R7 filter drive direction Pancam panoramas along the traverse toward the summit. So this material may be more widespread than accounted for in in situ observations. We cannot determine the relative stratigraphic positions of the Independence and Voltaire outcrops and here place them within the same unit. A second type of substrate exposure is the bench-shaped and more jointed outcrop Voltaire. Tracking of relative stratigraphic positions of units suggests that the Voltaire outcrop is low in the stratigraphic sequence [*Arvidson et al.*, 2008]. Whereas most of the outcrops on the west flank of Husband Hill dip more or less conformably with the surrounding slopes, estimates of the strike and dip for Voltaire [*Arvidson et al.*, 2008; *McCoy et al.*, 2008] range from approximately northwesterly to southeasterly into the hillslope.

[86] These are coarse clastic rocks with characteristics of breccias or conglomerates. The campaign at Voltaire, an orthogonally jointed outcrop consisting of several separate target areas (Descartes, Bourgeoisie, and Haussmann), is described by *Arvidson et al.* [2008], and the results are compelling evidence for mixtures of multiple lithologies. The centimeter-scale clasts within Bourgeoisie consisting of Wishstone class materials appear to be set in a fine matrix of nanophase iron oxides and high ferric-ferrous ratio materials [*Morris et al.*, 2008]. A probable origin of nanophase iron oxides common in many Columbia Hills rocks is the alteration of a mafic-rich glass [*Arvidson et al.*, 2008]. Elemental abundances [*Ming et al.*, 2008] are, however, distinct between the outcrops Independence and Voltaire. Independence is anomalously low in Fe, and Voltaire is high in Cr.

[87] Clasts littering the soils within this unit are among the largest on the Columbia Hills [*Yingst et al.*, 2008] with a mean size up to 15 mm. Either the outcrops are more competent here or the large angular clasts in the observed exposures are weathering out and account for the relatively low sphericity [*Yingst et al.*, 2008] of clasts in this unit. On the basis of Min-iTES observations, there is an unusual mix of rock classes represented in individual float rocks immediately upslope [see *Arvidson et al.*, 2008, Figure 8]. Therefore, a breccia bearing fragments from multiple lithologies would be consistent with that observation.

[88] In terms of visible and near infrared spectra from Pancam, the rocks at the Voltaire outcrop show some heterogeneity, but are typified by the rock Descartes and are spectrally similar to the Methuselah spectral class of rocks [*Farrand et al.*, 2008]. Descartes, however, has a shorter-wavelength reflectance maximum at 673 nm, shallower blue to red slopes, and a band minimum at 934 (instead of 900) nm. So there are detectable differences in the spectra of Descarte and Methuselah.

4.11.3. Analysis and Interpretation

[89] The rough texture at short scales and absence of mixed blocks and fines typical of most of the slopes of Husband Hill are characteristics suggestive of the exposure of bedrock material rather than loose debris. Overlapping relations with surrounding units imply that it lies beneath the general debris mantle and is either stratigraphically correlated to the northwest Cumberland Ridge outcrops (unit lcr), or stratigraphically lower. The sharp transition from a surface of trough and ridge relief upslope to one of bland block aggregations downslope is consistent with an unconformable surface stripped of float, or exhumed along an unconformity. This would account for the step up in relief on the downslope side of the contact between surrounding mantles and this surface.

[90] The low-angle attitude of this outcrop and distinctive elemental abundances of the sampled areas distinguishes it from the other outcrops in the Columbia Hills. Given the breccia-like texture of the rock, a mixed impact melt and breccia origin is likely, the variations in elemental abundances may reflect the heterogeneity of the target materials. In addition, the melts have incorporated some of the rock classes from the preexisting areas of Husband Hill.

[91] The matrix of nanophase oxides, interpreted as originally glassy, and breccia-like textures bearing clasts of another distinctive regional rock (Wishstone class rocks) [*Arvidson et al.*, 2008] are evidence that this is an early impactite. The fact that clasts of the lower stratigraphic materials (Wishstone class rocks) of the Columbia Hills have been incorporated into it is also significant constraint on the stratigraphic position of this unit. Unless this outcrop is rotated from its original position, these orientations are indicative of emplacement prior to development of the current shape of Husband Hill. A working hypothesis for this orientation would be early emplacement of the Voltaire outcrop rocks, possibly as part of the original Columbia Hills massif formation, followed by erosion, development of an unconformity, and subsequent deposition of the Summit and lower Cumberland Ridge (lcr) materials as a drape of successive air fall layers.

4.12. Haskin Ridge (Unit h)

[92] The upper surface of Haskin Ridge forms a spur that juts eastward on the east side of Husband Hill much like the West Spur does on the west side of Husband Hill (Figures 2 and 3e). But there are more apparent impact craters here

than anywhere else along the traverse, and from rover perspective the rocks are more massive, and laminated structure is absent. The terrain relief is also more rugged and blocky at meter scales than elsewhere in the Columbia Hills, giving the overall impression of fewer mobile fines and exposures of more strongly consolidated bedrock that has been rubblized in situ. These characteristics, in combination with the stratigraphically higher materials on the flanks of Haskin Ridge suggest that the rocks here are stratigraphically low. Possibly relevant is the granular petrographic characteristic that appears similar to Wishstone class rocks (upper Cumberland Ridge Materials, unit ucr), the stratigraphically lowest material identified. Rover based observations place the Haskin Ridge unit stratigraphically low and suggest it is exposed because an overburden of less competent materials may have been stripped off.

4.12.1.   Orbital Observations

[93]   The ridge extending eastward from Husband Hill is a distinct surface of rugged relief of blocky surface texture and a somewhat greater population of small impact craters than elsewhere along the traverse. This is a relatively old surface texturally more comparable to the summit outcrops (ch) and the caprock of West Spur (uws) than other areas within the Columbia Hills. The contact to the south with underlying units on the south flank of Haskin ridge is relatively abrupt, there are several debris chutes, and the unit terminates abruptly at a bench of the upper Inner Basin unit (uib). Also similar to the West Spur, this unit appears to cap a ridge crest and based on orbital images alone could be stratigraphically high like the caprock of West Spur. HiRISE stereo relief data show the presence of prominent benches and steps in the southern hillside suggestive of thick relatively flat-lying layers making up the south side of Husband Hill.

4.12.2.   Field Observations

[94]   Haskin Ridge was traversed between sols 655 and 679 and representative outcrops were examined at Larrys Bench (sol 659–663) near the crest of the ridge and Seminole (sol 671–677) on the south flank of the ridge. The relative stratigraphic position of Haskin Ridge outcrops with respect to the west side of Husband Hill is uncertain because the contact with the rocks of Husband Hill is covered by thick float. Spirit drove 90 m down this float-covered contact on sol 655 after leaving the Columbia Hills unit (ch) and the outcrop Kansas.

[95]   Many small impact craters are visible from the rover perspective in agreement with their abundance in orbital images (see Figures 2, 3e, and 17). As a result, there are few, if any, undisturbed outcrop exposures, so information on orientation of the Haskin Ridge rocks is restricted. Most of Haskin Ridge consists of outcrops that are blocky or angular at meter length scales. Rubble consists of subangular blocks 10 to 30 cm, and local bench-like ledges of suborthogonally jointed rock up to 1 m in size.

[96]   The interpretation from orbital images that the ridge is a flat-lying stack of depositional units is not supported by in situ observations. In eastward directed panoramas from the west end of Haskin Ridge, the upper surface presents the impression of a surface or cap that dips gently southward. Measurements at outcrops farther southward [*McCoy et al.*, 2008] in the next lower geologic unit (uib) certainly indicate southward dips at low angles there. The steps in the relief

of the southeast side of Husband Hill roughly match the benches associated with mapped units like the Haskin Ridge unit (H) and the Inner Basin units. The transition from the summit to Haskin Ridge is just the uppermost of these. Additional steps occur at the transition from Haskin Ridge to the Inner Basin. Each of these steps continues somewhat subdued westward beneath the thick mantle of float on the south side of Husband Hill.

[97]   Large exposures of rock are present and planar fabrics and laminations seen in other outcrops of the Columbia Hills are generally absent. Joints have no strong orientation and are mostly massive rock masses fractured possibly from impact rather than from far-field stress. The outcrop surfaces consist of roughly planar faces derived from irregular to suborthogonal jointing and bearing a megascopic polygonal roughness at a scale of a few millimeters. The outcrop surface at Larrys Bench was RAT brushed but remained largely obscured with dust because the irregularities associated with the millimeter-scale roughness act as a trap for mobile fines and obscure most of the petrographic character. In MI images a few small areas within the brushed area of the target Thrasher on Larrys Bench (Figure 10) consists of coarse, granular patterns of lineation, comparable in texture to the target Jambalaya at the Alligator outcrop (unit lcr) on the northwest flank of Husband Hill. An overall knob and pit morphology at the scale of the grains is consistent with either a poorly cemented clastic rock or alteration of an igneous rock matrix supporting angular microxenoliths and megacrysts. The composition is basaltic with slightly higher P and Ti, and moderate to low Fe^{3+}/Fe_T somewhat comparable to Wishstone class rocks [*Squyres et al.*, 2006; *Ming et al.*, 2008; *Clark et al.*, 2007] but with a dominant olivine phase [*Morris et al.*, 2008; *McSween et al.*, 2008]. The morphology of the outcrop Seminole is similar to the outcrop Alligator from the northwest side of Husband Hill and consists of a light-toned and granulated appearing planar outcrop surface broken by an array of obliquely intersecting joints at intervals of several centimeters.

[98]   In situ observations at the outcrop Seminole (Figure 11) were done on a brushed surface, as were all in situ studies after about sol 419 following failure of the RAT abrasion tool, so details of the petrography are difficult to compare with previous samples. But elemental and mineral abundances appear similar to Larrys Bench, namely, enriched in Fe and Mg, depleted in Al, and dominated by olivine, nanophase oxides, and pyroxene [*Ming et al.*, 2008]. Alligator, a Peace class outcrop on the other side of Husband Hill [*Squyres et al.*, 2006; *Ming et al.*, 2006] is texturally similar to some Haskin Ridge rocks, and it contains slightly more olivine and pyroxene. The surface is distinct from the Algonquin and Comanche outcrops farther downslope. MI images for this outcrop reveal a surface texture that is similar to the texture in MI images of Larrys Bench, bearing a polygonal relief on scales of 2 to 4 mm and trace lineations of possible grain alignment (bedding?) across the rock face, and a few dark clasts 1 to 3 mm in size resting in a granular, poorly sorted matrix. In Pancam multispectral data, the Haskin Ridge outcrops, Larrys Bench and Seminole have deep 904 nm band depths, a characteristic shared with Methuselah outcrop rocks (unit lcr), Cumberland Ridge, and Columbia Hills Summit rocks (unit ch). The 673 nm reflectance maximum appears to be a characteristic of the
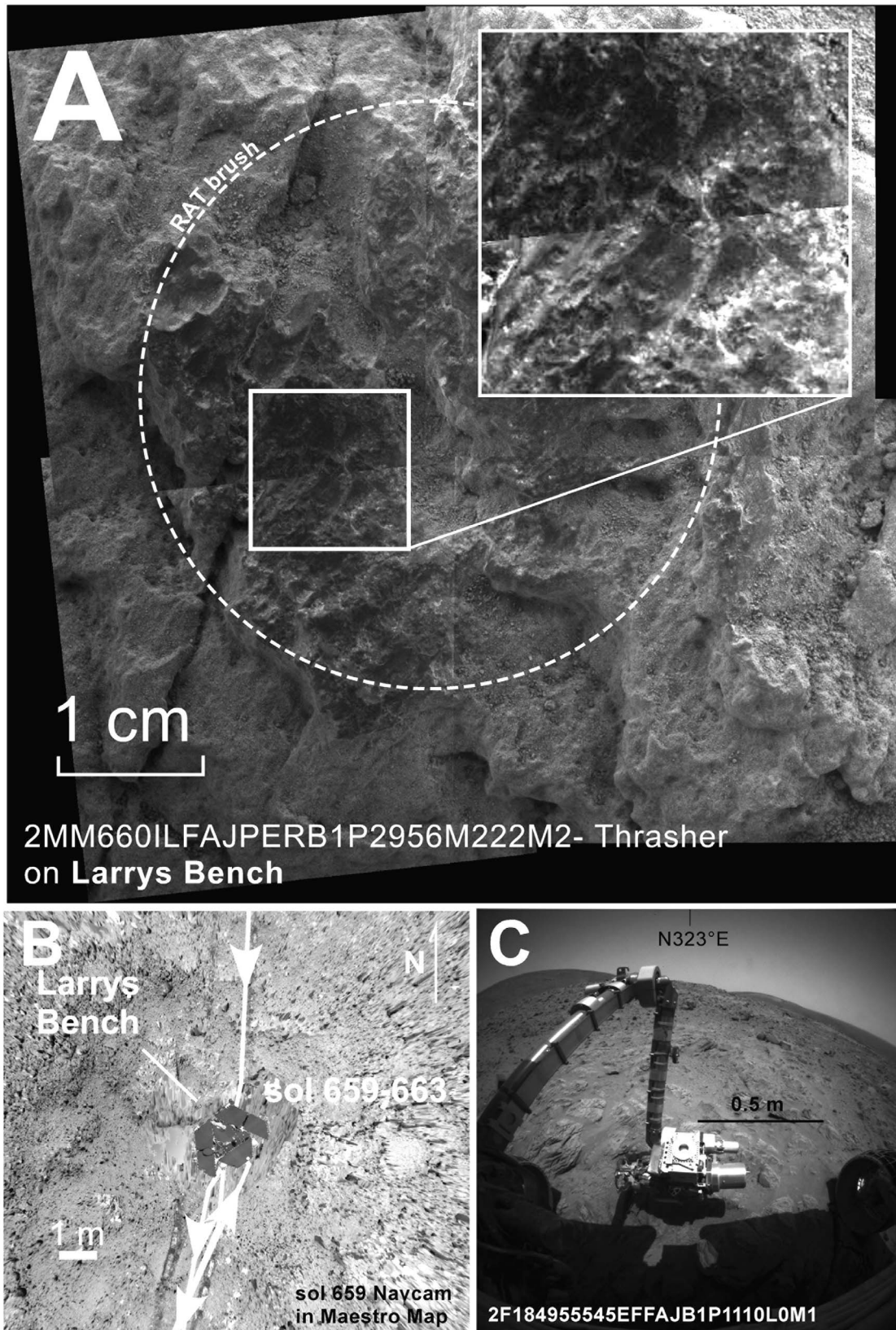
Figure 10. (a) Sample of the Haskin Ridge unit in the MI target Thrasher on the outcrop Larrys Bench. The rough microscale polygonal character of the outcrop surface impeded RAT brushing. MI mosaics show small areas of 1 mm roughness elements that may be granularity. (b and c) The outcrop is part of a rocky terrain bearing minimal drifted fines.
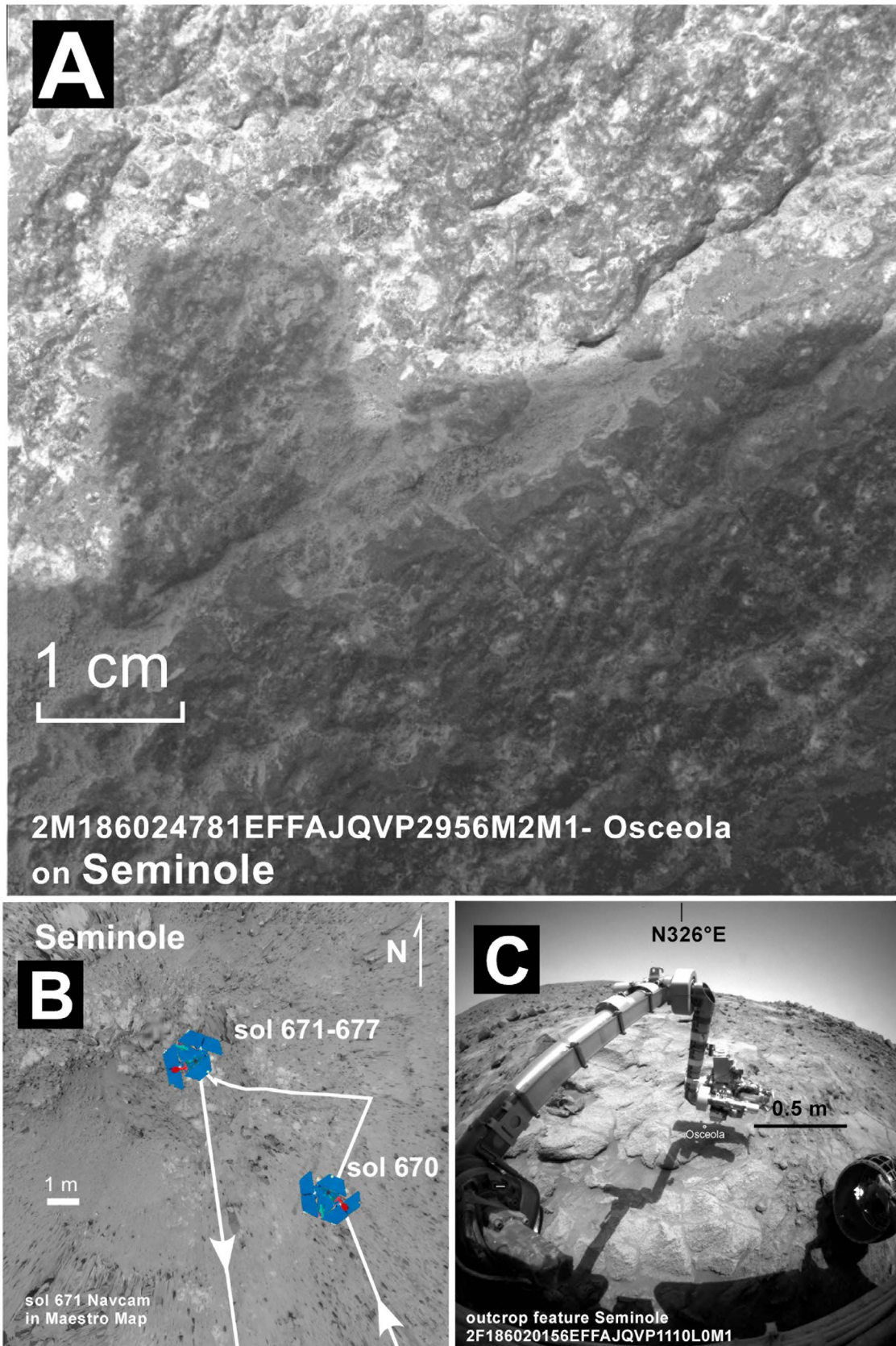
Figure 11. (a) MI on the outcrop Seminole consists of a (poorly sorted) millimeter-scale granularity similar to that in the target Thrasher on Larrys Bench. The dynamic range of the lower half of this mosaic was shadowed and has been stretched to enhance details. (b and c) Locations and terrain.

Haskin Ridge rocks, especially the Seminole outcrop (H) and it distinguishes it from outcrops southward in the Inner basin such as Comanche. This shift to a shorter reflectance maximum is consistent with the olivine-rich character of these rocks. *Farrand et al.* [2008] interpret this distinction in Pancam as resulting from the higher fraction of pyroxene in Comanche relative to Seminole, an interpretation that must now be reconsidered considering the carbonate-rich nature of the material [*Morris et al.*, 2010] and corresponding apparent absence of pyroxene. The outcrop morphologies and rock textures are decidedly different between Comanche and Seminole and might in part reflect the striking mineralogical differences.

4.12.3. Analysis and Interpretation

[99] It is unclear whether the Haskin Ridge outcrops are a continuation of the same sequence of materials that caps the summit of Husband Hill (ch), whether it is another unit that laps onto the summit outcrop unit, or whether it is a local exposure of an even deeper unit forming the core of the Columbia Hills. The relatively greater number of impact craters either means that Haskin Ridge outcrops are an older surface, a preserved and exhumed surface, or a relatively resistant material retaining impact craters against long-term ablation that removes them in softer units. The surface of Haskin Ridge appears to be an area of extensive in situ rubblization based on the widespread occurrence of rocky materials and limited fines and mixed float as compared with many other areas along the traverse. The fragmented substrate outcrops consist of a poorly laminated, mostly granular clastic rock.

[100] There are some petrographic, mineralogic, and elemental similarities between the rocks of the Haskin Ridge area and rocks on the northwest side of Husband Hill (such as Wishstone). On the basis of the similarity to other rocks on the west side and its high position in the local relief, it is tentatively correlated with the lithologies present in the upper Cumberland Ridge unit (ucr). Like the source of the upper Cumberland Ridge unit lithology, which was interpreted as likely to be remobilized via impact from some of the lower stratigraphic sections, we consider the Haskin Ridge unit (H) to be potentially correlated stratigraphically and lithologically with the source of Wishstone class materials.

4.13. Upper Inner Basin (Unit uib)

[101] From orbital data this material is fairly distinctive because of the prevalence of small knobs across its surface, but there is nothing in the orbital perspective to indicate that this is not a flat-lying material and part of the Haskin Ridge outcrops in general (Figures 2 and 3e). However, significant planar structure is present in rover based observations and the attitude supports an interpretation that the stratigraphic sequence on this south flank of Haskin Ridge is actually the inverse of that predicted from orbital observations. The petrography of the rock appears to be more coarse grained than the outcrops from upslope, so it is a different lithology than the exposures of the Haskin Ridge unit (H) along the crest of Haskin Ridge. But it is also lithologically different from the more lapilli-tuff type character of outcrops downslope at the outcrop Comanche (and apparent up section; see below). For this reason we accord it a distinct unit designation. As is the case with western Husband Hill (wh) unit,

once characterized in outcrop, MRO-HiRISE images were used to help define the lateral extent.

4.13.1. Orbital Observations

[102] This unit is restricted to the upper slopes of the inner basin and is populated by widespread knobs and ridges in the upper elevations of the basin south of Haskin Ridge. The knobs and ridges are from 2 m to 10 m in width and separated by 30 to 40 m from adjacent knobs and ridges. The contact coincides with a prominent bench separating Haskin Ridge from the interior of the basin to the south. The bench on which it occurs is a distinctly flat-lying based on HiRISE stereoscopic views, so the inference is that this unit is a flat-lying resistant layer exposed by backwasting of the flanks of Haskin Ridge, and that the layer underlies the Haskin Ridge unit (H) and overlies the unit within the basin to the south (lower Inner Basin unit, lib).

4.13.2. Field Observations

[103] The only outcrop examined (Algonquin, sol 685–689) consists of scattered exposures finely fractured along obliquely intersecting joints, and somewhat laminated in appearance (Figures 12a and 12d). The laminations dip 15° south [*McCoy et al.*, 2008] somewhat more steeply than the regional slope down to the outcrop Comanche and into the Inner Basin. Down dip projection of this unit implies that it lies stratigraphically below the outcrops of Comanche and the inner basin (unit lib), unless abrupt changes in dip or faulting occur, neither of which are evident. On the basis of this attitude, the unit thickness is in excess of 23 m.

[104] Microscopic Imager mosaics from sol 688 (Figure 12) of the RAT brushed surface Iroquois on the outcrop Algonquin are distinctly coarse grained and consist of 0.5 mm angular grains and apparent grain sockets. Some grains as large as a few millimeters, possibly olivine megacrysts [*McSween et al.*, 2008], appear darker and more angular.

4.13.3. Analysis and Interpretation

[105] Because the contact with Haskin Ridge is a step in relief, it was interpreted from the mapping in HiRISE data as a flat-lying (layer) contact, in this case overlain by the Haskin Ridge unit (H) and underlain by the lower Inner Basin unit (lib). Arguments for descending into the Inner Basin south of Haskin Ridge during planning for long-term traverse options were based on the possibility that this unit and the unit upslope and downslope were all part of a stack of layered materials, roughly horizontal. Descent would ultimately enable sampling lower and lower stratigraphic units. However, the rover-based observation of the strike and dip of the unit imply instead that this unit probably overlies the Haskin Ridge unit (H) and is overlain by the lower Inner Basin unit (lib). This is an example where we have tested a stratigraphic interpretation based on the best available orbital image data and have rejected that interpretation by observations from the surface. The lesson learned is that information about the attitude of a material unit may occur at a small scale within small outcrops, and below that detectable from remote images alone. Large-scale relief characteristics may be correspondingly misleading regarding the attitude and incorrect stratigraphic interpretations can result.

[106] The origin of the characteristic knobby texture of this unit is not clear. Some debris slide sheets on Earth are hummocky at scales of tens of meters, although other than being adjacent to prominent ridges or slopes, there is
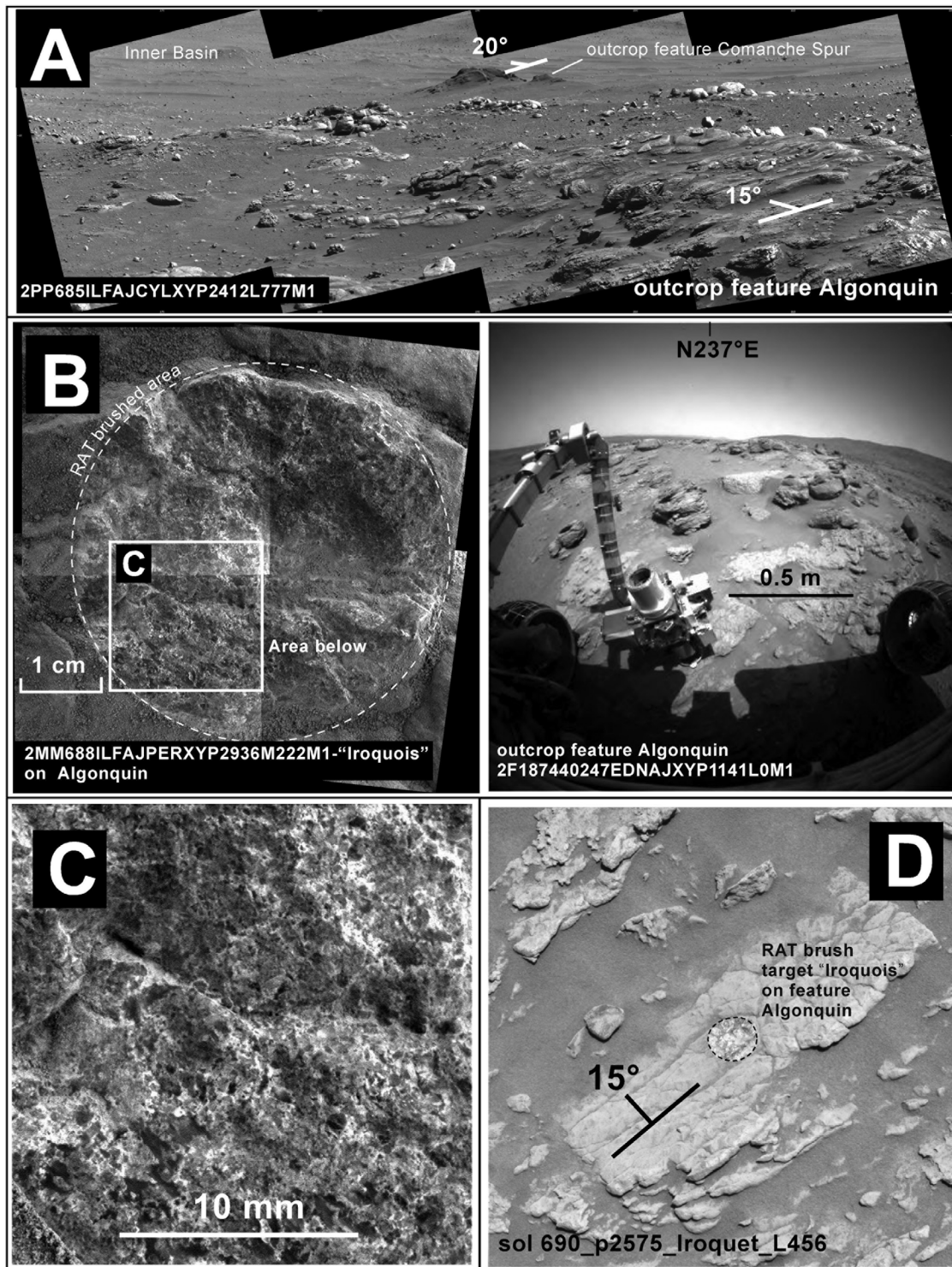
Figure 12. The outcrop "Algonquin," (a) Laminations in the outcrops at Algonquin dip southward at an angle (15°) that is steeper than the local slopes. This means that outcrops to the north (upslope) are stratigraphically below the Algonquin outcrop and that outcrops to the south (downslope), including the outcrop Comanche and Comanche Spur (in the distance at top), are stratigraphically higher. (b) (left) An MI mosaic on the target Iroquois on the outcrop Algonquin and (right) the location on the outcrop where the mosaic was acquired. (c) The MI enlargement shows a coarsely sorted but immature sandstone texture bearing some lithic fragments. High porosity is implied since there are apparent openings between grains. Petrologically this rock is distinct from the underlying units. (d) a Pancam image view down at the top of the Algonquin outcrop showing the planar south dipping textures. The brushed circle shown in the MI images is clearly visible on the planar surface.

nothing that particularly supports a debris slide origin for this unit. Alternately, since it is mostly adjacent to the relatively competent ridge forming material of Haskin Ridge, it is possible that the knobs are residual fragments of the Haskin Ridge outcrop material armoring a more easily, and now widely ablated underlying unit.

[107] An unusual drop in sphericity of surface clasts is reported by *Yingst et al.* [2008] during the circuit around the knob Miami (sol 690–692) just after leaving the Algonquin outcrop. We speculate that the transition in float derived from the relatively chunky and rubblized competent rocks of Haskin Ridge to the coarse-grained, somewhat more laminated clastic outcrops of Algonquin could be responsible. Alternatively, the greater sphericity of clasts and the bench-like character of the relief that forms the surface on which the outcrop Algonquin is located may result from an unusual weathering environment prior to the back wasting that opened the inner valley. These are igneous rocks of unknown emplacement, possibly altered. Mechanisms for generating laminated granular rocks of fundamentally ultramafic lineage are limited. Either this is an unusual type of cumulate or they are pulverized mantle materials explosively emplaced on the surface (deeply derived impactite). An open network of vugs or pits is similar in form to a moldic porosity. In this case, it could arise from cementation of a coarse clastic rock or pervasive alteration of a finer intergranular matrix in primary igneous rock.

[108] The coarse poorly sorted aspect of these rocks is similar to the rocks Wishstone and Champagne on the northwest side of Husband Hill. However, chemically and mineralogically, Wishstone and Champagne bear little similarity to this unit where it was sampled (Iroquois) at the outcrop Algonquin. Wishstone is elevated in plagioclase and phosphates, whereas Algonquin and the Haskin Ridge rocks in general are notably olivine rich. The Haskin Ridge rocks are chemically characterized as ultramafic [*McSween et al.*, 2008; *Mittlefehldt et al.*, 2006] which raises the question of whether they are clastic, derived from ultramafic parent materials, or a primary ultramafic rock possibly isochemically weathered. Visible and near infrared spectral character of the Algonquin rocks are very similar to the outcrop Seminole from the Haskin Ridge unit (h).

4.14. Lower Inner Basin (Unit lib)

[109] The upper slopes of the basin south of Husband Hill and adjoining Haskin Ridge on the south are examples of the importance of surface observation in establishing the overlapping relations for units observable in orbital data (Figures 2, 3f, and 3f). It is distinctive in both orbital and surface images due to the light-toned characteristic of outcrops. From rover perspective there is a distinctively southward dipping laminated structure to this unit. Up dip projection at the contact with the Haskin Ridge unit implies it overlies the Haskin Ridge outcrops. Prior to the traverse, it was mapped from orbital interpretations as flat lying, and therefore basal to the Haskin Ridge outcrops. It is similar petrographically to the lapilli tuffs on the flanks of Husband Hill and both are of similar estimated stratigraphic position. This material includes the unusually carbonate-rich outcrop Comanche; therefore, the stratigraphic position determined from this study implies that the environment and the processes responsible for the carbonates postdate the deposition of some of the stratigraphically higher materials of the Columbia Hills.

4.14.1. Orbital Observations

[110] This is a distinctive unit in HiRISE images because of the relatively light-toned and subpolygonal patterns of outcrop. It occurs over a series of benches down which the surface descends from Haskin Ridge into the Inner Basin south of Husband Hill. The exposures appear to be relatively flat lying and without obvious relief knobs or scarps. On the basis of mapping the materials around the periphery of the Inner Basin, this material appears to occupy the lowest surfaces. By inference it was assumed to be among the lowest stratigraphic materials exposed.

4.14.2. Field Observations

[111] Only one outcrop, Comanche was examined within this unit (sols 697 to 703). The Comanche outcrop (Figures 13a and 13b) is a bedrock knob 8 m wide and about 4 m high, the base resting on a broad bedrock bench that slopes toward the Inner Basin. The surface of the outcrop has a granular texture consistent with a massive material and fin-like traces of what appear to be slightly more resistant bedding planes slanting across the outcrop face. On the basis of the moderately uniform grain size and massive bedding planes, we would characterize this petrographically as a lapilli tuff, although some grains might be described as more angular than typical of lapilli.

[112] In at least two places, a dominant orientation set and minor set of these planar traces intercept obliquely. The minor set may be a joint plane subparallel to bedding. The facing side of Comanche in approach images is characterized by several throughgoing fractures or joints oriented at roughly right angles to these bedding traces suggesting expansion joints in an otherwise coherent rock of sufficient competence to fracture along roughly planar extension joints. One or two shorter fractures are oriented obliquely, and in local vertical orientation, to this first set. Terrestrially similar patterns occur only in fine-grained massive sandstones or fine-grained igneous rocks. If it is an igneous rock, then the bedding planes are cumulate structures that are coincidentally roughly parallel to local slopes.

[113] The Comanche outcrop could be an outlier of the upper inner basin unit (uib) and correlative with the upper parts of the Algonquin outcrop upslope which lies well within the upper Inner Basin unit (uib). Structural contours projected linearly southward from Algonquin intercept the base of Comanche outcrop assuming a relief (~10 m) and profile as determined from adjusted rover telemetry [*Li et al.*, 2008] and separation between the two outcrops of about 90 m. The general dip of what appears to be bedding planes in the Comanche outcrop is comparable to that in the outcrop Algonquin. However, if it is part of the upper Inner Basin unit (uib) it bears little chemical or mineralogical similarity to Algonquin or even Seminole, with the exception that all of these are fundamentally ultramafic [*McSween et al.*, 2008; *Ming et al.*, 2008; *Morris et al.*, 2008]. On the basis of the above analysis of the attitude of laminations dipping southward, the Comanche outcrop (unit lib) stratigraphically overlies the unit exposed in the Algonquin outcrop (uib). On the basis of a dip of at least 15° south, unit lib is a minimum of 10 m thick, the upper surface being a current erosion surface.

[114] Observations from the one visited location did not resolve whether Comanche is representative of the larger
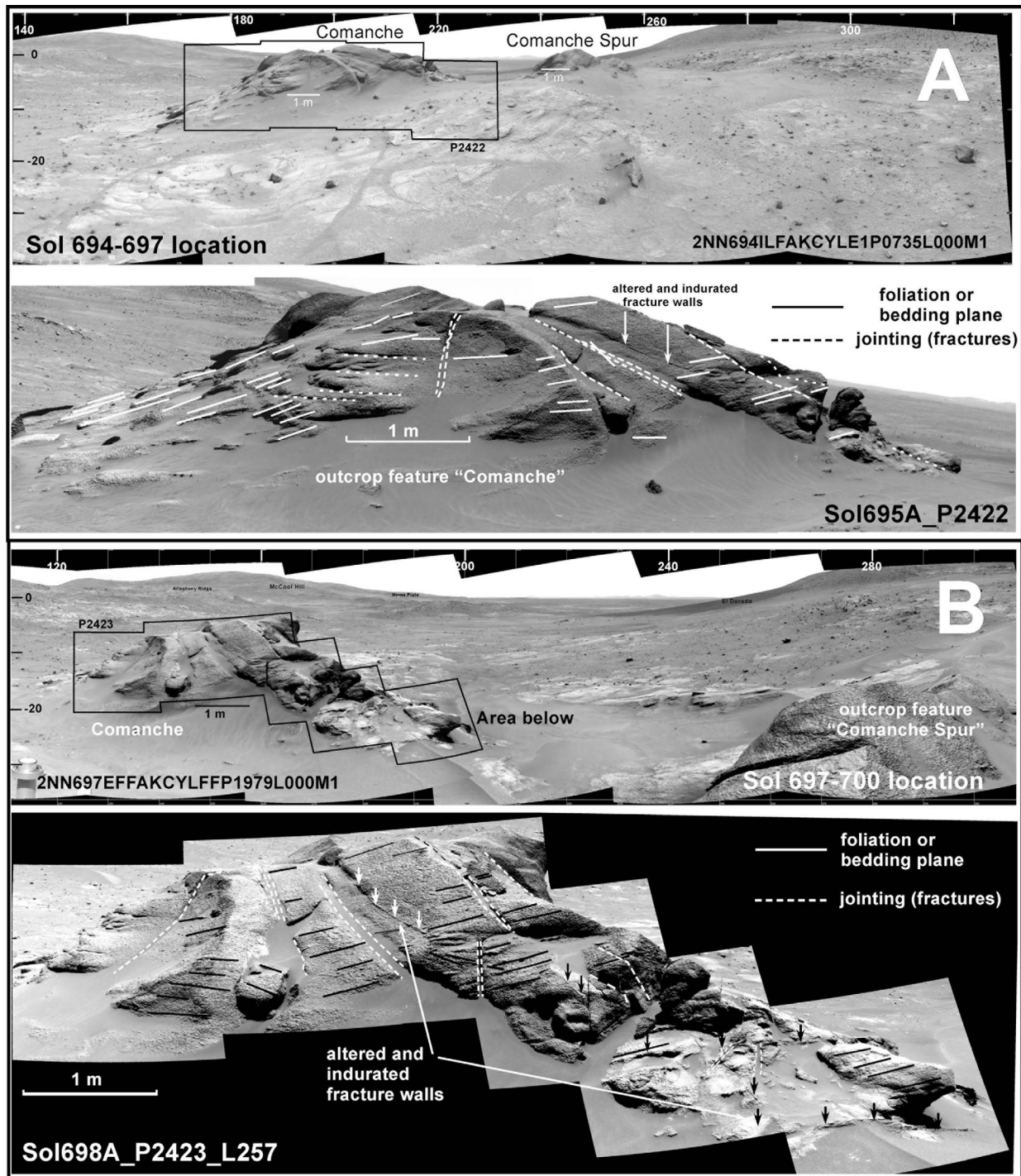
Figure 13. (a) Navcam and Pancam approach mosaics of the outcrop Comanche and (b) from the location near the outcrop Comanche Spur: (top) Navcam and (bottom) Pancam. Comanche and Comanche Spur are a residual knobs resting on a generally south dipping (left) layered sequence. Two sets of lineation are present. Solid lines indicate the general trend of parallel bedding planes. Cross lamination is minor, if present. Dashed lines denote throughgoing fractures. The vertical fractures are fin-like and may be the results of fluid alteration along vertical fractures in the rock mass. (c) Pancam mosaic of Comanche Spur, a smaller outlier 3 m north of the Comanche outcrop where in situ observations were made. (d) Proximal Pancam image with locations of MI shown. Note that the outcrop has an overall stair-step pattern likely from the oblique section through a series of dipping laminations. (e) MI mosaic of the target Palomino on Comanche Spur. In the MI data there is an overall granularity consisting of 1 mm size rounded particles similar to lapilli seen elsewhere in layered materials on Husband Hill and the basin to its south.
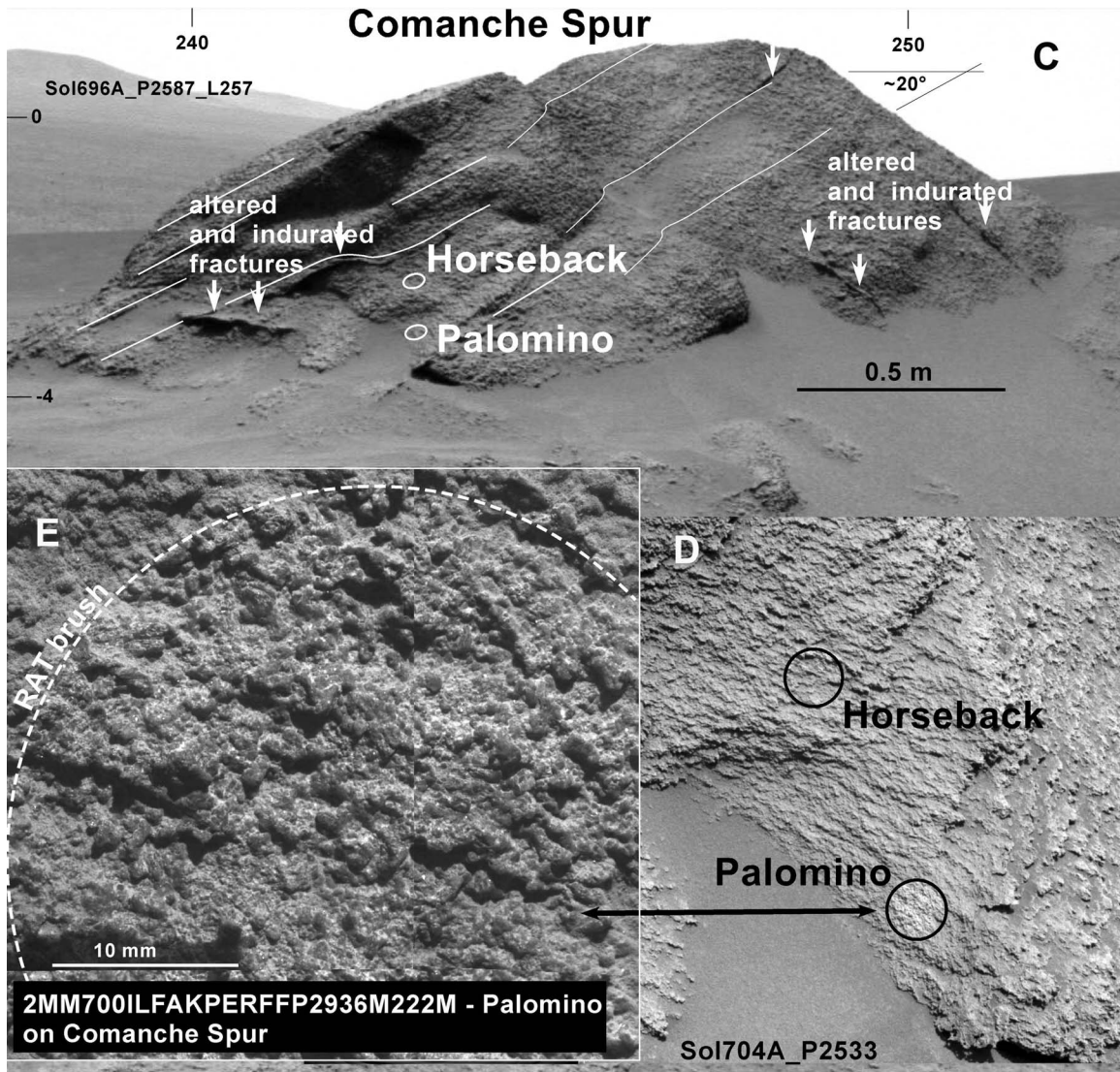
Figure 13. (continued)

expanse of the lower Inner Basin unit as mapped in HiRISE or whether it is a sole residual of an upper darker member of this unit. Beyond Comanche several meters to the west are low ledge-like exposures with similar apparent southward dipping planes suggesting that the southward dipping planar features of Comanche are consistent at least with it being a residual knob on a more extensive unit of the same bedding sequence. These dips are roughly conformable to the local slope leading into the Inner Basin. Although it is interpreted from the regional view provided by HiRISE to be a stratigraphically lower unit in the overall stratigraphic sequence traversed on Husband Hill, we cannot discount the possibility that it is actually a much later material that conformably fills the depression south of Husband Hill. Contact relations with the nearby upper Inner basin unit (Algonquin area) appear consistent with Comanche underlying that outcrop, but contacts can featheredge in misleading ways in some cases.

[115] In situ observations were done on a smaller knob, Comanche Spur (Figures 13c, 13d, and 13e), occupying a short ridge to the north of the main outcrop Comanche. Microscopic Imager results (Figure 13e) on the brushed surface of an adjoining outcrop, Comanche Spur, show individual grains less than 1 mm and traces of planar grain alignment. There are few obvious clasts or inclusions, but otherwise the appearance in hand specimen scale is similar to the lapilli tuff-like exposures at the outcrop Methuselah (target Keystone), the outcrop Jibsheet (target Davis), and the outcrop Larrys Outcrop (target Pequod).

[116] These outcrops are ultramafic compositions, a characteristic of Haskin Ridge outcrops (Larrys Bench and Seminole) in general [*McSween et al.*, 2008; *Mittlefehldt et al.*, 2006]. Although the chemistry is similar among the Haskin Ridge outcrops, the Mössbauer and Min-iTES spectra of the Comanche outcrops are decidedly different from the other outcrops [*McSween et al.*, 2008; *Morris et al.*, 2008] because they indicate the presence of major mineralogical

component in addition to olivine. Subsequent reanalysis of the APXS, Mössbauer, and Min-iTES data for the Comanche outcrops and additional laboratory studies show that this component is Mg-Fe carbonate [*Morris et al.*, 2010].

[117] In terms of Pancam spectra, Comanche, is similar to the Seminole spectral class [*Farrand et al.*, 2008] but has a shallower 900 nm band depth, a higher 535 nm band depth, and a relative reflectance maximum at 754 instead of 673 nm. The higher 535 nm band depth is consistent with a greater content of oxidized materials and the change in position of the relative reflectance maximum, originally thought to be consistent with more pyroxene in Comanche than in Seminole, is now suspected to reflect the presence of carbonate.

4.14.3. Analysis and Interpretation

[118] Map relations determined from orbital data suggested that this is the lowest stratigraphic unit encountered. But in situ observations support the alternative view, that this unit is among the stratigraphically higher materials and fills a preexisting basin. The question remains why the outcrop Comanche occurs as a knob if the surrounding materials have been eroded so deeply. It is possible that the noneroded material of this layer was locally indurated through one or more processes. For example, it could be a subsurface zone of fluid movement at the site of a former mineral-enriched spring, with corresponding greater cementation of the parent material and subsequent resistance to erosion. Or it could be compacted and shocked material from beneath the floor of impact crater exposed as a remnant by erosion.

[119] These are mafic to ultramafic igneous rocks with character of lapilli tuffs. We cannot say whether the carbonates characteristic of the Comanche outcrop prevails over a broader area or whether it is restricted to just a local occurrence because there were no additional in situ observations of this unit. If it is restricted in occurrence, then the Comanche outcrop may be a local mineralized zone in a former subsurface fluid pathway, or a shallow exposure of former spring. Vertical fracture zones that cut across the face of the outcrop and the unusually wide fins associated with some of them could easily represent former pathways for fluids bearing dissolved carbonate that have cemented lapilli of an existing fall deposit in the vicinity of greatest fluid flow. If so, then this outcrop may well be the subsurface expression of a spring deposit. Martian spring deposits have been predicted to occur and have been sought in remote sensing data [*Crumpler*, 2003a, 2003b] because of their potential as sites of prebiotic chemistry and habitability. If these outcrops are lapilli tuffs, then they have been altered and infused with significant carbonates subsequent to desposition.

4.15. Float (Unit f)

[120] Because of the great age, general fragmentation of outcrops, and extensive occurrence of mobile fines, float consisting of loose clasts in a matrix of fines is possibly the most common surface unit [*Yingst et al.*, 2008] (Figures 2 and 3). In many places it is thin enough that the character of underlying materials asserts characteristics that are mappable. Float is by definition widespread and locally of variable thickness and it has correspondingly irregular, discontinuous, and commonly feather-edged contacts. Rover observations show that in many places it has the character of a distinct epiclastic unit subject to erosion and deflation along

underlying unconformities much like any bedrock unit. This is significant because much of the float appears to have accumulated rapidly, may simply be a relic of environments of rapid erosion early in the history of the Columbia Hills. Instead of being a late surficial material unrelated to deep geologic time as it is on Earth, it may actually record characteristics from an environmentally more dynamic earlier time of Martian geologic history.

4.15.1. Orbital Observations

[121] This is the most widespread map unit and appears to consist of accumulated debris of both blocks and fines forming thick mantles, ramps, and fans on the mid to lower flanks of steep hills and ridges throughout the Columbia Hills. Whereas the upper slopes are generally topographically rough, the downslope areas of hills and massifs bear very little roughness or relief other than individual blocks. In places a mantle of mobile aeolian materials overlies this yet may be thin to absent along the crests of most of the ridges and hills.

4.15.2. Field Observations

[122] Float is more pervasive than it appears from the mapping based on the HiRISE image. Although widespread it may locally be relatively thin, and where it is thick it may not mask the large-scale texture of a geologic unit. Several areas mapped as bedrock in the remotes sensing data are in traverse-based observations actually veiled with a layer of loose debris. The pervasive character of float was used to good advantage in analysis of clast survey images [*Yingst et al.*, 2008], systematically acquired single frame Pancam images directed at high incidence at the ground near the rover. Changes in the morphology, size, and abundance of clasts occurring as float in local soils appear to represent changes in bedrock units and were used as additional information on the character of the geologic units being traversed.

[123] In the Columbia Hills float appears to occur as a debris-mantling layer of moderately uniform thickness. We consider float to be a distinct epiclastic deposit throughout much of the Columbia Hill. Examples of the layer-like character in surface panoramas and observation while ascending West Spur around sol 192 and 193 (Figure 14a) where light-toned float of cobble-sized and finer material form a layer or mantle that covers and armors the slopes to depths of at least 10 to 20 cm. This layer has locally ablated exhuming an underlying unconformity developed on the slopes of West Spur. From the rover perspective this pervasive float has the appearance of fragmented clasts derived from more resistant material upslope. It is undetermined whether the float developed from downslope movement or ballistic and air fall accumulation. Some of the ablation may result from small impact craters, as many of the float-free area appear to be local depressions.

[124] Another example occurs near the outcrop Voltaire on the west side of Husband Hill, where loose debris and fines typical of float elsewhere form a distinct mantle on the substrate that has been subject to local thinning and removal. Immediately downslope from the Voltaire outcrop, a small ledge delineates the contact between a layer of typical float type debris and the underlying bedrock of the Voltaire outcrop. In stereo HiRISE images the flat iron characteristic of the float mantle results in float-bedrock contact forming a relatively flat, natural grade through undulations in the hillside along which Spirit ascended
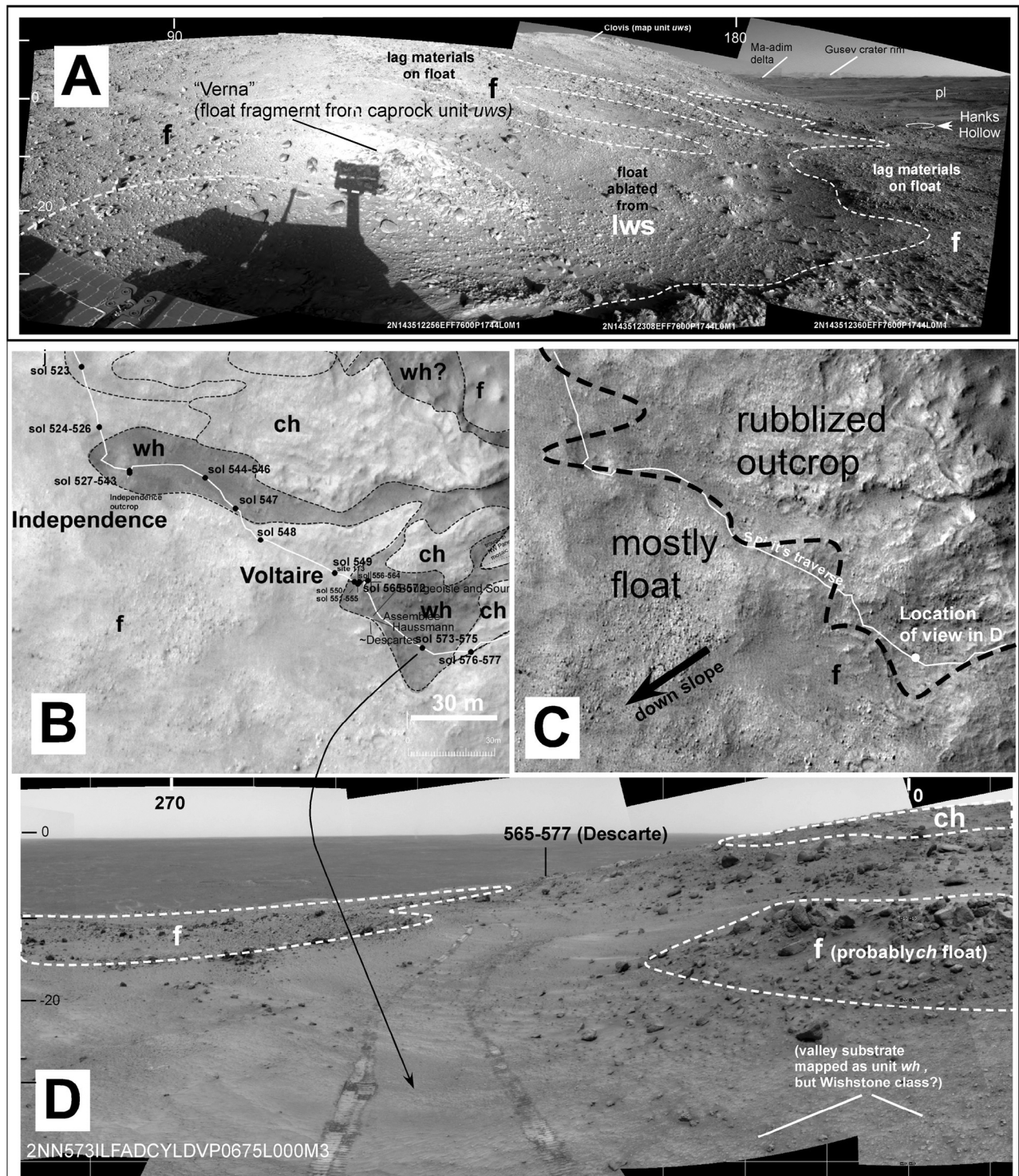
Figure 14. Float acts as a distinct mantling unit that may be locally stripped exposing the underlying bedrock. (a) At West Spur, float forms an epiclastic mantle, now partially striped, on an underlying unconformity. (b) Segment of the geologic map on the western slope of Husband Hill near the outcrop Descartes/Voltaire. The traverse followed the contact between an overlying float layer and the erosional unconformity developed on stratigraphically low breccias observed in the Voltaire outcrop. (c) In the corresponding HiRISE image the textural distinction is pronounced between mixed rock and fines debris on the lower left and rugged and rubblized bedrock surfaces on the upper right. Dashed line indicates the generalized contact between the two surface textures. (d) On sol 573 after leaving the outcrop Voltaire and Descartes the traverse followed a bedrock valley flanked by flat-iron layers of mantling float on the south (left) and rocky float derived from local outcrops of unit ch on the north (right).

beginning on sol 523. The contact is apparent from HiRISE perspective (Figures 14b and 14c) according to the distinction in surface texture between the blocky float and the rugged relief of the outcrop upslope. The abundance of float downslope and the rugged rubblized outcrop upslope can be seen in Navcam panoramas throughout the traverse along this contact. In a Navcam panorama on sol 573 looking back at this contact (Figure 14d), it appears as step or ramp of loose rocks typical of float, while the floor of the trough just upslope appears to be outcrop. The float is acting like a clastic layer in this case and is draped on an unconformity. Removal of the float layer has created a flat iron type layer or skin; the contact with the underlying unconformity follows local variations in relief.

4.15.3. Analysis and Interpretation

[125] From orbital images this material is interpreted as surficial debris and soils covering bedrock. General downslope transport and overlapping accumulations of rubblized and disaggregated bedrock appear to contribute to this surficial debris and soil, and forms unconsolidated mantles on hillsides. The widespread occurrence probably represents long-term erosion by both low-energy (aeolian deflation) and energetic (impact cratering) processes over significant intervals of geologic time.

[126] Rover-based observations show that float occurs nearly everywhere in the Columbia Hills [*Yingst et al.*, 2008]. It encompasses many parent lithologies and many time scales of emplacement, and has accumulated from individual clasts for the most part but locally it may be part of slides, debris flows, and downslope creep all leading to thick accumulations locally on the mid to lower flanks of hills. Simple tracking of changes in clast morphology and lithology in local float throughout the Columbia Hills [*Yingst et al.*, 2008] shows that it is probably representative of the underlying bedrock through rubblization of the substrate, downslope transport, and overlapping accumulation of debris fragmented by long-term (aeolian deflation) and energetic (impact cratering) erosion.

[127] In the long term, small impacts could act as mechanical erosion agents, gradually move float off of upper slopes of hills, and accumulate it on the lower slopes. Several observations show that there are substantial float mantles, that it behaves as an epiclastic layer, and that it is subject to erosion, stripping, and subsequent reexposure of the underlying outcrop much as with any other clastic layer. In several locations float forms a distinct layer on an underlying disconformity and has been partially stripped off. In this respect it behaves now in many places as a distinct ancient epiclastic layer.

[128] If the characteristics of float here in the Columbia Hills are representative of float elsewhere on Mars, then outcrops of bedrock are most likely to occur near crests of relief features simply because float, as well as mobile fines, are thinner to absent on the upper slopes. Float accumulations or layers may be important stratigraphic markers that are common on Mars, are restricted to one or a few time stratigraphic positions, and have developed on significant geologic unconformities. The role of float on Mars as a geologic record of changing environments is unlike its role on Earth where it is of importance principally as a surficial material of very recent age.

4.16. Bright Unconformable Debris of Cumberland Ridge (Unit dcr)

[129] This surface is prominent in both orbital images and rover-based images, but for different reasons (Figures 2, 3a, and 3b). In orbital data it is clear that this is a bright streaked material, that it includes many blocks, and that the streaks trend downslope and over significant breaks in slope. Taken together these imply a likely zone of high downslope mobility of clasts derived from some rocky source upslope. From rover perspective this a steep sloping area occupied by many large (20–30 cm) clasts resting on and within mobile fines. It appears to be an area of competition between aeolian fines moving upslope with prevailing westerlies, and blocks moving downslope derived mostly from unit ucr. The clasts themselves may be representative of the lowest observed materials.

4.16.1. Orbital Observations

[130] Bright-toned, streak-like patterns and linear boulder trains occur on the northwest side of Cumberland Ridge, the west rim of Tennessee Valley, a deep cleft on the north slope of Husband Hill. The streaked appearance consists of trails of aligned boulders and cobbles, many brighter in tone than the surroundings. The continuity of the streaks across significant changes in relief is apparent in stereo image data and illustrates its association with steep slopes in general.

4.16.2. Field Observations

[131] The surface consists of abundant angular to subangular blocks resting on, and within, thick mantles of fines where this unit was crossed during the initial ascent of Husband Hill between sols 317 and 380 (Figure 15). The fines resulted in significant impairment of mobility. A buried 3 to 4 cm clast churned up by the wheels during drives was temporarily wedged in the right rear wheel. Buried clasts occurred in at least two or three other sites where thick, nearly cohesionless, soils were present, mostly in areas characterized as mobile fines (dmf) adjoining slopes where downslope movement of rocky debris also occurred (Dead Sea adjacent to Lorre Ridge south of Husband Hill and Troy, a site on the west base of the Inner Basin feature Home Plate).

[132] The rocks (Wishstone, sol 332–337, and Champagne, sol 353–358) are two well-studied examples of these blocks examined in situ. Their relatively low alteration and relatively higher RAT SGE (15 to 24 J mm-3) compared to other classes of rocks such as the Clovis class [*Squyres et al.*, 2008] is consistent with a competent rock mass that has been broken into multiple subangular fragments instead of simply disintegrating as would a materials with poor cohesion. On the basis of the high RAT SGE, the overall blockiness of these materials is therefore not surprising. No outcrops of comparable mineralogy were encountered farther upslope, but the presence of a moderately fresh impact crater near the crest, and small clasts of this rock class in outcrops (Voltaire) of what are interpreted to be impact breccias and melts, suggests a possible source as deeply excavated substrate material.

[133] In an MI mosaic of the RATed surface, Wishstone is characterized as a poorly sorted clastic rock. Angular dark grains 1 mm in diameter are set in a matrix of smaller lighter grains and a subresolution matrix. Texturally the character is similar to that of some terrestrial volcanic tuffs [*Squyres et al.*, 2006], including ash flows, but we cannot exclude the pos-
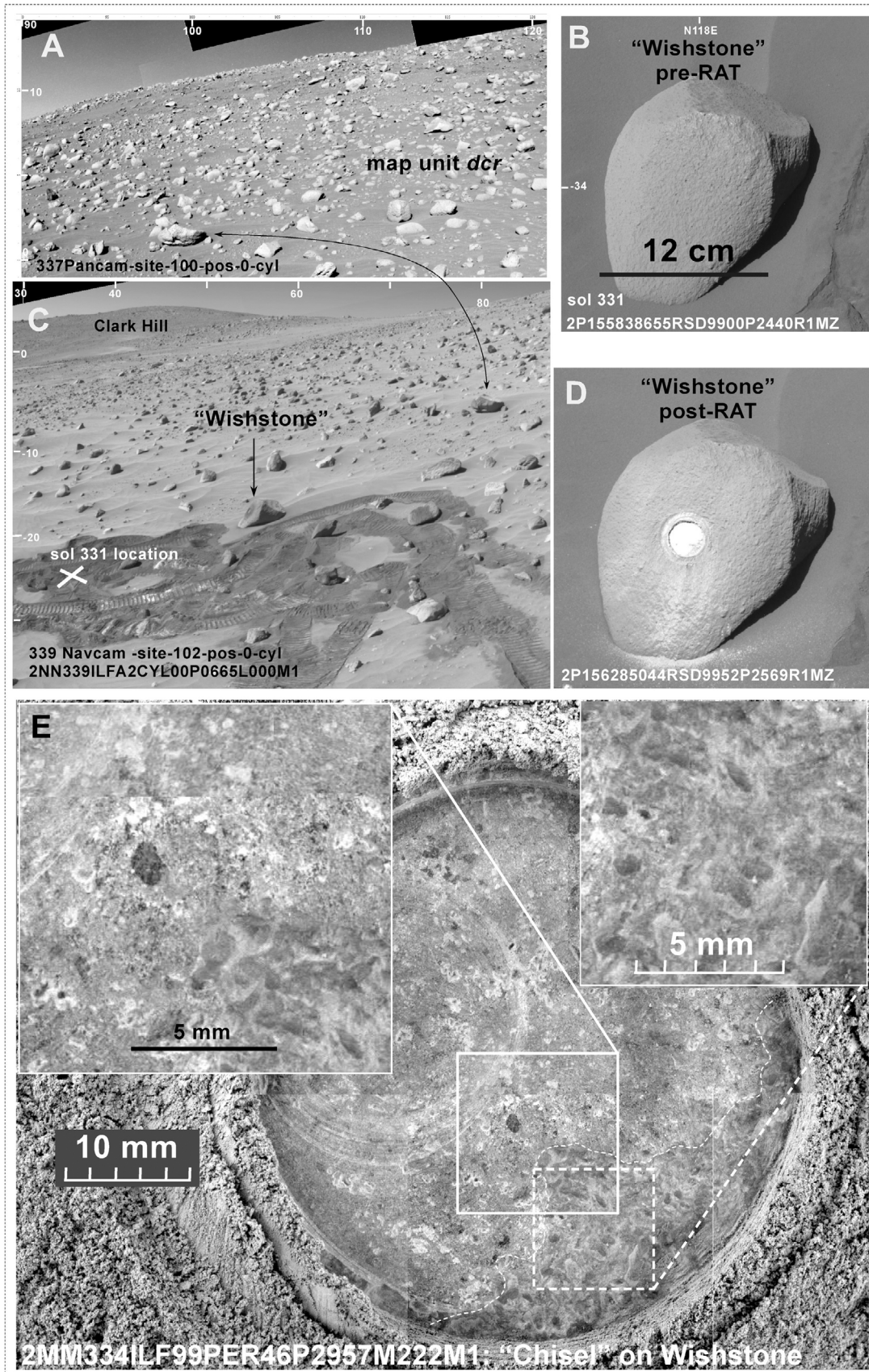
Figure 15
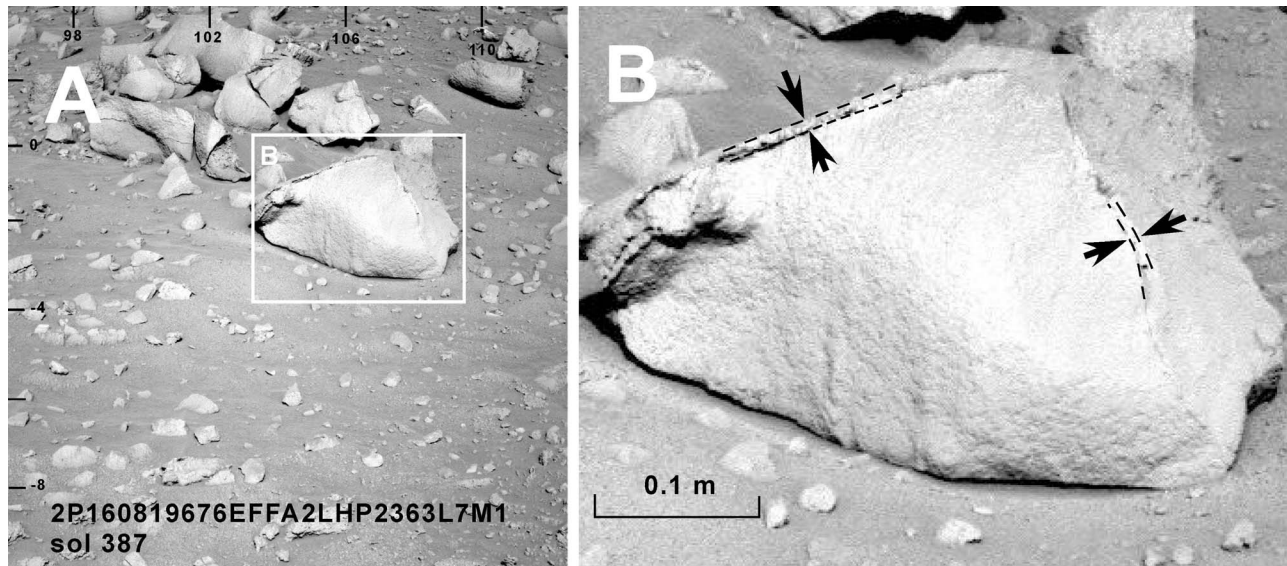
Figure 16. (a) Pancam mosaic directed south at scattered float rocks, part of the bright unconformable deposits of Cumberland Ridge on the northwest flank of Husband Hill. (b) In full resolution, one rock bears a distinct rind or coating (indicated by arrows between dash lines. The surface of this rock appears texturally similar to Wishstone. The presence of a rind or coating along relatively planar faces is suggestive of alteration along joint (fracture) planes when the rock was part of a larger substrate rock mass.

sibility that it is a porphyritic lava or an impactite derived from igneous country rock.

[134] Wishstone is so distinctive as to represent a class of rocks that is relatively less altered compared with most of the other rocks on Husband Hill. Wishstone *class* rocks have high Ti and P [*Clark et al.*, 2007], signatures of some exotic alkali basaltic rocks on Earth, although the P content exceeds common high values and is best explained as the result of some type of weathering and alteration [*Ming et al.*, 2008; *Hurowitz et al.*, 2006]. Nonetheless, apatite, the common repository for significant phosphorous concentrations in igneous rocks (characteristically in intermediate alkalic volcanic rocks on Earth) does not appear to fit Min-iTES spectra [*Ruff et al.*, 2006]. According to *Ruff et al.* [2006], mini-TES deconvolution runs fit well only for P present in wavellite, a phosphate of secondary origin, together with some sulfates and a significant fraction of plagioclase. Infiltration and in situ secondary mineralization of a porous ash or impactite is one possible way to impart excess P in a primary ash. Olivine and pyroxene are relatively minor phases. Iron oxides are relatively low, and Fe^{3+}/Fe_T of 0.42 [*Morris et al.*, 2008] is among the lowest of any Columbia Hills rocks, suggesting relatively little alteration compared with many rocks in the Columbia Hills, additional evidence that these rocks were isolated from many of the alteration fluids that affected other rocks in this region.

[135] Wishstone class rocks appear similar to the Methuselah rocks in Pancam spectral analysis [*Farrand et al.*, 2008]. Some of the similarity may reflect the comparable levels of olivine and pyroxene, and low goethite and Fe^{3+}/Fe_T ratios [*Morris et al.*, 2008], but proximity in occurrence of Methuselah rocks and Wishstone is notable.

[136] Some of the blocks characteristic of the bright unconformable debris of Cumberland Ridge are scattered on the surface of the adjacent map unit lcr. One polygonal rock encountered on sol 387 as loose float while traversing lcr is notable because the nearly planar faces of this rock have a rind several millimeters thick (Figure 16). On the basis of min-TES character and in Pancam images it appears granular or textured at a millimeter-scale consistent with the character of Wishstone class materials. The coating is (1) compacted dusty material originally filling thin joint planes when the rocks were part of a local bedrock, (2) fluid-altered joint walls, or (3) weathering rinds developed after the blocks were excavated. The exterior bears some similarity to the case hardened exteriors of rocks like those at Hanks Hollow (e.g., Breadbox). Unfortunately, no in situ or remote sensing comparisons of the rinds and the interiors of these rocks were done. But they remain as possible examples of how fractures in the substrate of the Columbia Hills could have facilitated both the movement of fluids in the past and the formation and distribution of polygonal blocks.

Figure 15. (a) The bright unconformable debris of Cumberland Ridge (unit dcr) is a surficial deposit of relatively lighter-toned subangular blocks scattered on the steep slopes of the northwest flank of Husband Hill. (b) The clean face of one rock, Wishstone was examined following application of (c and d) the Rock Abrasion Tool (RAT). (e) The MI mosaic on the abraded surface shows that this rock consists of poorly sorted light and dark rock fragments on the order of 1 mm in size cemented by a microgranular matrix. A part of the surface remained un-RATed (lower right corner of MI mosaic) because of local relief on the rock face. This surface bears the small-scale polygonal or faceted character typical of many of the rocks on the east flanks of Husband Hill at Haskin Ridge (Seminole and Larrys Bench).

4.16.3. Analysis and Interpretation

[137] In the HiRISE images vectors for some of the streaks place the up hill source in the ejecta of a relatively deep 15 m diameter impact crater situated on the crest of Cumberland Ridge. From the rover perspective, the abundance of rocky debris and moderate angularity of the blocks is evidence for relatively short transport from the source, and the rim and ejecta of a small impact crater farther upslope would explain their abundance. The rock Wishstone, which bears several unusual characteristics that distinguishes it from other rocks examined in the Columbia Hills [*Squyres et al.,* 2006], is a representative of these rocks. On the basis of the fact that Wishstone class materials occur as fragments within one of the lowest stratigraphic units encountered (Voltaire outcrop, see discussion of unit wh), it is likely that Wishstone along with many of the other blocks in the bright unconformable debris of Cumberland Ridge unit (ucr) are currently, as exposed, are disaggregated and out of position in the stratigraphic sequence. If these are derived from the ejecta of a crater farther upslope, then they could easily be among the lowest materials encountered and are representative of lower stratigraphic materials not exposed elsewhere along the traverse. The rind-like coatings along angular boundaries of at least one of these rocks, along with chemical evidence for relatively minor alteration in the surrounding rocks, would be consistent with a source in moderately competent and jointed bedrock of low permeability and high hydraulic conductivity in which fluids moved primarily along planar joints and fractures. Subsequent excavation of the blocks by impacts scattered fragments on the upper slopes of Husband Hill where they were included in the loose unconformable surficial deposits. To summarize, these deposits are likely to be a mixture of debris slide fines and excess deeply derived blocks from an impact crater ejecta field migrating downslope and mobile fines migrating up the west-northwest slope of Husband Hill.

4.17. Unconformable Debris of Allegheny Ridge (Unit da)

[138] This is an anomalously sinuous ridge that extends across the surface of the basin south of Haskin Ridge (Figures 2 and 3f). In HiRISE images the ridge has the appearance of developing from confinement of a material along a sinuous trace, which suggests and inverted channel the material of which could be anything from mudflows or impact debris to lava flows or streambeds perched through subsequent erosion of the surrounding landscape. Proximal, although not in situ, observations indicate that the outcrop material along the crest contains clasts of blocks and cobble size, so we suggest that this is a debris channel that has been topographically inverted.

4.17.1. Orbital Observations

[139] A narrow and elongate ridge in the floor of the valley south of Husband Hill, Alleghen*y* Ridge, stands out as unusual because its narrow planform curves southward across another larger ridge. Where it terminates it is a broader lobate platform with steep margins descending directly onto the inner basin valley floor. It also appears to overlie the contact between two map units implying that it represents something unconformable that was emplaced after the exposure of the contact between the two underlying units

and was therefore emplaced late in the morphologic development of the Columbia Hills.

4.17.2. Field Observations

[140] This material was not traversed, but on sol 716, Spirit passed within 100 m of its steep western margin. Pancam images acquired near the closest approach between sol 723 and sol 724 (Figure 17) show resistant outcrops 1–2 m thick resting on a light-toned unit that appears similar from the distal perspective to outcrops of the lower Inner Basin unit (lib). There is no evidence for large clasts within the outcrops, yet the crest and slopes of the ridge are covered with large equant blocks. So we cannot say with certainty that the Allegheny Ridge material is fine grained, or whether it is a gravel and cobble deposit.

4.17.3. Analysis and Interpretation

[141] The sinuous form and the exposure of distinct outcrops of moderately resistant material in the upper slopes of the ridge implies that the ridge form is the results of topographic inversion through erosion of up to several meters of material from the surroundings. A likely upstream source for a well-developed channel is not obvious, and the overall broadening near its western terminus appears similar to the patterns seen in other slide and debris deposits identified within the Columbia Hills. If it is a former valley, then it is just as likely that it was filled by debris derived from local more competent rock type materials and persisted as a resistant caprock following deflation within the inner basin.

4.18. Unconformable Boulder Debris of West Spur (Unit bws)

[142] This is one of the more distinct surface units in both orbital and rover images (Figures 2 and 3a). Unfortunately, it was not visited, and it appears to be limited in lateral occurrence. The relatively high concentration of equant blocks compared to the flat-lying and laminated rocks that make up the rest of the West Spur, and the abruptness with which it strikes across the West Spur imply a significant localized angular unconformity. On the basis of rover proximal perspectives it appears to be a blocky deposit, possibly debris flow materials from farther up Husband Hill that have collected in a structural valley transecting West Spur (graben?) and subsequently exposed by back wasting of the margins of West Spur.

4.18.1. Orbital Observations

[143] This, like the western Husband Hill (wh) unit, is another example of a unit that is too limited in occurrence to have been mapped in pretraverse orbital image base photogeologic mapping exercises. Only after detecting this material during surface traverse was it subsequently possible to identify its surface characteristics well enough to map its extent in a HiRISE image. In plan view this is an elongated area of unusually abundant blocks but limited apparent bedrock outcrop occurring as a low ridge diagonally transecting the roughly east-west strike of West Spur. The east and west contacts of this unit with West Spur are abrupt and linear suggesting either a preexisting linear valley or graben-bounding normal fault crosscutting West Spur.

4.18.2. Field Observations

[144] This is a distinctive terrain from the rover perspective and it was imaged from several locations (Figures 18a, 18b, and 18c) while Spirit was located on the upper slopes of West Spur (sol 313 to ~sol 324). It appears as a cluster
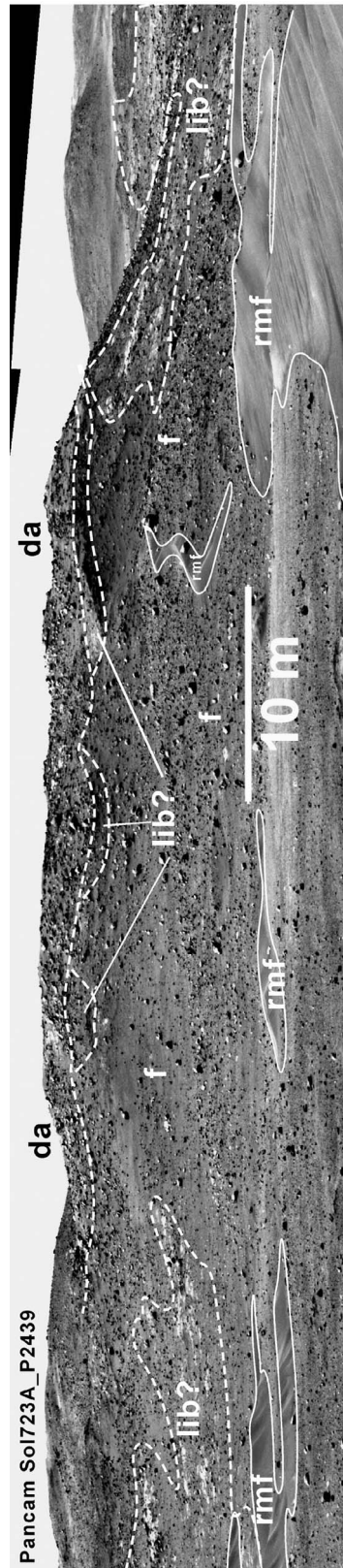
Figure 17. Pancam mosaic of Allegheny Ridge. This is an oblique, nearly end-on view of the ridge. The upper meter consists of concentrated blocks and small clasts. Outcrops just below these are of an undetermined lithology. The upper meter may be representative of whatever material filled the original sinuous depression that is now inverted to form Alleghany Ridge.
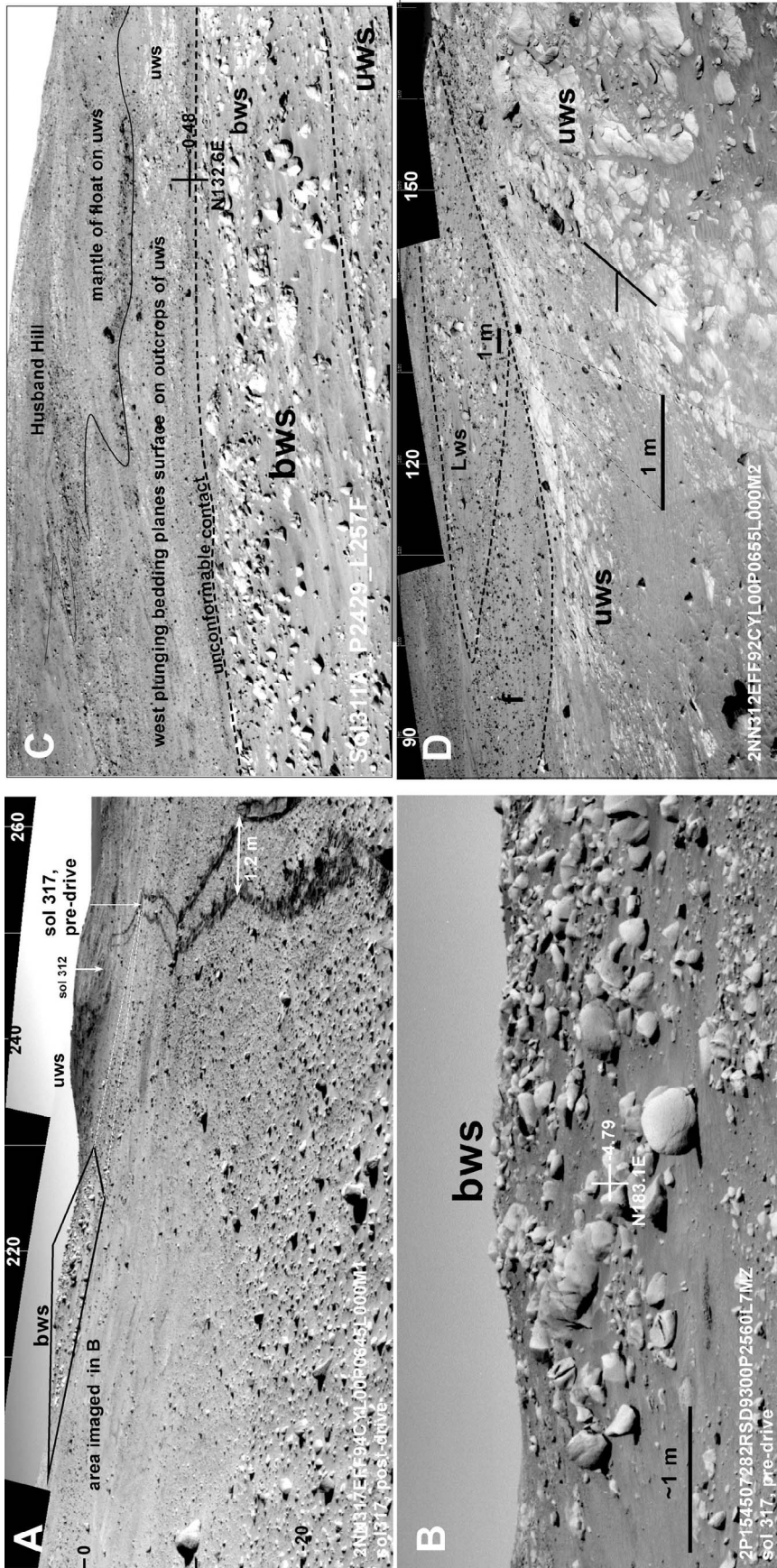
Figure 18. Unconformable boulder debris of West Spur (bws). (a) View from rover location on sol 313 looking back toward the West Spur from which the rover has just descended on the previous few sols. The unconformable boulder debris of West Spur occurs as a distinct cluster of boulders along a short segment of West Spur. Polygon shows area acquired in predrive Pancam of sol 317. (b) Pancam image acquired on sol 317 (location shown in Figure 18a) during closest approach to the unconformable deposits of West Spur. The overall texture and size of blocks are similar to those in the bright unconformable debris of Cumberland Ridge (unit dcr). It is interpreted that this a residual accumulation in a former trough filled with debris sourced in materials from farther upslope and comparable to unit dcr materials (Wishstone class?). (c) View east from West Spur across anomalous block and boulder concentration. The caprock of West Spur (unit uws), exposed as outcrops on the far east side of the deposit, appears to plunge beneath the deposit. (d) Observations here during the decent of West Spur show that the caprock of West Spur (uws) plunges eastward underneath the unconformable deposits of West Spur.

of 10 cm and larger subrounded, light-toned blocks and boulders in an area where most of the rocks are tabular or laminated (unit uws). It occupies a roughly northeast trending linear trough into which the normally horizontal laminations forming the caprock of West Spur (unit uws) appear to plunge or dip (sol 312, Figure 18d). In observations around sol 313 near the east end of West Spur (Sol313A_P2431_L357) the caprock outcrop (uws) locally has an apparent easterly tilt toward the contact with this unit.

4.18.3.   Analysis and Interpretation

[145] The morphology and texture as seen from rover perspective contrasts strongly with surroundings and is one of the clearer examples of a geologic unit mappable from the ground. Because all of the rocks are large, moderately round, and morphologically distinct from the slab like rocks of West Spur, it is unlikely that the material is associated with the surrounding ridge. Instead it appears to be a collection of disaggregated blocks of a distinctly different lithology than local rocks and outcrops of West Spur.

[146] In HiRISE stereo data the crest of the crosscutting ridge clearly lies below the elevation of the surrounding West Spur caprock (uws) in support of the hypothesis that it is a blocky deposit that has filled a tough-shaped discontinuity cutting diagonally across the West Spur ridge form. If so, the fact that the west Spur caprock appears to dip toward the unit on the east and west sides might imply that the trough was either present prior to the deposition of West Spur caprock or the graben developed subsequently with blind boundary faults resulting in surface drag fold rather than scarps. Distinct linear terminations of bedding planes on the far wall of the trough (Figure 18b) are suggestive of either a fault line scarp or the strike line of dipping bedding plane. On the basis of the linear boundaries and the crosscutting character of this unit in HiRISE stereo data, either (1) it is slope debris and debris slide materials collected in a former valley, possibly a graben that cuts across the West Spur, and is now topographically inverted by differential erosion of a less resistant substrate or (2) it is a fault sliver uplifting a block of Columbia Hills bedrock or dropping formerly overlying units within a narrow graben.

[147] In the absence of compositional or spectral data on these rocks, we cannot say how they differ from the observed West Spur mineralogies. But on the basis of the restricted occurrence the most likely interpretation is that it is debris collected in a former valley cutting across West Spur. The equidimensional form of many of the blocks and the relatively light tone are similar to blocks (like Wishstone) in the light unconformable deposits on the northwest side of Husband Hill (dcr) or the Cumberland Ridge (ucr?).

[148] Our interpretation based on limited proximal remote sensing is that these deposits are the results of early landslide or debris flow of materials from the upper slopes of a formerly steeper Husband Hill. A sequence that could account for the observed exposure is the development of a graben in the lower West Spur unit (lws), followed by air fall draping of the material that became the West Spur caprock (uws), and then unconformable emplacement of the boulder deposit. Alternatively, normal faults could have dropped a segment of the West Spur along a crosscutting graben, cantilevering segments of the West Spur caprock into the margins of the graben, followed by deposition of the unconformable boulder deposit.

4.19.   Unconformable Debris and Chute Materials (Unit d)

[149] The lower slopes of the Columbia Hills in HiRISE images are characterized by debris aprons, deep valleys and ravines, and streaks similar to that generally interpreted on Mars as evidence for significant downslope migration of loose materials and disintegrated bedrock (Figures 2 and 3e). From the rover perspective, some areas on the slopes of the Columbia Hills, particularly the south face of Husband Hill and Haskin Ridge, and the north face of McCool Hill, appear more organized as chutes with adjoining fan-like arrangements of deposits at their lower termini. We interpret these as debris slides and chutes but cannot say whether they form as single slide events or are the results of long-term accumulation. Exposures of the terminus of the McCool Hill debris slide show that at least some of these are emplaced as distinct thin layers implying that they are emplaced as thin, spreading flows possibly over many events.

4.19.1.   Orbital Observations

[150] Hillside chutes, lobe-shaped areas at the foot of slopes, and linear boulder trains and streaks are present in a few locations, mostly on the steeper slopes of the Columbia Hills. Significant examples near Spirit's traverse occur on the north and south flanks of Husband Hill and the south flank of Haskin ridge. In HiRISE image data, the surfaces of debris flows appear to consist of loose debris of mixed fines and some rocks. The uphill termination of the more lobe-shaped examples are frequently defined by scallop-shaped alcoves or small scarps while the margins of larger examples like that on the north flank of Husband Hill are bounded by lateral ridges or levee-like arrangements in midslope. The terminus of the two larger lobe-shaped examples is hummocky, yet the interiors are relatively smooth. The linear boulder trains and streaks differ in that the plan shape is more irregular. The two type examples are on the northwest flank of Husband Hill and appear to be sourced at prominent scarps in flat-lying benches.

4.19.2.   Field Observations

[151] None of the areas mapped as this material were traversed and only the occurrences on the eastern end of West Spur and the south face of Husband Hill were observed with proximal remote sensing during the traverse. The example on the eastern end of West Spur is imaged in the south-southeast quarter of the Thanksgiving Pan (NASA PIA 07734) (Figure 19a) but is unrevealing other than that the slope is excessively rocky and undulating with local swells several meters across and up to 50 cm deep. A prominent debris chute on the south side of Husband Hill was imaged in super resolution Pancam data on sol 1513 (Figure 19b). Only the upper end of this was acquired, but it does reveal that the interior of the chute is hummocky, more finely textured than the surrounding much rockier flanks of Husband Hill, and the contact between the surroundings and the chute are defined by an abrupt ridge or scarp.

4.19.3.   Analysis and Interpretation

[152] From orbital images alone these areas are interpreted as debris chutes and fans that have developed following fluid downslope movement of unconsolidated and unstable materials, including blocks and fines together. Alternately, instead of coherent mass movement as a loose debris flow, these could be long-term accumulation of materials along
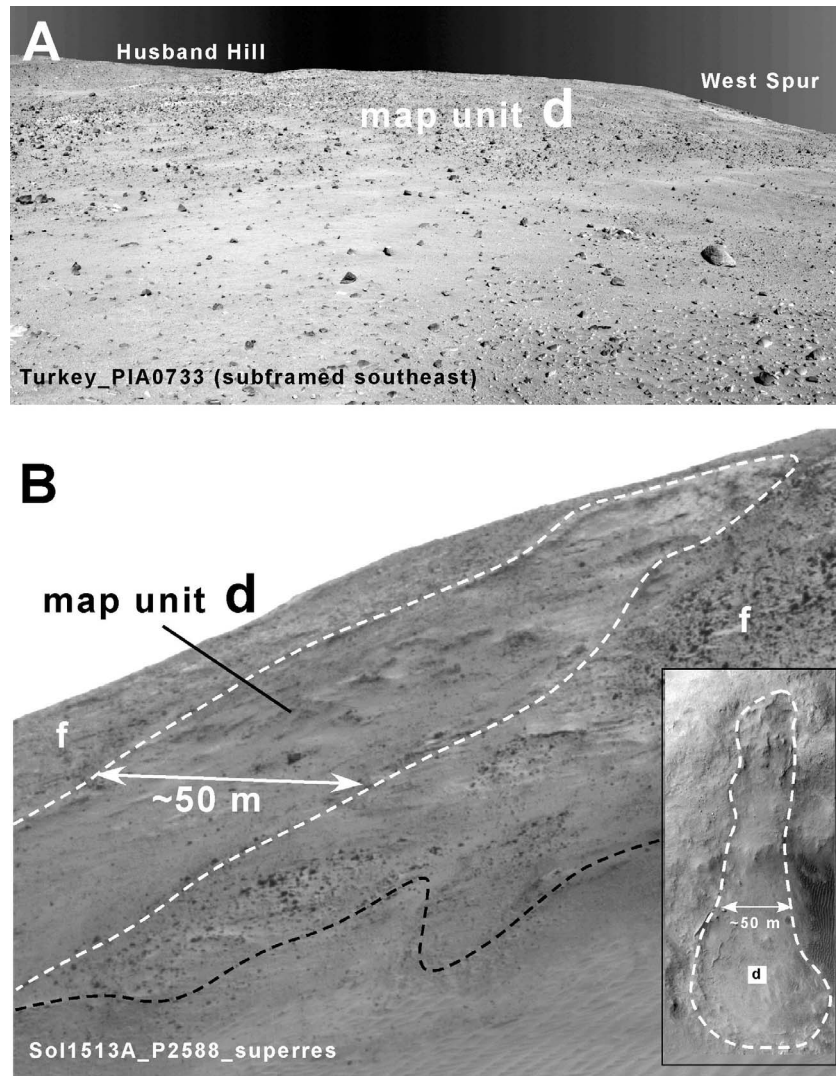
Figure 19. (a) Rover perspective on NW Husband Hill looking upslope at thick, rocky debris mantle that drapes over the steeper slopes on the northwest flank of Husband Hill. (b) Pancam "super resolution" view of feature/frame AuthorC.Clarke (Sol 1513A_P2588), a debris chute or slide on the south side of Husband Hill, as seen from the third winter location on the north edge of Home Plate. Inset shows perspective from HiRISE.

chute-like corridors. The lobe-shaped examples appear to be well-confined flows of aggregated debris mass in which terminal run out included large, possibly matrix-supported blocks.

[153] Comparison of landscape characteristics from the rover perspective and the location and plan view lobate shape of these surfaces in HiRISE images are consistent with the more coherent flow of material *en mass* to as debris flows. The smooth, rolling surface of some of these as seen in superresolution Pancam images (Figure 19b) is similar to the fine-dominated and character of debris slides on Earth. The location on relatively steep slopes, particularly where outcrops are few and the surface is bland and apparently loaded with fines supports this interpretation. We suspect that these are examples of a form of mass movement that has been common during the landscape evolution throughout the Columbia Hills [*Rice et al.*, 2010]. Other areas identified

as this unit may be areas of confined downslope accumulation rather than cohesive flows.

5. Impact Craters

[154] Distinct differences in the density of impact craters within the Columbia Hills are notable in a map based on identification of all impact crater rims and circular residual impact depressions using stereo HiRISE images (Figures 20a and 20b). Three distinct groups of surface units were grouped for counting and include the plains unit (Ba), Float materials (F), and capping or outcrop units. The capping or outcrop units include several widely separated Columbia Hills outcrops and rock types: West Spur (uws), Haskin Ridge (H), Cumberland Ridge (ucr), Columbia Hills summit (ch), and upper Home Plate (R).

[155] The results show that where the float (unit F) is common, which is mostly on slopes, there is a dearth of small
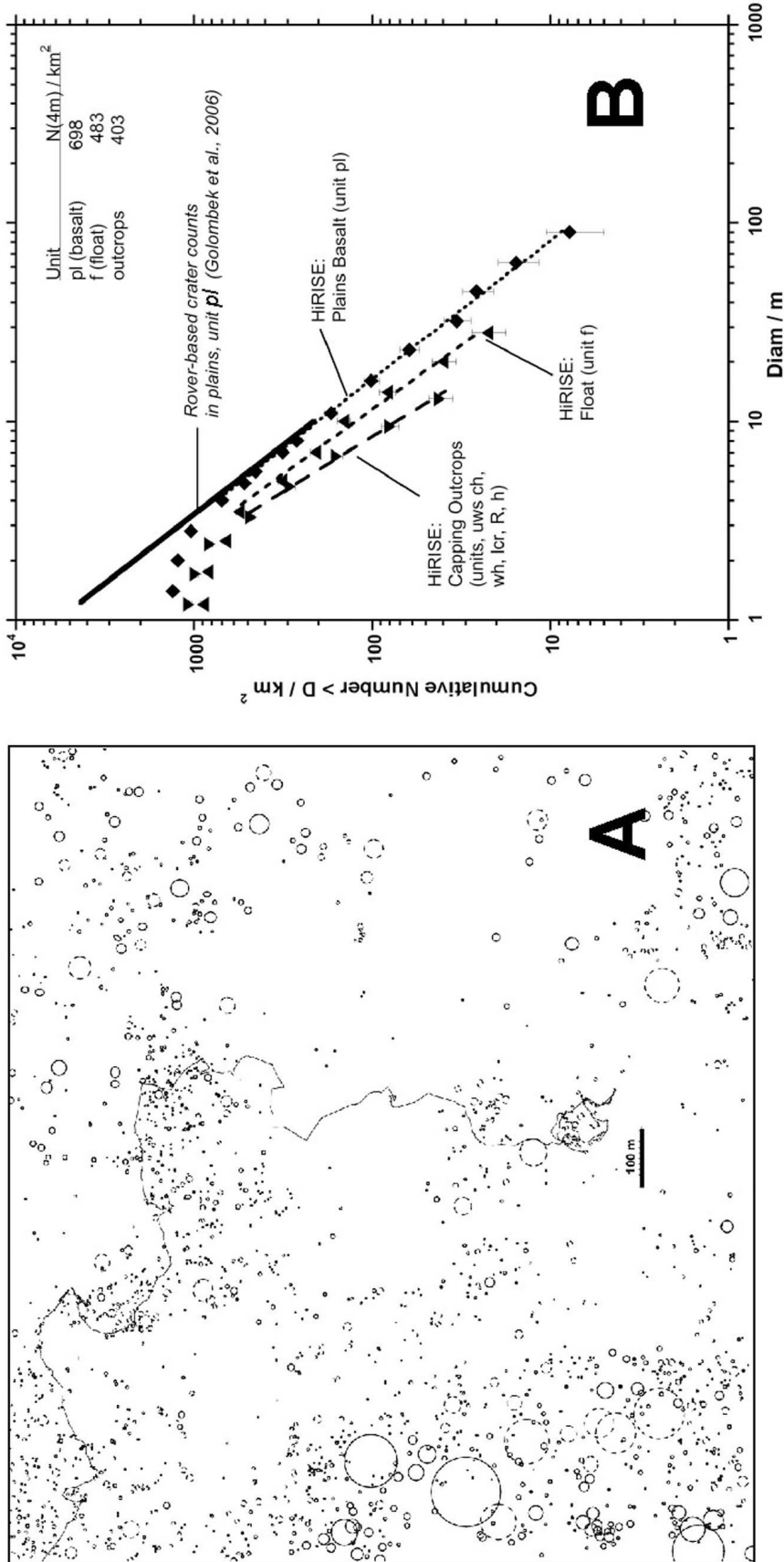
Figure 20. (a) Map of all identifiable impact craters in HiRISE images covering the area shown in Figures 1 and 2a. Some variations in crater density are notable throughout the Columbia Hills. Areas of obviously lower impact crater concentration are not correlated with stratigraphically higher (younger) materials but instead are correlated with areas where significant erosion has occurred, or where slope debris is abundant. (b) Size-frequency distribution of small impact craters in three of the broad surface types, plains lavas (unit pl), float covered slopes (unit f), and units representing outcrops and capping ridges (units uws, lcr, ch, h, R). Areas covered by mobile materials (units rmf and dmf) were not counted. Impact crater abundances in the plains determined from counts on the HiRISE image base (dotted line) is comparable to the findings from rover-based counts (solid line) along Spirit's traverse within the plains. At this scale the synoptic overhead view afforded by HiRISE is more useful for crater inventories because it assesses greater areas than ground-based crater identification.

impact craters, whereas later plains lavas tend to have slightly more impact craters. As a check, in Figure 20b we directly compare the results for counts on the plains unit in HiRISE image data with impact craters distributions identified from the rover perspective [*Golombek et al.*, 2006] and find that crater counts based on HiRISE data are capable of detecting small impact craters nearly as well as ground-based counts from rovers and certainly over larger areas.

[156] Compared with the small impact craters that were easily identified from the rover perspective within the plains [*Golombek et al.*, 2006], impact craters are not as obvious along the traverse within the Columbia Hills. Only a few small impact craters are easily identifiable from rover perspective (sols 200, 310, 317, 520, 639, 655, 1886) whereas numerous depressions, troughs, and hillside scalloped depressions were traversed. The latter are likely remnants of small impact craters although there is nothing distinctive other than the absence of other reasonable alternative methods to create hollows and arcuate scarps to confirm this origin. At least two localities of outcrop exposure on the traverse over Husband Hill (Independence and Kansas) (see Figure 2) appear to lie in broad depressions that are sharply separated from the thick mantles of surrounding float. These coincide with (roughly circular) depressions and are identifiable in HiRISE image data as probable small impact craters. There is some suggestion that among small impact crater populations, low-velocity impacts, presumably secondary craters, are more common [*Golombek et al.*, 2006; *Grant et al.*, 2006]. The depressions with little float are intriguing inasmuch as they support some basic concepts about the dispersal of impact energy in targets of variable strength. For example, low- to moderate-velocity impacts into layered targets [*Melosh*, 1989], where a low-strength material overlies a hard substrate (a reasonable description for float-covered bedrock), the impact energy can be diverted in lateral expulsion of upper layers and relatively little excavation. These observations may support the general conclusion that low-velocity impacts on slopes with thick float may be capable of removing significant covers of loose debris and result in exposure of the bedrock substrate. In the long term, the process exposes bedrock to erosion and breakdown while mostly moving existing loose material downslope.

[157] The variation in the local impact crater distribution at this scale bears little relation to the stratigraphy determined from geologic mapping. For example, overall abundances of impact crater are greater in the plains than within the Columbia Hills [*Haldemann et al.*, 2004], in apparent contradiction to the fact that onlapping relations, visible in orbital images [*Kuzmin et al.*, 2000] as well as from Spirit's traverse [*Crumpler et al.*, 2005], show that the Columbia Hills are much older than the surrounding plains. The lower crater abundances for the stratigraphically older Columbia Hills most likely reflect differences in crater retention rather than age, a difference that is almost certainly a result of the more resistant plains lavas relative to the less competent clastic lithologies that dominate the shallow surface and outcrops of the Columbia Hills. The greater strength of plains rocks relative to rocks of the Columbia Hills was confirmed directly by recorded Rock Abrasion Tool (RAT) Specific Grind Energies (SGE) [*Gorevan et al.*, 2003; *Bartlett et al.*, 2005]. The SGE recorded the energy consumed to excavate a RAT hole of a given volume and represents a

reliable quantitative proxy for laboratory rock compressive strength measurements. The average SGE of plains rocks (50–60 J mm^{-3}) is several times higher than typical rocks of the Columbia Hills (2 to 24 J mm^{-3}) [*Bartlett et al.*, 2005; *Arvidson et al.*, 2006; *Squyres et al.*, 2006]. Rocks of the plains are likely to erode at rates proportionally slower than the rocks within the hills therefore yielding a net higher crater retention rate within the plains.

6. Stratigraphy and Geologic History of the Columbia Hills Interpreted From Field Results

[158] At least 60 m of vertical stratigraphic section has been examined as outcrop within the Columbia Hills. Where benches, ridges, and ledges were traversed on the flanks of Husband Hill, the dip of local outcrop layers, or structural surfaces, generally exceeded the topographic slopes. From this general arrangement of bedding planes, the Columbia Hills are interpreted to have an eroded antiformal structure, that is, older materials are generally exposed at higher elevations, although this is modified at the highest elevations by local caps of higher, more resistance stratigraphic units. Exposure of older rocks at higher elevations was accomplished through general effects of ablation wearing away the summits and depositing debris on the lower flanks. During the traverse, the contact between the exposed bedrock outcrops and the debris-laden lower slopes appeared to be distinct and the debris itself had begun to be ablated as a later epiclastic unit. The ability to measure the dimensions of the observed sections from the rover enabled sections to be roughly correlated for the first time at meter scales on the surface of Mars. The summary sketch of stratigraphic results (Figures 21a and 21b) plotted on the general profile of the Columbia Hills along with the measured sections and lithostratigraphic relations permits the development of some general hypotheses for the regional geologic history of the Columbia Hills.

[159] Sections on the northwest flank of Husband Hill (the Methuselah–Larrys Lookout region) and on the south flank of Haskin Ridge bear some similarities in their petrography and overlapping position with other units. In both sections an early poorly sorted material (Larrys Bench and Seminole) with abundant nanophase oxides, interpreted as severely altered matrix glass groundmass and microshards (Voltaire and Wishstone source), is overlain by somewhat coarser, but poorly laminated lapilli tuffs (Larrys Lookout and Algonquin–Comanche Spur). The latter bear evidence for explosive emplacement, abundant altered glassy groundmasses, and incorporation of Wishstone clasts (Voltaire). We interpret this sequence as the result of at least one significant impact into a Wishstone class material substrate that generated impact melts, along with other impacts into basaltic material, and followed by later volcanic air fall deposits. Pervasive and thick lapilli tuffs resting on these rocks are possible volcanic deposits from local Plinian to sub-Plinian eruptions, either vents within the floor of Gusev crater, or more distal volcanoes typified by those in the surrounding highlands. Lapilli of the observed dimension, on the order of 1 to 2 mm, can be transported from several hundred kilometers [*Wilson and Head*, 2007].

[160] The outcrop Clovis (the caprock of West Spur, unit uws) in general is interpreted as a fundamentally basaltic

volcanic ash (size fraction) fall deposit from a distal source. The unusual enrichment in Cl (1.4 wt %) bears some similarity to the high Cl concentrations determined from Mars Odyssey Gamma Ray Spectrometer results for the equatorial region immediately to the north [*Keller et al.*, 2007]. This broad region corresponds with the mapped extent of the Medusae Fossae mantling deposit, a material that unconformably buries significant preexisting relief and is generally compared with deposits of ashfall derivation [*Mandt et al.*, 2008]. The proximity of Gusev crater to the region over which Medusae Fossae Formation occurs, together with the chlorine anomaly, makes the Clovis class material (unit
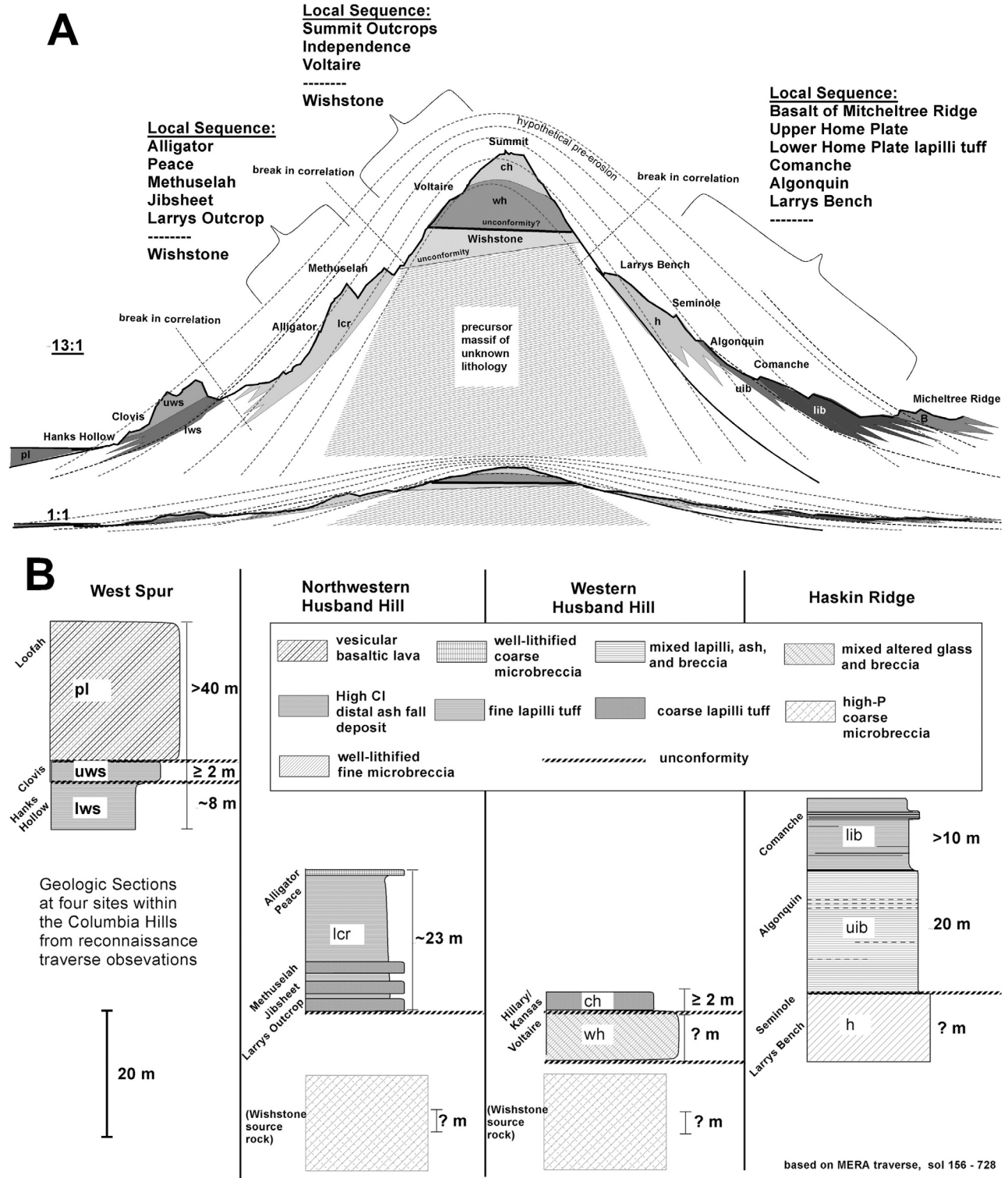

Figure 21

uws) a viable candidate as a distal outlier of the Medusae Fossae Formation. If this were so then we could speculate that the entire Columbia Hills stratigraphic sequence predates the end of the Ma'adim Vallis incursion into Gusev crater, because the channels at the terminus of Ma'adim cut Medusae Fossae materials. The presence of a surrounding lake or throughgoing channels after the protolith rocks of Columbia Hills had been emplaced would be consistent with the greater availability of fluids in the environment that ultimately played a role in chemically altering the rocks. The extreme backwasting of the lower slopes of the Columbia Hills, such as that seen at West Spur and significant development of slope debris and thick epiclastic deposits would also be consistent with enhanced mechanical erosion afforded by significant water and corresponding physical erosion.

[161] From Spirit's traverse we now know from direct observation that significant geologic time transpired before the emplacement of the plains basaltic lavas in Gusev crater. The Columbia Hills side of the lava contact is an angular unconformity. Yet this unconformable surface is covered with float derived from some of the higher stratigraphic units (Clovis and Hanks Hollow, units uws and lws) and the sequence of clastic rocks in West Spur are truncated by back wasting beneath the resistant cap of Clovis class rock. Erosion sufficient to generate this scale of unconformity was accomplished by some extremely energetic erosion process or by a less energetic process operating over a long period. Either intense activity or long intervals of activity are implied, which is geologically significant in either case, and the regional volcanism occurred long afterward. This follows a pattern of former fluvial valleys reoccupied by later lava flows that appears common to much of Mars [e.g., *Crumpler et al.*, 2007].

[162] All rocks measured, even the distal ash deposits like Clovis, and with the exception of Wishstone, are extensively altered by fluids. So, a fluid-rich environment and potential for erosive environments continued long after the original impacts and pyroclastic eruption events responsible for them. Wishstone appears to represent a substrate, possibly an early core massif of the Columbia Hill that was not subjected to the abundance of fluids that affected later rocks, although the presence of rind-coated angular blocks (sol 387) and possible secondary P implies that at least a limited amount of fluids were present.

[163] The following geologic history of the Columbia Hills is based on the observations outlined above and cur-

rent understanding of their implications. The Columbia Hills were initiated as a floor relief feature in Gusev crater, likely a central peak. At some point structural deformation occurred. Both a series of wrinkle ridges and numerous impact craters across the floor may have helped shape the hills. Tectonic deformation may have continued through later times both as wrinkle ridges and late floor isostatic adjustments. Thermal events may also have affected the basement rocks throughout this period.

[164] During this earlier and more dynamic period, deep erosion and modification of the central peaks between intervals of modification, and regional impact crater fall deposits were probably occurring and contributed to a series of deposits and unconformities further obliterating any original central peak rocks or their associated landscape. Fluvial events (Ma'adim Vallis) were active on the Gusev crater floor at some point during these events or immediately following them, but there is no evidence to indicate whether or not the Columbia Hills were directly affected mechanically. There is evidence that moderately high water-to-rock ratios were present during the time that most of the clastic rocks of the Columbia Hills were being deposited as fall deposits, including both impactites and pyroclastic deposits. These were all subsequently altered significantly by fluids moving through the rocks.

[165] Proximal volcanic vents, possibly local, deposited volcanic air fall materials throughout the hills. Small tectonic movements possibly associated with continued wrinkle ridge type deformations may have occurred during this phase as well. Local volcanic vents may have been the source of the widespread pyroclastic deposits or they may have been simply a part of the regional rise in volcanism that also contributed to the stack of volcanic fall deposits draped over the hills. Substantial time elapsed after, and likely between, these eruptions for early erosion of the Columbia Hills, including backwasting of ridges and peaks draped by regional fall deposits. The early, more altered, and softer core rocks acted as slope formers and later pyroclastic sequences were caprocks. Accumulated hillslope debris aided by local small impact cratering events initiated many debris slides and slumps. Wind redistributed some of the ash and eroded volcanic rocks throughout the time of active volcanism, filling local hollows with secondary, mobile sands of composition similar to the local primary volcanic rocks. Finally the floor of Gusev crater was flooded by lava flows that encroached on the eroded margins of the

Figure 21. (a) Summary schematic section of Husband Hill and adjoining ridges on an elevation plot along the traverse route. The profile represents elevations of the traverse from sol 156 to sol 720 based on the rover tracking reported by *Li et al.* [2008]. Sols of significant back tracking (sols 423–434; 454–513; 582–605; 619–635; 668–664; 667–678) have been removed, and the profile laterally collapsed into a serial ascent and descent traverse from left to right from the West Spur on the left, across Husband Hill in the center, and into the Inner Basin near Lorre and Mitcheltree Ridges on the right. On the basis of recorded structure at laminated outcrops, and the apparent down-stratigraphic sequence of exposures with upslope traverse, the Columbia Hills are interpreted to consist of multiple draped deposits, now mostly stripped from the crest so that stratigraphically higher materials tend to occur topographically lower on the hills. An unconformity on the core massif materials and on the Wishstone parent material, shown only graphically, predate and form the substrate over which most of the other outcrops visited during the traverse are draped. (b) Measured stratigraphic sections at four locations along the traverse through the Columbia Hills. The total apparent section is about 60 m. Early impactites and microbreccias are followed in succession by thick lapilli tuffs, fine ashfall deposits, and late basaltic lava flows. A significant erosion unconformity postdates the high-Cl ash of West Spur (Clovis outcrop, unit uws) unconformity. Note that breaks in the lateral correlation of these four sites result in considerable uncertainty regarding their relative vertical positions in the regional stratigraphy.

Columbia Hills. Continued, but significantly reduced, impact cratering modified the hills and the lava plains. Even though the period of intense geological activity and surface modification had ended by this point in the sequence, repetitive cycles of moist climatic events over the course of the next (few) billion years that followed, together with the acidic character of fluids and their sequestering in the substrate between moisture events, were sufficient to further erode and alter rocks at depth and leach fines exposed at the surface. Sulfate seeps and springs may have continued until the relatively recent past.

7. Conclusions

[166] Spirit conducted a geologic reconnaissance traverse on Mars and field checked a photogeologic map prepared from orbital remote sensing data. From the results of the traverse mapping, we conclude that stratigraphic complexity occurs at submeter scales on Mars, field geologic mapping is possible at meter (outcrop) scales, and elements of regional geologic history may be preserved and subsequently interpreted by terrestrial type field methods. The tools of field geology were an important part of the mission design criteria and these results confirm that the use of standard field geologic methods and field tools is appropriate to understanding the geologic history of Mars. This first walk through and geological characterization of a complex geologic setting on Mars also demonstrates that Mars is as geologically complex as Earth. But whereas the most complex preservation on Earth records the last half billion years of geologic activity, on Mars the activity was earlier and equally well preserved as young events on Earth, though no less complex. The main impediment to accurate unit mapping on the surface in rugged terrains on Mars will be float. Slumped blocks and residual fragments of hard caprocks on a softer undermined substrate can almost entirely cover retreating slopes leaving very little of any softer substrate exposed for sampling. In terrains where float is abundant, a successful in situ sampling strategy might include focusing on small impact craters. Because small impacts may be dominated by low-velocity secondary impacts [*Golombek et al.*, 2006], and the kinetics is insufficient to substantially damage the substrate, loose (float) overburden resting on harder bedrock appears to be swept laterally by the impact.

[167] The geology along the entire traverse through the Columbia Hills consists of scattered outcrops, mostly of tuffs and breccias, thick accumulations of float, and mobile fines. Spirit's in situ studies were unable to examine the deep substrate materials of the Columbia Hills but it is likely that the precursor hills were part of an original central peak massif consisting of breccias and uplifted deeper crustal materials. Following development of one or more unconformities and intervening fall deposits, the precursor hills were draped with various later air fall deposits to form the outcrops that were examined. Many of the variations in microscopic texture, abundances of small lithic fragments (clasts) and evidence for predepositional and postdepositional nonisochemical alteration are consistent with local and regional fallout and ejecta from impacts of differing sizes and depth of excavation in target materials of diverse initial alteration state. In some cases, these may have been altered subsequently by secular and episodic events in which fluids circulated through the

rock masses. Differing proximity and differing alteration and petrologic state of nearby target materials are possible origins of variations in observed protolith chemistries for these deposits. Other materials are volcanic fall deposits from distal and proximal ash and lapilli sources. The Clovis class materials that cap West Spur and the Medusae Fossae Formation of equatorial Mars may be part of the same regional volcanic fall deposit.

[168] The documentation of the great differences in alteration and weathering of rocks on either side of the geologic unconformity between the plains and Columbia Hills represents the first direct validation of the general inference from remote sensing that the Martian climate has become dryer and less energetic with time. The general stratigraphic trend in the Columbia Hills records a geologic history that progresses from time of higher water-rock ratios, through a period of predominant influences of impact ejecta and fallout, then to predominantly volcanic, and subsequently a longer period of small secular changes in fluid abundance and pervasive aeolian erosion. A sequence of environments, the decline in vigorous geologic activity punctuated by cycles of fluid interaction, periods of volcanism, and some intervening periods of erosion are all documented in the Columbia Hills through direct observation of exposed outcrops. This geologic history, determined with basic field geologic techniques, in the Columbia Hills is similar to current hypotheses of global Martian geologic history, and may be applicable to interpreting global processes and secular changes that have affected many as yet unvisited areas of Mars.

References

Arvidson, R. E., et al. (2003), Physical properties and localization investigations associated with the 2003 Mars Exploration rovers, *J. Geophys. Res.*, *108*(E12), 8070, doi:10.1029/2002JE002041.

Arvidson, R. E., et al. (2004), Initial localization and physical properties experiments conducted with the Mars Exploration Rover Mission to Gusev crater, *Science*, *305*(5685), 821–824, doi:10.1126/science.1099922.

Arvidson, R. E., et al. (2006), Overview of the Spirit Mars Exploration Rover Mission to Gusev crater: Landing site to Backstay Rock in the Columbia Hills, *J. Geophys. Res.*, *111*, E02S01, doi:10.1029/2005JE002499.

Arvidson, R. E., et al. (2008), Spirit Mars Rover Mission to the Columbia Hills, Gusev crater: Mission overview and selected results from the Cumberland Ridge to Home Plate, *J. Geophys. Res.*, *113*, E12S33, doi:10.1029/2008JE003183.

Arvidson, R. E., et al. (2010a), Spirit Mars Rover Mission: Overview and selected results from the northern Home Plate Winter Haven to the side of Scamander crater, *J. Geophys. Res.*, *115*, E00F03, doi:10.1029/2010JE003633.

Arvidson, R. E., et al. (2010b), Recent scientific results from Spirit's observations of sulfate sands on the side of Scamander crater, Columbia Hills, Mars, *Lunar Planet. Sci.*, *41*, Abstract 1247.

Barnes, J. (1981), *Basic Geological Mapping*, 119 pp., Open Univ. Press, London.

Bartlett, P. W., L. E. Carlson, P. C. Chu, K. R. Davis, S. Gorevan, A. G. Kusack, T. M. Myrick, and J. J. Wilson (2005), Summary of Rock Abrasion Tool (RAT) results pertinent to the Mars Exploration Rover science data set, *Lunar Planet. Sci.*, *36*, Abstract 2292.

Bell, J., et al. (2003), Mars Exploration Rover Athena Panoramic Camera (Pancam) investigation, *J. Geophys. Res.*, *108*(E12), 8063, doi:10.1029/2003JE002070.

Cabrol, N. A., E. A. Grin, R. Landheim, R. O. Kuzmin, and R. Greeley (1998), Duration of the Ma'adim Vallis/Gusev crater hydrologic system, *Icarus*, *133*, 98–108, doi:10.1006/icar.1998.5914.

Cabrol, N. A., et al. (2003), Exploring Gusev crater with Spirit: Review of science objectives and testable hypotheses, *J. Geophys. Res.*, *108*(E12), 8076, doi:10.1029/2002JE002026.

Carr, M. H. (1996), *Water on Mars*, 229 pp., Oxford Univ. Press, New York.

Christensen, P. R., et al. (2003), The Miniature Thermal Emission Spectrometer for the Mars Exploration Rovers, *J. Geophys. Res.*, *108*(E12), 8064, doi:10.1029/2003JE002117.

Clark, B. C., et al. (2007), Evidence for montmorillonite or its compositional equivalent in Columbia Hills, Mars, *J. Geophys. Res.*, *112*, E06S01, doi:10.1029/2006JE002756.

Compton, R. (1985), *Geology in the Field*, 398 pp., John Wiley, New York.

Crumpler, L. S. (2003a), Spring deposits on Mars: Physical processes from terrestrial analogs, *Lunar Planet. Sci.*, *XXXIV*, Abstract 2002.

Crumpler, L. S. (2003b), Physical characteristics, geologic setting, and possible formation processes of spring deposits on Mars based on terrestrial analogs, in *Sixth Mars Conference* (CD-ROM), Abstract 3238, Lunar and Planet. Inst., Houston, Tex.

Crumpler, L. S., and the Athena Science Team (2005), MER field observations and analysis of vesicles in the Gusev plains: Significance as records of emplacement environment, *Lunar Planet. Sci.*, *XXXVI*, Abstract 2122.

Crumpler, L. S., et al. (2005), MER geologic traverse science by the Spirit Rover in the Plains of Gusev crater, Mars, *Geology*, *33*, 809–812, doi:10.1130/G21673.1.

Crumpler, L. S., L. P. Keszthelyi, W. L. Jaeger, A. McEwen, and the HiRISE Science Team (2007), High-resolution imaging of lava flow terrains on Mars by MRO HiRISE, *Eos Trans. AGU*, *88*(52), Fall Meet. Suppl., Abstract P34A-03.

Delmelle, P., and J. Stix (2000), Volcanic gases, in *Encyclopedia of Volcanoes*, edited by H. Sigurdsson, et al., pp. 803–815, Academic, San Diego, Calif.

Easterbrook, D. J. (1999), *Surface Processes and Landforms*, Prentice Hall, Upper Saddle River, N. J.

Evans, T. J. (2007), General standards of geologic maps, in *The Geoscience Handbook*, edited by J. D. Walker and H. A. Cohen, pp. 23–26, Am. Geogr. Inst., Alexandria, Va.

Farmer, J. D. (2005), Case-hardening of rocks on Mars: Evidence for water-mediated weathering processes, paper presented at Annual Meeting, Geol. Soc. of Am., Salt Lake City, Utah.

Farrand, W. H., et al. (2008), Rock spectral classes observed by the Spirit Rover's Pancam on the Gusev crater plains and in the Columbia Hills, *J. Geophys. Res.*, *113*, E12S38, doi:10.1029/2008JE003237.

Fleisher, M., T. Liu, W. S. Broecker, and W. Moore (1999), A clue regarding the origin of rock varnish, *Geophys. Res. Lett.*, *26*, 103–106, doi:10.1029/1998GL900229.

Gellert, R., et al. (2004), Chemical composition of Martian rocks and soils at the Spirit Landing Site in Gusev crater: Initial results of the Alpha Particle X-ray Spectrometer, *Science*, *305*, 829–832, doi:10.1126/science.1099913.

Gellert, R., et al. (2006), Alpha Particle X-Ray Spectrometer (APXS): Results from Gusev crater and calibration report, *J. Geophys. Res.*, *111*, E02S05, doi:10.1029/2005JE002555.

Golombek, M. P., et al. (2003), Selection of the Mars Exploration Rover landing sites, *J. Geophys. Res.*, *108*(E12), 8072, doi:10.1029/2003JE002074.

Golombek, M. P., et al. (2006), Geology of the Gusev cratered plains from the Spirit rover transverse, *J. Geophys. Res.*, *111*, E02S07, doi:10.1029/2005JE002503.

Gorevan, S. P., et al. (2003), Rock abrasion tool: Mars Exploration Rover mission, *J. Geophys. Res.*, *108*(E12), 8068, doi:10.1029/2003JE002061.

Grant, J. A., et al. (2006), Crater gradation in Gusev crater and Meridiani Planum, Mars, *J. Geophys. Res.*, *111*, E02S08, doi:10.1029/2005JE002465.

Greeley, R., and R. M. Batson (1990), *Planetary Mapping*, 296 pp., Cambridge Univ. Press, New York.

Greeley, R., et al. (2005), Fluid lava flows in Gusev crater, Mars, *J. Geophys. Res.*, *110*, E05008, doi:10.1029/2005JE002401.

Greeley, R., et al. (2006), Gusev crater: Wind-related features and processes observed by the Mars Exploration Rover, Spirit, *J. Geophys. Res.*, *111*, E02S09, doi:10.1029/2005JE002491.

Greeley, R., et al. (2008), Columbia Hills, Mars: Aeolian features seen from the ground and orbit, *J. Geophys. Res.*, *113*, E06S06, doi:10.1029/2007JE002971.

Haldemann, A. F. C., et al. (2004), Survey of craters by Spirit in Gusev crater and Opportunity in Meridiani Planum, paper presented at Mars Crater Consortium 7th Meeting, Flagstaff, Ariz.

Hartmann, W. K. (2005), Martian cratering 8: Isochron refinement and the chronology of Mars, *Icarus*, *174*, 294–320, doi:10.1016/j.icarus.2004.11.023.

Haskin, L. A., et al. (2005), Water alteration of rocks and soils on Mars at the Spirit rover site in Gusev crater, *Nature*, *436*, 66–69, doi:10.1038/nature03640.

Herkenhoff, K. E., et al. (2003), The Athena Microscopic Imager Investigation, *J. Geophys. Res.*, *108*(E12), 8065, doi:10.1029/2003JE002076.

Herkenhoff, K. E., et al. (2006), Overview of the Microscopic Imager Investigation during Spirit's first 450 sols in Gusev crater, *J. Geophys. Res.*, *111*, E02S04, doi:10.1029/2005JE002574.

Herkenhoff, K. E., et al. (2008), Surface processes recorded by rocks and soils on Meridiani Planum, Mars: Microscopic Imager observations during Opportunity's first three extended missions, *J. Geophys. Res.*, *113*, E12S32, doi:10.1029/2008JE003100.

Hurowitz, J. A., et al. (2006), In situ and experimental evidence for acidic weathering of rocks and soils on Mars, *J. Geophys. Res.*, *111*, E02S19, doi:10.1029/2005JE002515.

Keller, J. M., et al. (2007), Equatorial and mid-latitude distribution of chlorine measured by Mars Odyssey Gamma Ray Spectrometer, *J. Geophys. Res.*, *112*, E03S08, doi:10.1029/2006JE002679.

Kerber, L., and J. W. Head (2010), The age of the Medusae Fossae Formation: Evidence of Hesperian emplacement from crater morphology, stratigraphy, and ancient lava contacts, *Icarus*, *206*, 669–684, doi:10.1016/j.icarus.2009.10.001.

Klingelhöfer, G., et al. (2003), Athena MIMOS II Mössbauer spectrometer investigation, *J. Geophys. Res.*, *108*(E12), 8067, doi:10.1029/2003JE002138.

Kuzmin, R. O., R. Greeley, R. Lanheim, N.A. Cabrol, and J. Farmer (2000), Geologic map of the MTM-15182 and MTM 15187 quadrangles, Gusev crater-Ma'adim Vallis region, Mars, *U. S. Geol. Surv. Misc. Invest. Map, 1-2666*.

Li, R., et al. (2005), Initial results of rover localization and topographic mapping for the 2003 Mars Exploration Rover Mission, *J. Photogramm. Eng. Remote Sens.*, *71*, 1129–1142.

Li, R., et al. (2006), Spirit rover localization and topographic mapping at the landing site of Gusev crater, Mars, *J. Geophys. Res.*, *111*, E02S06, doi:10.1029/2005JE002483.

Li, R., et al. (2008), Characterization of traverse slippage experienced by Spirit Rover on Husband Hill at Gusev crater, *J. Geophys. Res.*, *113*, E12S35, doi:10.1029/2008JE003097.

Liu, T., and W. S. Broecker (2000), How fast does rock varnish grow?, *Geology*, *28*, 183–186, doi:10.1130/0091-7613(2000)28<183:HFDRVG>2.0.CO;2.

Maki, J. N., et al. (2003), Mars Exploration Rover engineering cameras, *J. Geophys. Res.*, *108*(E12), 8071, doi:10.1029/2003JE002077.

Mandt, K. E., S. L. de Silva, J. R. Zimbelman, and D. A. Crown (2008), The origin of the Medusae Fossae Formation, Mars: Insights from a synoptic approach, *J. Geophys. Res.*, *113*, E12011, doi:10.1029/2008JE003076.

Martínez-Alonso, S., B. M. Jakosky, M. T. Mellon, and N. E. Putzig (2005), A volcanic interpretation of Gusev crater surface materials from thermophysical, spectral, and morphological evidence, *J. Geophys. Res.*, *110*, E01003, doi:10.1029/2004JE002327.

McCoy, T. J., et al. (2008), Structure, stratigraphy, and origin of Husband Hill, Columbia Hills, Gusev crater, Mars, *J. Geophys. Res.*, *113*, E06S03, doi:10.1029/2007JE003041.

McEwen, A. S., et al. (2007), Mars Reconnaissance Orbiter's High Resolution Imaging Science Experiment (HiRISE), *J. Geophys. Res.*, *112*, E05S02, doi:10.1029/2005JE002605.

McEwen, A. S., et al. (2010), The High Resolution Imaging Science Experiment (HiRISE) during MRO's Primary Science Phase (PSP), *Icarus*, *205*, 2–37, doi:10.1016/j.icarus.2009.04.023.

McSween, H. Y., et al. (2006a), Characterization and petrologic interpretation of olivine-rich basalts at Gusev crater, Mars, *J. Geophys. Res.*, *111*, E02S10, doi:10.1029/2005JE002477.

McSween, H. Y., et al. (2006b), Alkaline volcanic rocks from the Columbia Hills, Gusev crater, Mars, *J. Geophys. Res.*, *111*, E09S91, doi:10.1029/2006JE002698.

McSween, H. Y., et al. (2008), Mineralogy of volcanic Rocks in Gusev crater, Mars: Reconciling Mössbauer, APXS, and Mini-TES Spectra, *J. Geophys. Res.*, *113*, E06S04, doi:10.1029/2007JE002970.

Melosh, H. J. (1989), *Impact Cratering: A Geologic Process*, 245 pp., Oxford Univ. Press, New York.

Milam, K. A., et al. (2003), THEMIS characterization of the MER Gusev crater landing site, *J. Geophys. Res.*, *108*(E12), 8078, doi:10.1029/2002JE002023.

Ming, D. W., et al. (2006), Geochemical and mineralogical indicators for aqueous processes in the Columbia Hills of Gusev crater, Mars, *J. Geophys. Res.*, *111*, E02S12, doi:10.1029/2005JE002560.

Ming, D. W., et al. (2008), Geochemical properties of rocks and soils in Gusev crater, Mars: Results of the Alpha Particle X-ray Spectrometer

from Cumberland Ridge to Home Plate, *J. Geophys. Res.*, *113*, E12S39, doi:10.1029/2008JE003195.

Mittlefehldt, D.W., R. Gellert, T. McCoy, H. Y. McSween Jr., R. Li, and the Athena Science Team (2006), Possible Ni-rich mafic-ultramafic magmatic sequence in the Columbia Hills: Evidence from the Spirit Rover, *Lunar Planet Sci.*, *37*, Abstract 1505.

Morris, R. V., et al. (2004), Mineralogy at Gusev crater from the Mössbauer Spectrometer on the Spirit Rover, *Science*, *305*, 833–836, doi:10.1126/science.1100020.

Morris, R. V., et al. (2006), Mössbauer mineralogy of rock, soil, and dust at Gusev crater, Mars: Spirit's journey through weakly altered olivine basalt on the plains and pervasively altered basalt in the Columbia Hills, *J. Geophys. Res.*, *111*, E02S13, doi:10.1029/2005JE002584.

Morris, R. V., et al. (2008), Iron mineralogy and aqueous alteration from Husband Hill through Home Plate at Gusev crater, Mars: Results from the Mössbauer instrument on the Spirit Mars Exploration Rover, *J. Geophys. Res.*, *113*, E12S42, doi:10.1029/2008JE003201.

Morris, R. V., et al. (2010), Identification of carbonate-rich outcrops on Mars by the Spirit Rover, *Science*, *329*, 421–424, doi:10.1126/science.1189667.

Newsom, H. E., et al. (2007), Geochemistry of Martian soil and bedrock in mantled and less mantled terrains with gamma ray data from Mars Odyssey, *J. Geophys. Res.*, *112*, E03S12, doi:10.1029/2006JE002680.

Norris, J. S., M. W. Powell, M. A. Vona, P. G. Backes, and J. V. Wick (2005), Mars Exploration Rover operations with the Science Activity Planner, paper presented at 2005 IEEE International Conference on Robotics and Automation, Barcelona, Spain.

Perry, R. S., and J. B. Adams (1978), Desert varnish: Evidence for cyclic deposition of manganese, *Nature*, *276*(5687), 489–491, doi:10.1038/276489a0.

Powell, M. W., T. M. Crockett, K. Shams, and J. S. Norris (2010), Geologic mapping in Mars Rover operations, paper presented at 2010 Space Ops Conference, Am. Inst. of Aeron. and Astron., Huntsville, Ala., April.

Ragan, D. M. (2009), *Structural Geology: An Introduction to Geometrical Techniques*, Cambridge Univ. Press, Cambridge, U. K.

Rice, J. W., Jr., et al. (2010), Geomorphology of the Columbia Hills Complex: Landslides, Volcanic Vent, and Other Home Plates, *Lunar Planet. Sci.*, *41*, Abstract 2566.

Rieder, R., et al. (2003), The new Athena Alpha Particle X-Ray Spectrometer (APXS) for the Mars Exploration Rovers, *J. Geophys. Res.*, *108*(E12), 8066, doi:10.1029/2003JE002150.

Ruff, S. W., et al. (2006), The Rocks of Gusev crater as viewed by the Mini-TES instrument, *J. Geophys. Res.*, *111*, E12S18, doi:10.1029/2006JE002747.

Rust, A. C., M. Manga, and K. V. Cashman (2003), Determining flow type, shear rate and shear stress in magmas from bubble shapes and orientations, *J. Volcanol. Geotherm. Res.*, *122*, 111–132, doi:10.1016/S0377-0273(02)00487-0.

Shea, T. B., et al. (2010), Textural studies of vesicles in volcanic rocks: An integrated methodology, *J. Volcanol. Geotherm. Res.*, *190*, 271–289, doi:10.1016/j.jvolgeores.2009.12.003.

Squyres, S. W., et al. (2003), Athena Mars rover science investigation, *J. Geophys. Res.*, *108*(E12), 8062, doi:10.1029/2003JE002121.

Squyres, S. W., et al. (2004), The Spirit Rover's Athena Science Investigation at Gusev crater, Mars, *Science*, *305*, 794–799, doi:10.1126/science.3050794.

Squyres, S. W., et al. (2006), Rocks of the Columbia Hills, *J. Geophys. Res.*, *111*, E02S11, doi:10.1029/2005JE002562.

Squyres, S. W., et al. (2008), Detection of silica-rich deposits on Mars, *Science*, *320*, 1063–1067, doi:10.1126/science.1155429.

Sullivan, R. R., et al. (2008), Wind-driven particle mobility on Mars: Insights from MER Observations at "El Dorado" and surroundings at Gusev crater, *J. Geophys. Res.*, *113*, E06S07, doi:10.1029/2008JE003101.

Tanaka, K. L., et al. (2009), Assessment of planetary geologic mapping techniques for Mars using terrestrial analogues: The SP Mountain area of the San Francisco Volcanic Field, Arizona, *Planet. Space Sci.*, *57*, 510–532, doi:10.1016/j.pss.2008.06.012.

Wang, A., et al. (2006), Evidence of phyllosilicates in Wooly Patch, an altered rock encountered at West Spur, Columbia Hills, by the Spirit rover in Gusev crater, Mars, *J. Geophys. Res.*, *111*, E02S16, doi:10.1029/2005JE002516.

Wang, A., et al. (2008), Light-toned salty soils and coexisting Si-rich species discovered by the Mars Exploration Rover Spirit in Columbia Hills, *J. Geophys. Res.*, *113*, E12S40, doi:10.1029/2008JE003126.

Wilhelms, D. E. (1990), Geologic mapping, in *Planetary Mapping*, edited by R. Greeley and R. M. Batson, pp. 208–260, Cambridge Univ. Press, New York.

Wilson, L., and J. W. Head (2007), Dispersal of tephra in explosive eruptions on Mars, *Lunar Planet Sci. Conf.*, *38*, Abstract 1117.

Yen, A. S., et al. (2008), Hydrothermal processes at Gusev crater: An evaluation of Paso Robles class soils, *J. Geophys. Res.*, *113*, E06S10, doi:10.1029/2007JE002978.

Yingst, R. A., et al. (2008), Morphology and texture of particles along the Spirit Rover traverse from sol 450 to sol 745, *J. Geophys. Res.*, *113*, E12S41, doi:10.1029/2008JE003179.

R. E. Arvidson, E. A. Guinness, and A. E. Wang, Department of Earth and Planetary Sciences, Washington University, 1 Brookings Dr., St. Louis, MO 63130, USA.

J. F. Bell III, M. Rice, and S. W. Squyres, Department of Astronomy, Cornell University, Ithaca, NY 14853, USA.

D. Blaney, J. Hurowitz, M. Powell, and A. Yen, Jet Propulsion Laboratory, Pasadena, CA 91109, USA.

N. A. Cabrol and D. DesMarais, NASA Ames Research Center, Moffett Field, CA 94035, USA.

B. Cohen, NASA Marshall Spaceflight Center, Huntsville, AL 35812, USA.

L. S. Crumpler, New Mexico Museum of Natural History and Science, 1801 Mountain Rd. NW, Albuquerque, NM 8710, USA. (larry.crumpler@state.nm.us)

P. deSouza, Tasmanian ICT Centre, CSIRO, Hobart, Tasmania, Australia.

W. Farrand, Space Science Institute, 4750 Walnut St., Ste. 205, Boulder, CO 80301, USA.

R. Gellert, Department of Physics, University of Guelph, Guelph, ON N1G 2W1, Canada.

J. Grant and T. McCoy, National Museum of Natural History, Smithsonian, Washington, DC 2001, USA.

R. Greeley, J. Farmer, and S. Ruff, School of Earth and Space Exploration, Arizona State University, Tempe, AZ 85287-1404, USA.

A. Haldemann, ESA/ESTEC, P.O. Box 299, 2200 AG Noordwijk ZH, Netherlands.

K. E. Herkenhoff and J. R. Johnson, U.S. Geological Survey, Flagstaff, AZ 86001, USA.

G. Klingelhöfer, Institut für Anorganische und Analytische Chemie, Johannes Gutenberg-Universität, D-55099 Mainz, Germany.

K. W. Lewis, Division of Geological and Planetary Sciences, California Institute of Technology, Mail Code 150-21, Pasadena, CA 91125, USA.

A. McEwen, Lunar and Planetary Lab, University of Arizona, 1541 E. Univ. Blvd., Tucson, AZ 85721, USA.

Y. McSween, Department of Earth and Planetary Sciences, University of Tennessee, 306 Geological Sciences Bldg., RM 306, Knoxville, TN 37996, USA.

D. W. Ming and R. V. Morris, Johnson Space Center, Mail Code KX, 2101 NASA Pkwy., Houston, TX 77058, USA.

J. W. Rice Jr., NASA Goddard Space Flight Center, Greenbelt, MD 20771, USA.

M. Schmidt, Department of Earth Sciences, Brock University, St. Catharines, ON L2S 3A1, Canada.

C. Schröder, Johnson Space Center, Houston, TX 77058, USA.

A. Yingst, Planetary Science Institute, 1700 East Fort Lowell, Ste. 106, Tucson, AZ 85719, USA.